The Spin Physics Detector (SPD) at NICA

Alexander Korzenev, LHEP JINR
on behalf of the SPD Collaboration

LHEP JINR seminar
19 Jan, 2024

SPD project at NICA (JINR, Dubna)

~300 participants from 32 institutes from 15 countries

- SPD (Spin Physics Detector) is a universal facility with the primary goal to study *unpolarized and polarized gluon content of proton and deuteron*
- SPD project was approved by PAC JINR and had its first proto-collaboration meeting in June 2019
- Conceptual Design Report (CDR) was released in January 2021, [arXiv:2102.00442]
- Official birthday of the SPD collaboration in June 2021
- Technical Design Report (TDR) v1 of SPD was released in January 2023, *http://spd.jinr.ru*

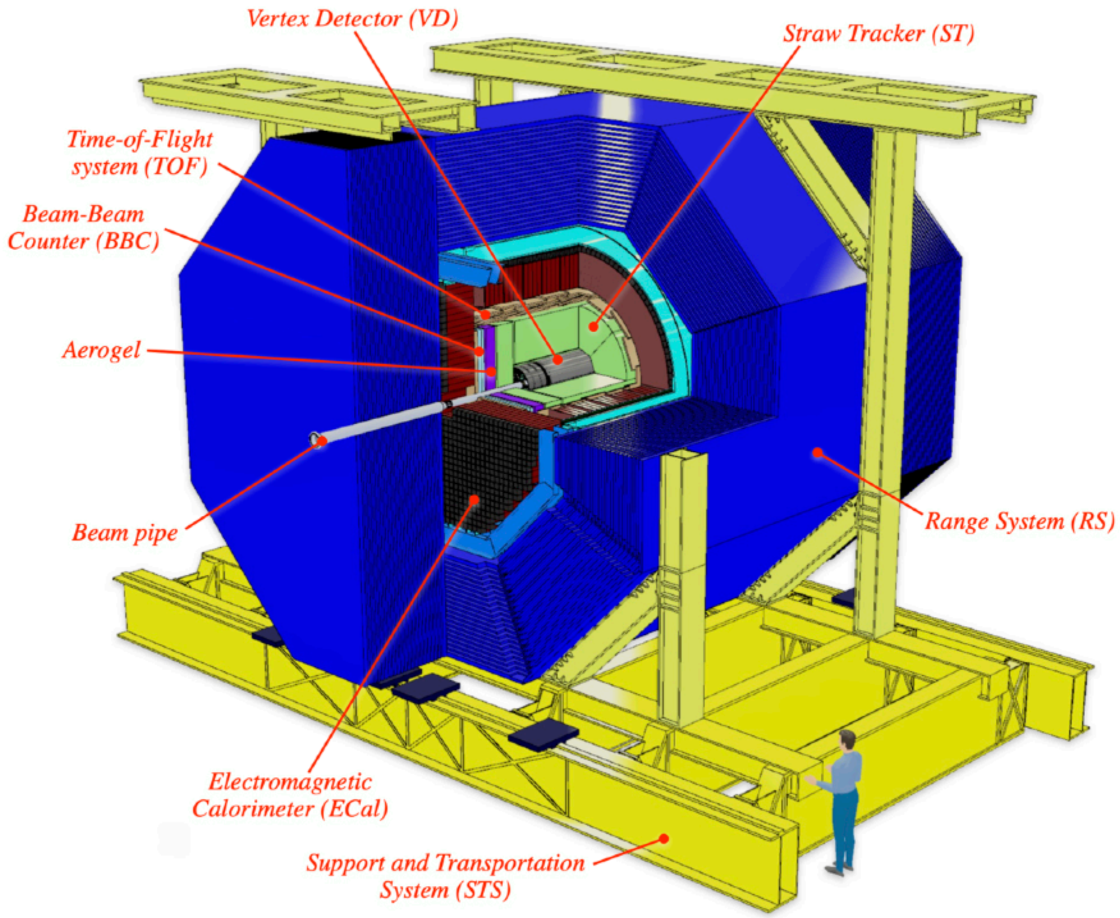

Physics program of SPD

- A.Arbuzov et al, *On the physics potential to study the gluon content of proton and deuteron at NICA SPD*, Prog.Part.Nucl.Phys. 119 (2021) 103858 [arXiv:2011.15005]
    - Probe gluon distributions in production of charmonia, open charm and prompt photons
- V.Abramov et al, *Possible studies at the first stage of the NICA collider operation with polarized and unpolarized proton and deuteron beams*, Phys.Part.Nucl. 52 (2021) 6 [arXiv:2102.08477]
    - Spin effects in elastic scattering and hyperon production, study of multiquark correlation, dibaryon resonances, exclusive reactions, open charm and charmonia near threshold, …

Accelerator complex NICA in JINR

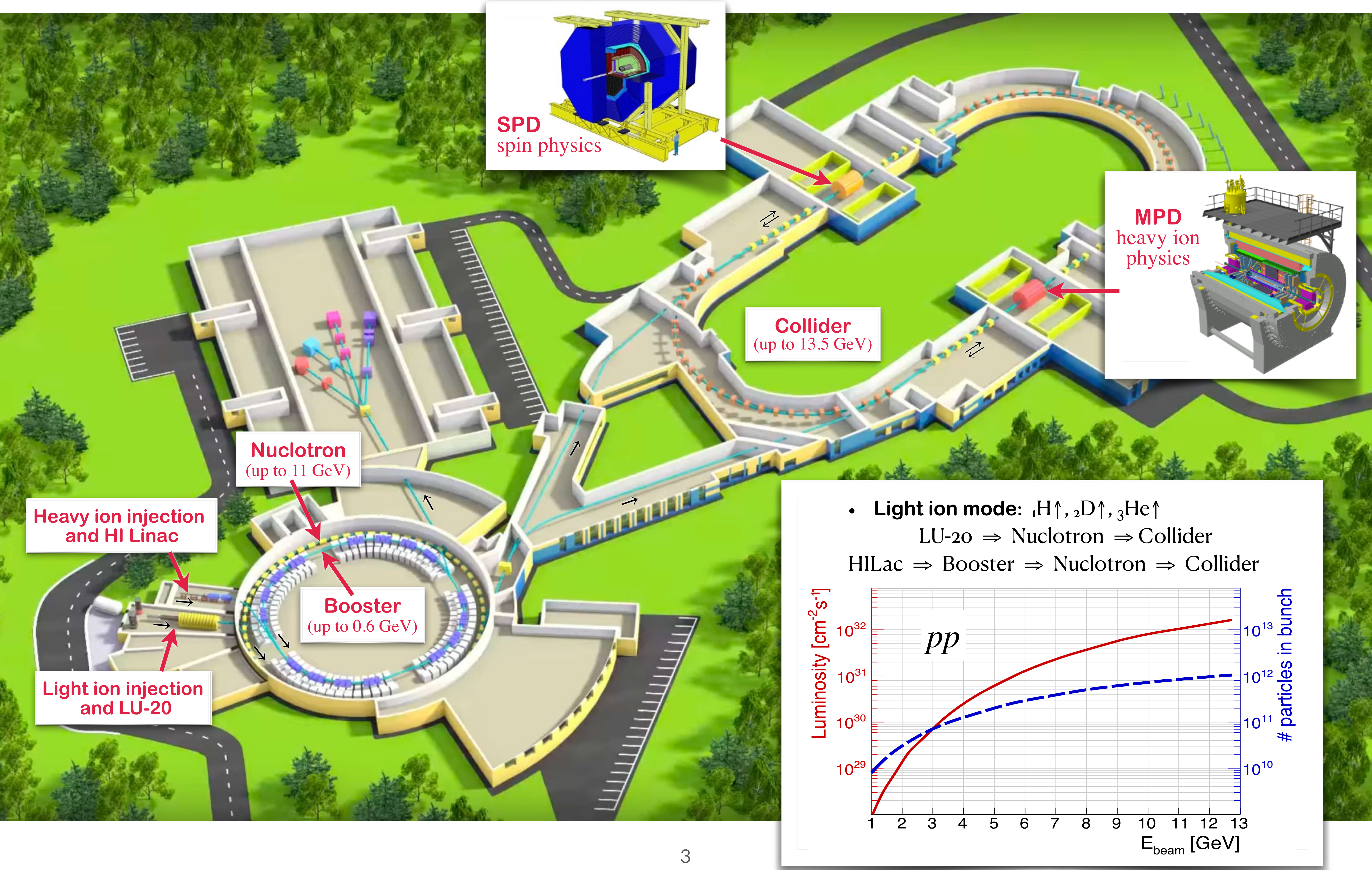

- **Light ion mode:** $_1H\uparrow$, $_2D\uparrow$, $_3He\uparrow$

LU-20 ⇒ Nuclotron ⇒ Collider

HILac ⇒ Booster ⇒ Nuclotron ⇒ Collider

SPD experimental hall in winter 2024

- The SPD hall is currently used for storing concrete blocks of biological protection and collider elements.
- The detector rail system will be installed upon arrival.
- Biological protection will be installed this year (extension of accelerator tunnel) and will remain until the construction of the SPD detector is completed.

Schematic view of the SPD setup

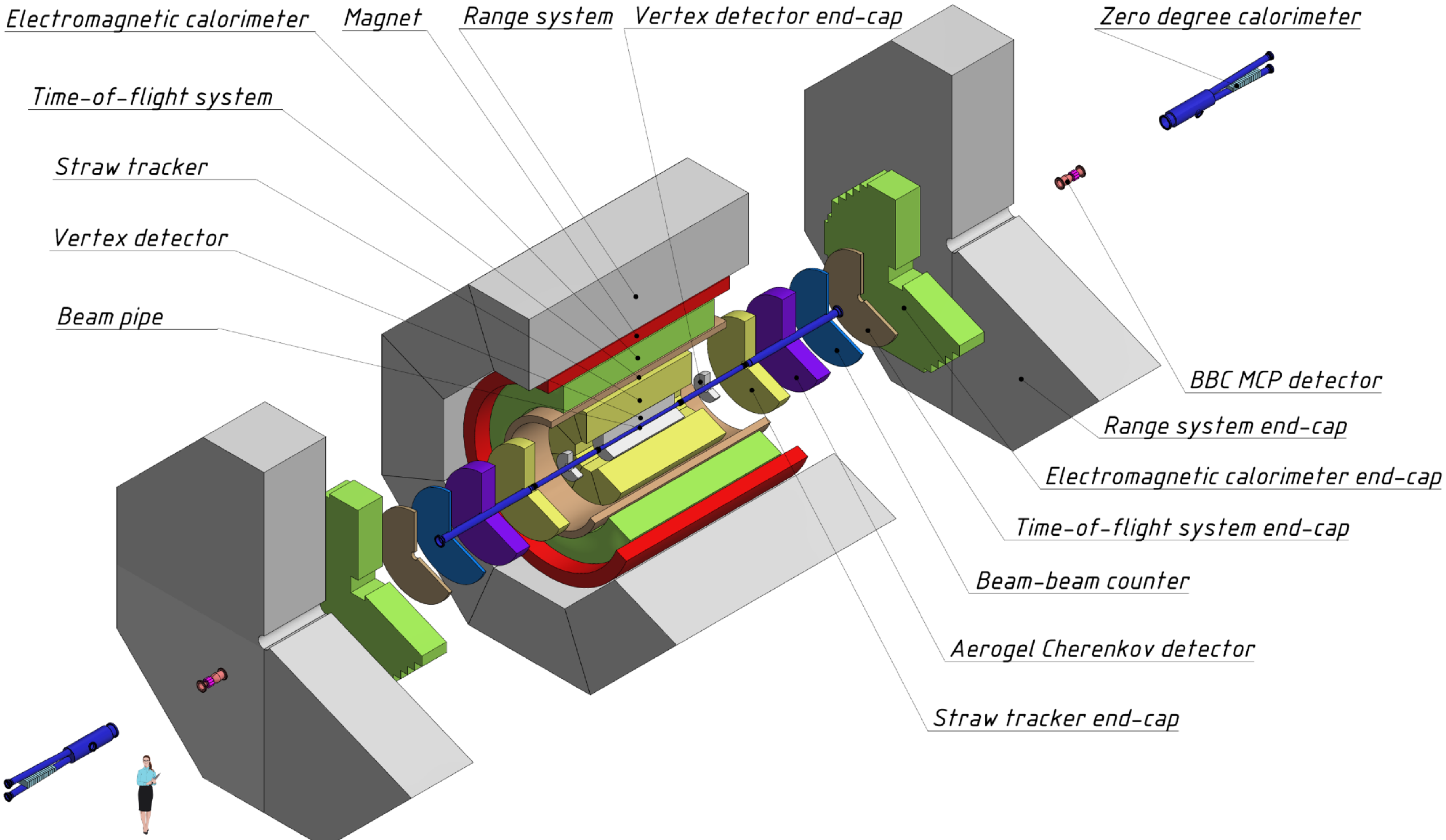

The total weight is ~1.3k tons

Detector requirements for the SSA/TMD measurement

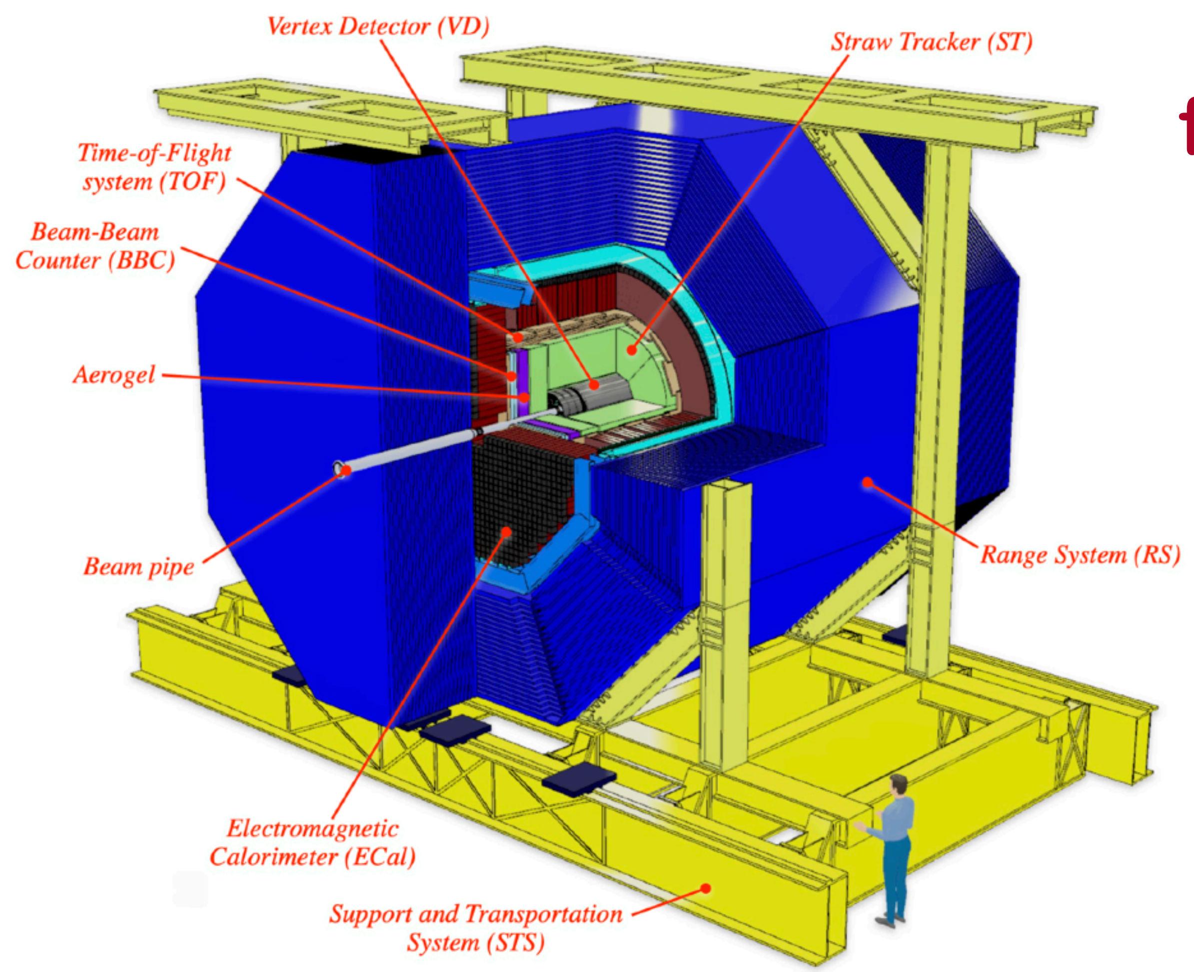

Gluon TMD: Charmonia (J/ψ) production

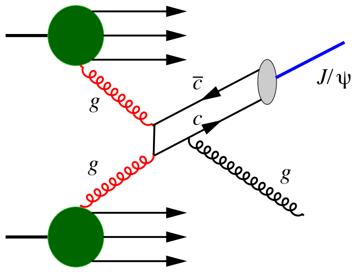

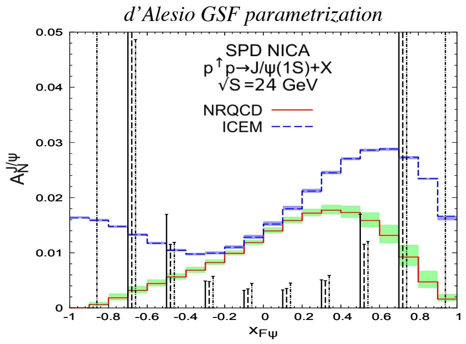

- Pair of muons from primary vertex to be identified
- **Range System** (iron interleaved by MDT detectors)
    - Thickness of $4\lambda_I$ or $4.5\lambda_I$ with ECal

Quark TMD: Light hadron π,K,p production

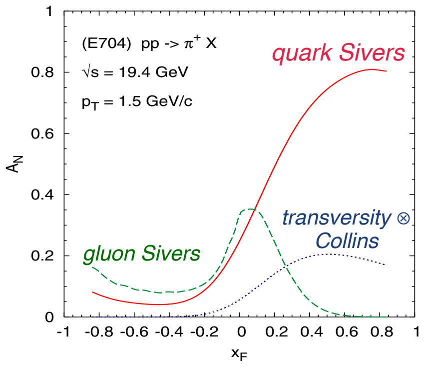

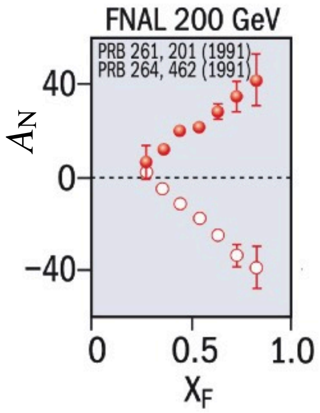

- High energy hadron identification (x_F>0.3)
- **FARICH** (Cherenkov photon detector)
    - Better than 3σ separation up to 6 GeV

Gluon TMD: Open charm ($D^{0,\pm}$) production

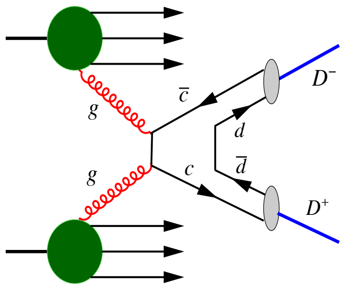

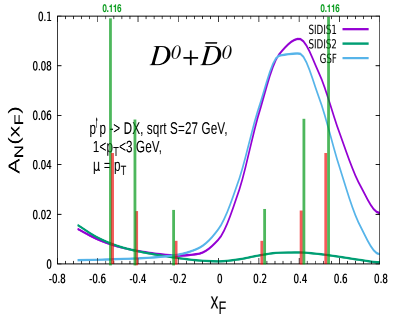

- Distinction of D-decay from primary vertex
    - Silicon detector (**DSSD** or **MAPS**)
- Identification of kaon from D-decay
    - **TOF** and **FARICH**

Gluon TMD: Prompt photon production

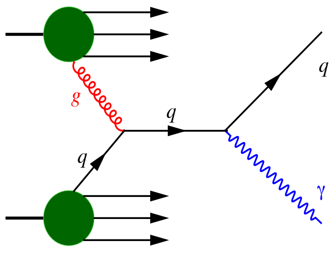

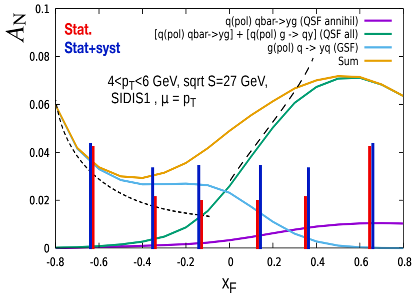

- High energy photons E>4 GeV to be detected
- **Electromagnetic calorimeter (ECal)**
    - 40 cm long cell = 200 layers of lead and scintillator
    - Thickness of $18.6X_0$

Comparison of SPD to MPD detector

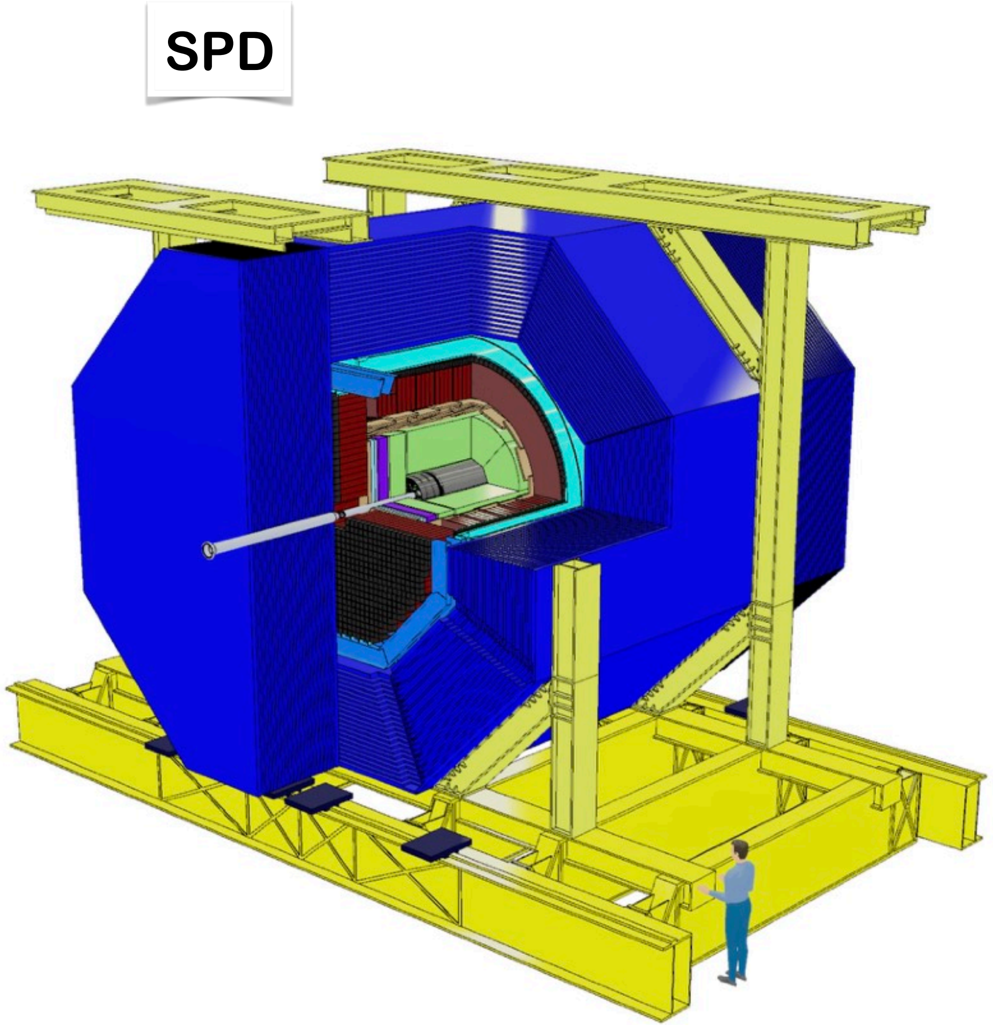

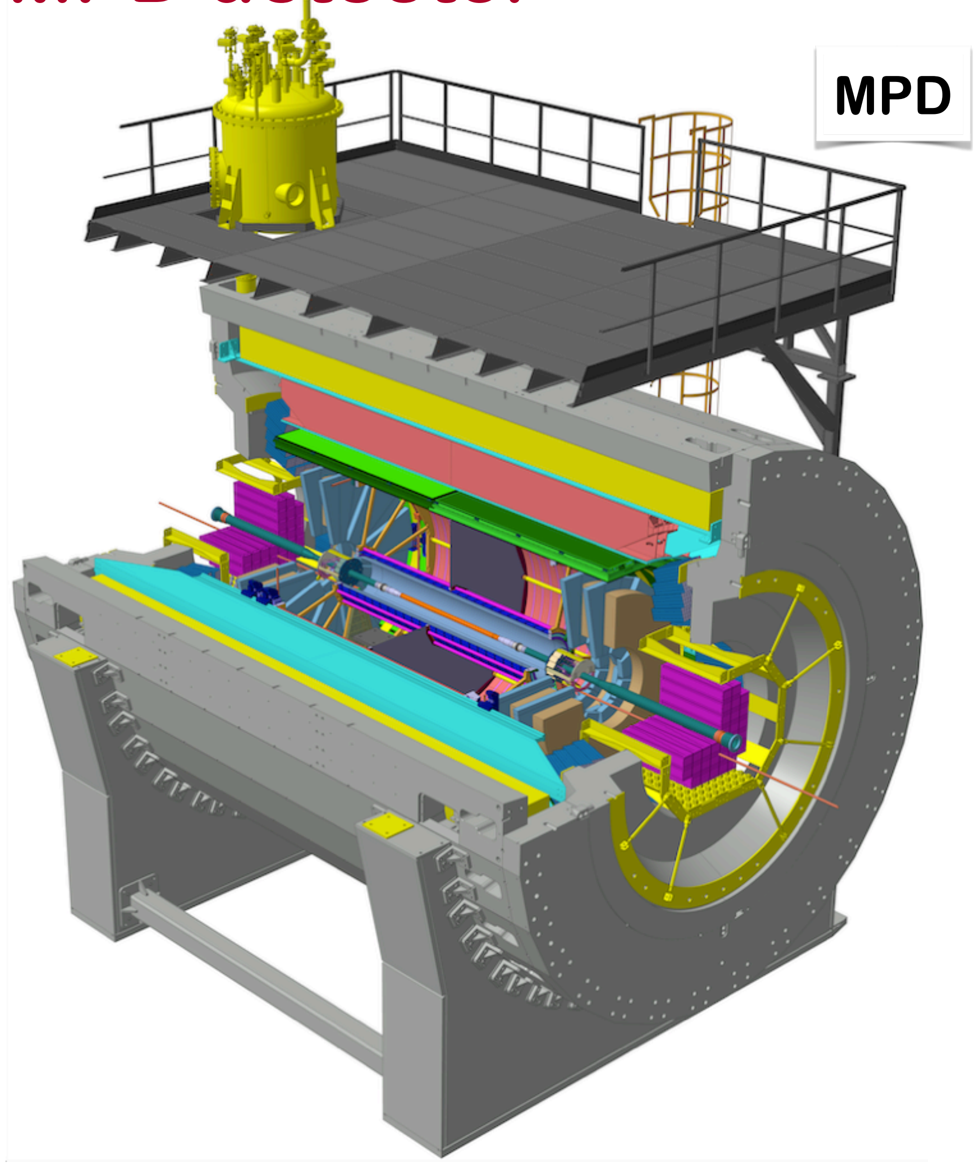

- **Event rate in SPD (~4MHz)**
  - About 250 ns between bunch interactions => Triggerless DAQ (online filter)
- **Low multiplicity events in SPD (~10 tracks)**
- **Muon detector in SPD (Range System)**
  - Physics of charmonia (J/ψ)
- **Tracking and hadron PID in SPD endcaps**
  - To measure large known asymmetry effects at small polar angles.
- **Magnetic field in SPD (1.2 T in center)**
  - To determine momentum of tracks in endcaps. Uniformity not important

E.Pyata (BINP)

Superconductive solenoid magnet

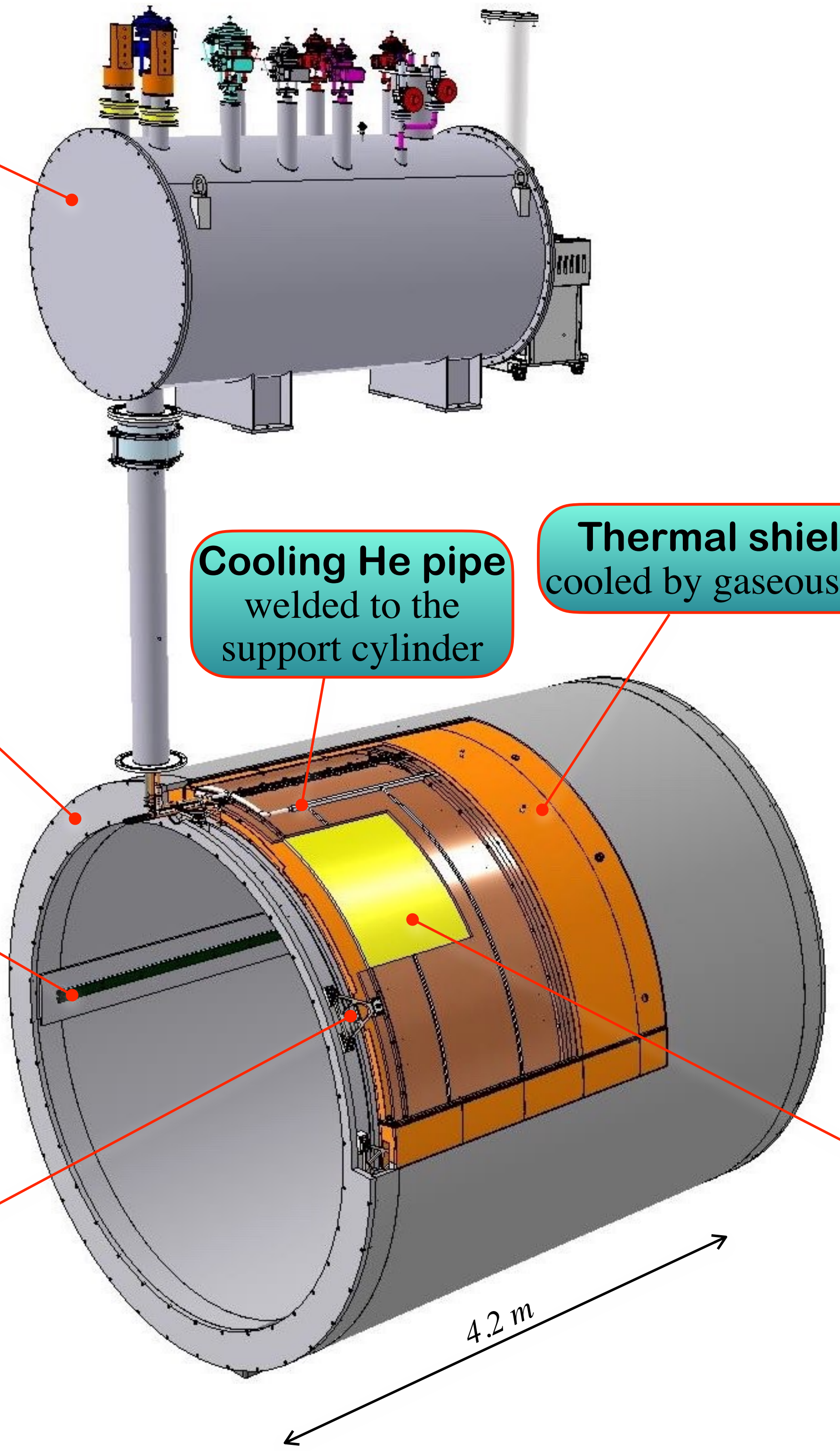

Control Dewar
The volume of the Dewar tank is enough to cool the magnet offline for about a day without an influx of helium from the outside

Steel cryostat
Outer diameter 4.01 m
Inner diameter 3.47 m
Thickness 27 cm
Length 4.2 m
Weight 22 tons

Cooling He pipe welded to the support cylinder

Thermal shield cooled by gaseous He

Linear guides used for positioning an electro-magnetic calorimeter

Triangular **supports** are used to suspend the “cold mass”.

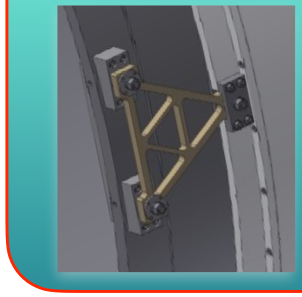

12 pieces on each side.

Made of fiberglass.

Magnetic field

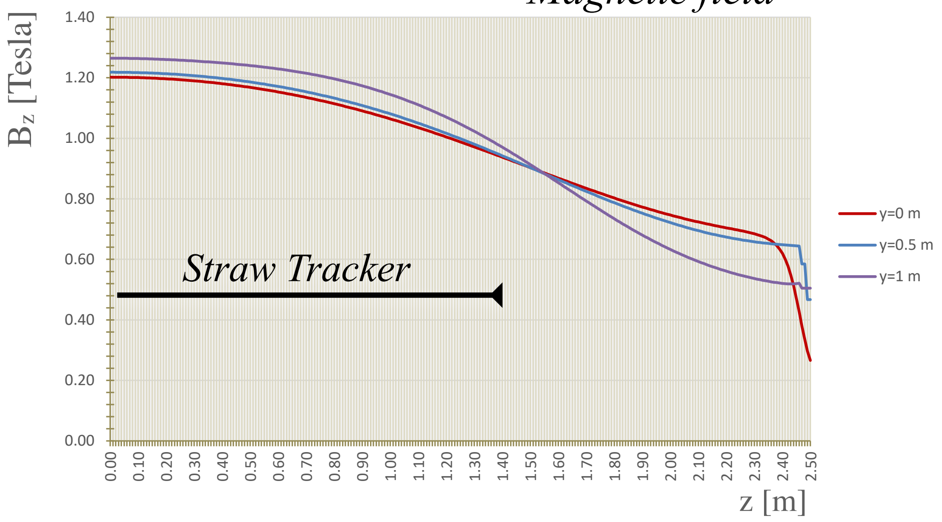

- 1.1 Tesla field with ±9% uniformity within ±1.4 m distance from center (tracking det.)
- Solenoid consists of 3 coils with 750 turns in total (two layer edge-wise winding)
  - central coil with 2×75=150 turns
  - 2 side coils with 2×150=300 turns
- The use of the *thermosyphon method* for cooling the superconducting coils (natural convection of two-phase helium at 4.5K)
- It will be constructed in BINP Novosibirsk

Rutherford-type cable made of 8-strands NbTi/Cu superconductor. The cable will be encased in an aluminum stabilizer using a co-extrusion process that provides a good bond between aluminum and superconductor in order to ensure quench protection during operation.

Cryostats of superconducting magnets of HEP experiments

∅ - outer diameter
ΔR - thickness
L - length
B - magnetic field

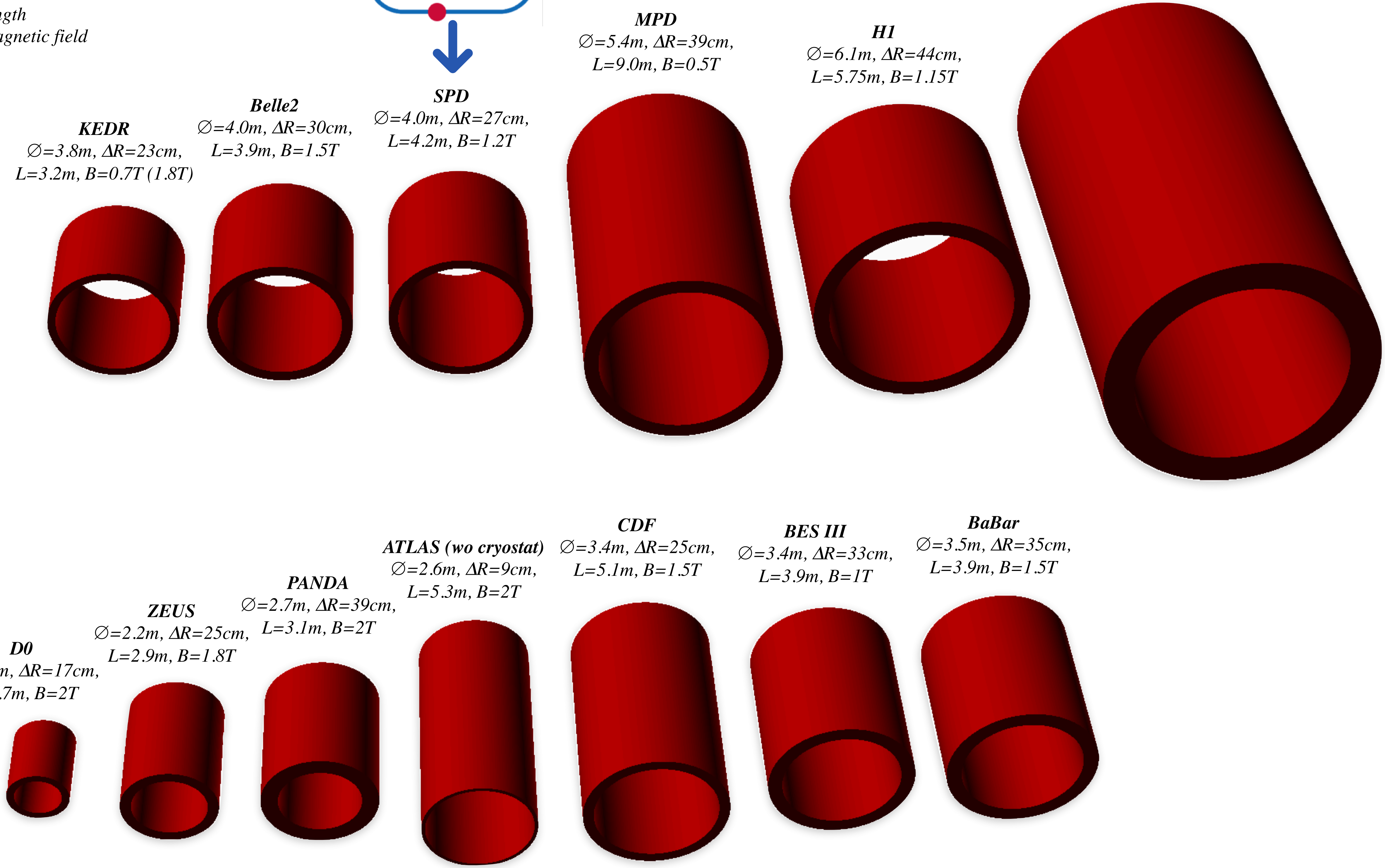

KEDR
∅=3.8m, ΔR=23cm, L=3.2m, B=0.7T (1.8T)

Belle2
∅=4.0m, ΔR=30cm, L=3.9m, B=1.5T

SPD
∅=4.0m, ΔR=27cm, L=4.2m, B=1.2T

MPD
∅=5.4m, ΔR=39cm, L=9.0m, B=0.5T

H1
∅=6.1m, ΔR=44cm, L=5.75m, B=1.15T

CMS
∅=7.6m, ΔR=85cm, L=12.9m, B=4T

D0
∅=1.4m, ΔR=17cm, L=1.7m, B=2T

ZEUS
∅=2.2m, ΔR=25cm, L=2.9m, B=1.8T

PANDA
∅=2.7m, ΔR=39cm, L=3.1m, B=2T

ATLAS (wo cryostat)
∅=2.6m, ΔR=9cm, L=5.3m, B=2T

CDF
∅=3.4m, ΔR=25cm, L=5.1m, B=1.5T

BES III
∅=3.4m, ΔR=33cm, L=3.9m, B=1T

BaBar
∅=3.5m, ΔR=35cm, L=3.9m, B=1.5T

Helium system

	Operating parameters	Unit
1	Cooling capacity (for 4.5 K)	100 - 130 l/h
	Cooling capacity (for 50 K)	150 W
2	Temperature of outlet flow	4.3 K (1.05 bar)
3	Temperature of inlet flow	4.5 K (1.15 bar)
4	Hydraulic resistance of the SC coil	0.1 bar
5	Cold weight	4000 kg
6	Maximum pressure in pipe	5 MPa
7	Heat load	60 – 80 W

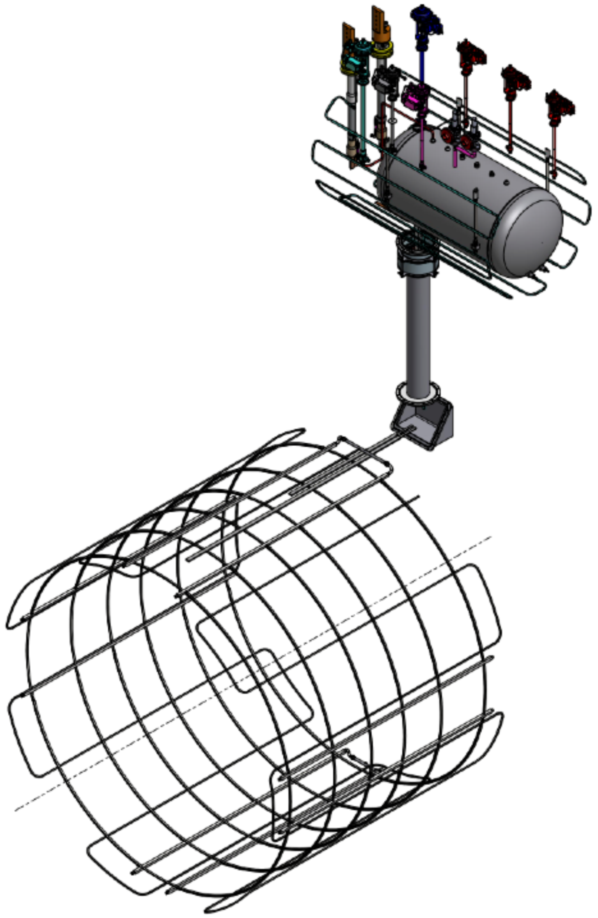

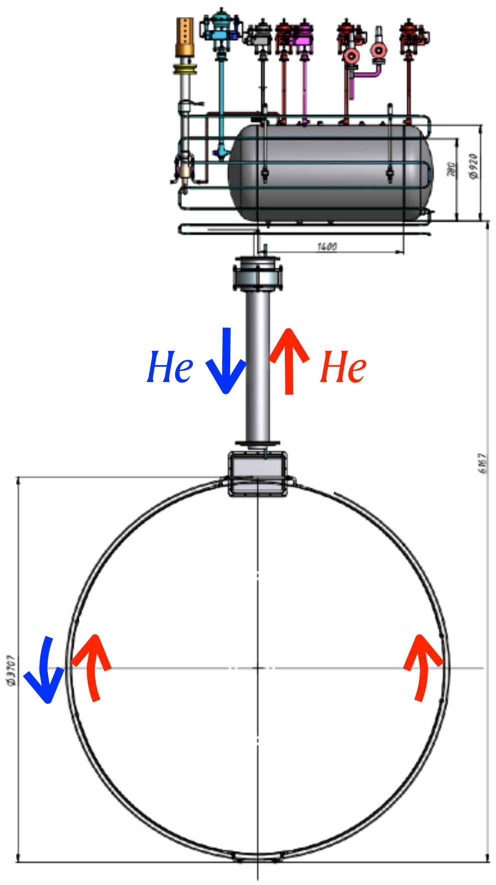

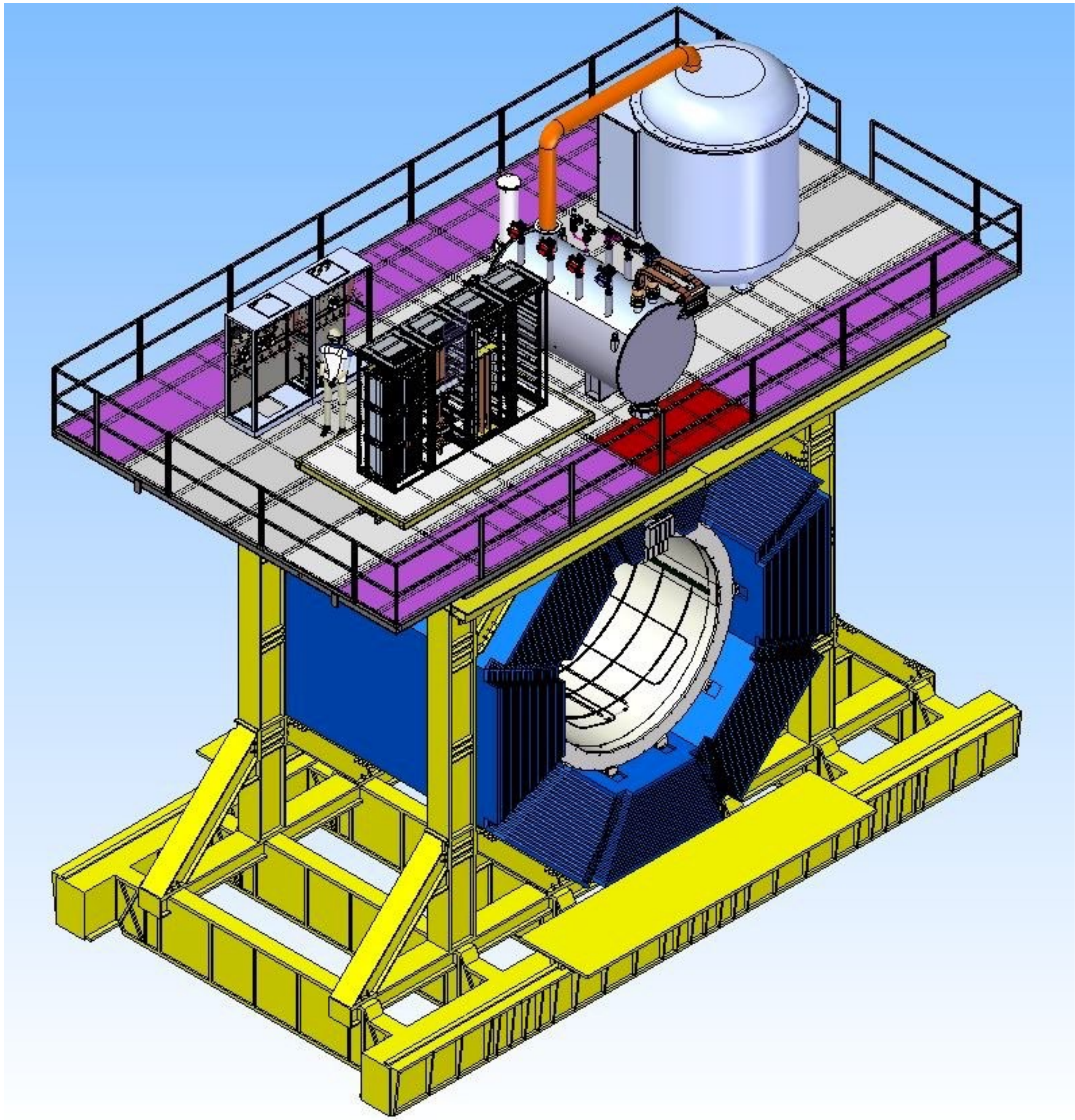

D.Nikiforov

Cryogenic system

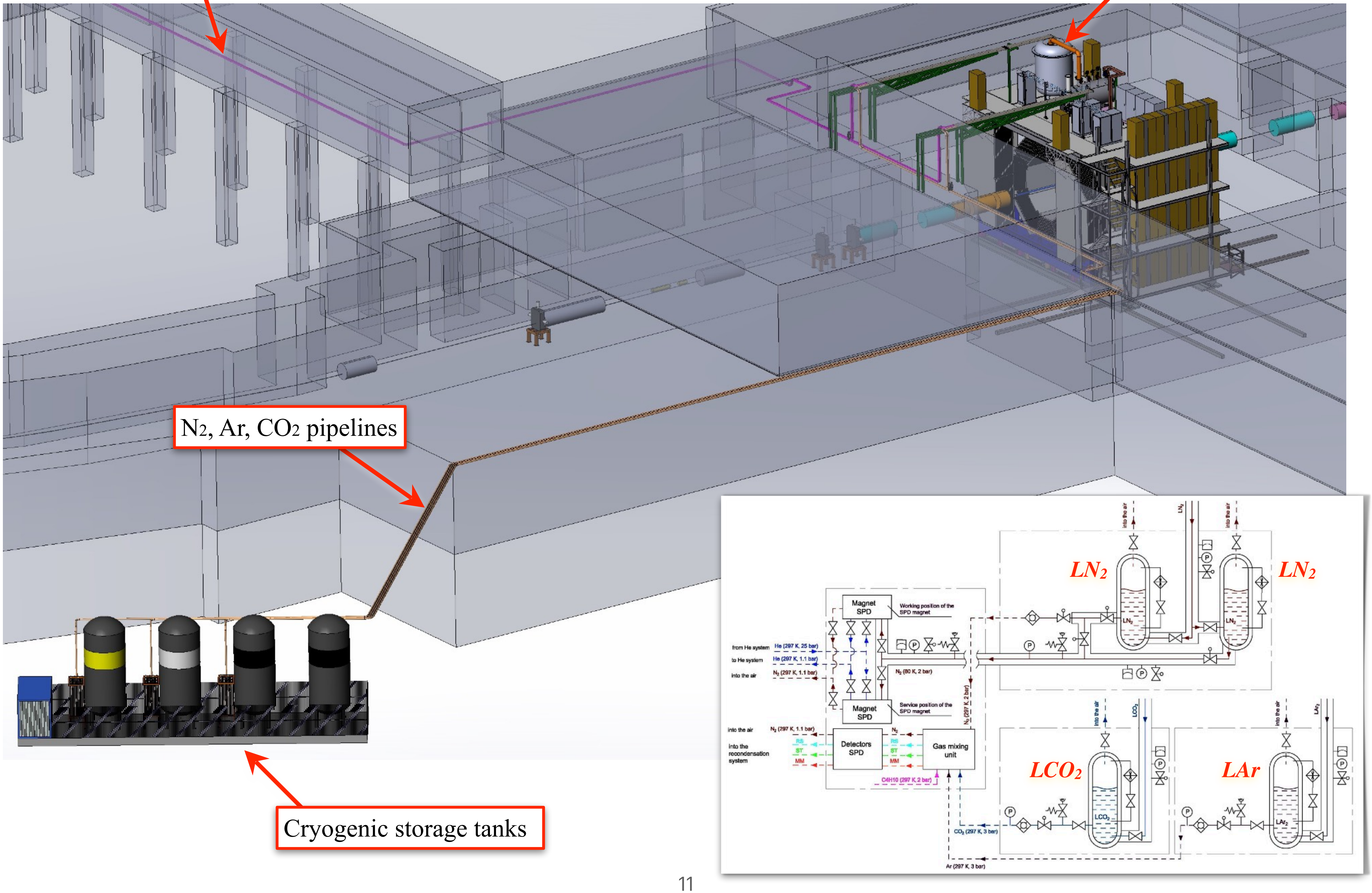

Helium pipelines

Helium liquefier

N_2, Ar, CO_2 pipelines

Cryogenic storage tanks

G.Alexeev,
A.Samartsev

Range System (RS)

- Purposes: μ identification, rough hadron calorimetry, iron return yoke of the magnet, mechanical support structure of the overall detector
- 20 layers of Fe (3-6 cm) interleaved with gaps for Mini Drift Tube (MDT) detectors
- The endcaps must withstand the ~100 tonne magnetic force
- Total mass ~1000 tons, at least $4\lambda_I$
- The design will follow closely the one of PANDA
- MDT provide 2 coordinate readout (~100 kch)
    - Al extruded comb-like 8-cell profile with anode wires + external electrodes (strips) perpendicular to the wires

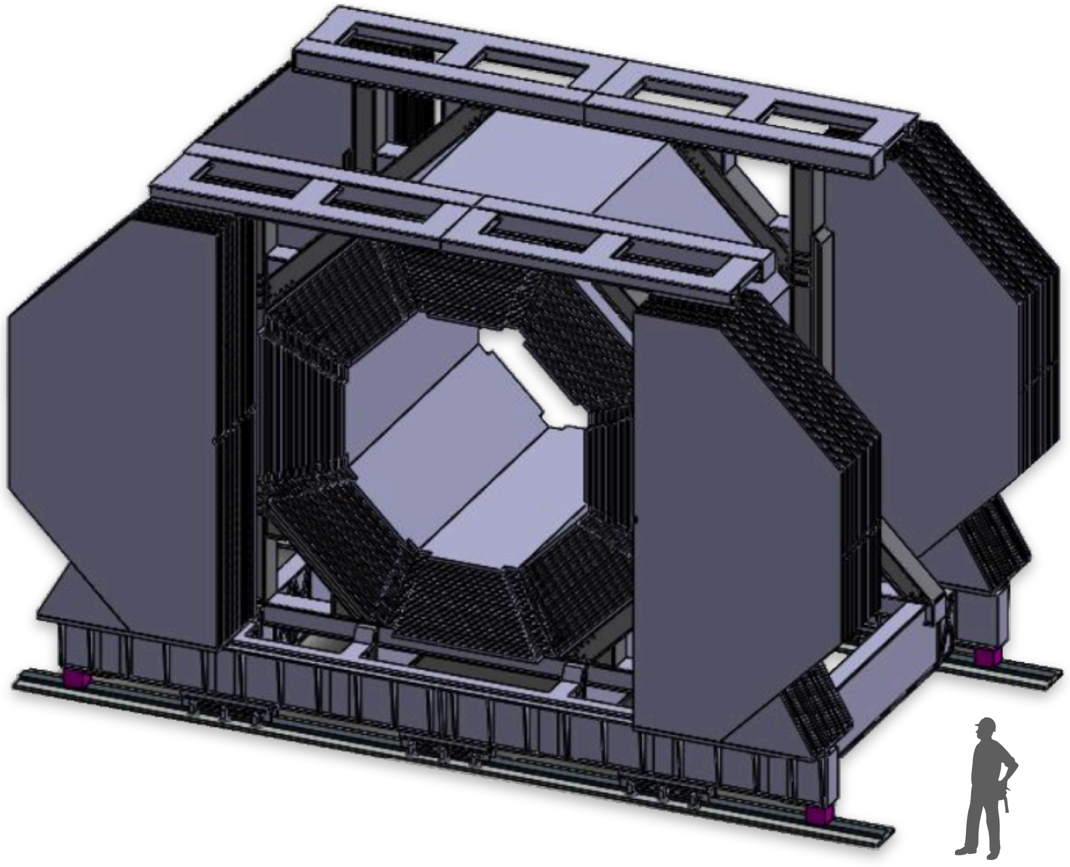

Results of beam tests of RS prototype (10 ton, 4k ch)

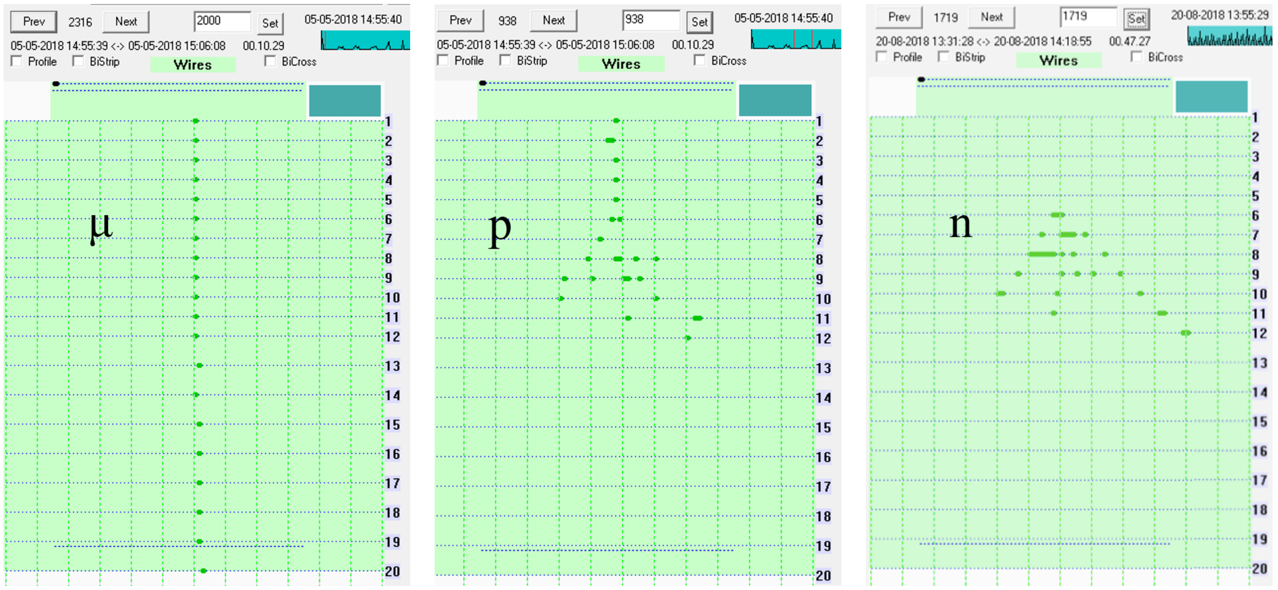

Mini Drift Tubes (MTD)

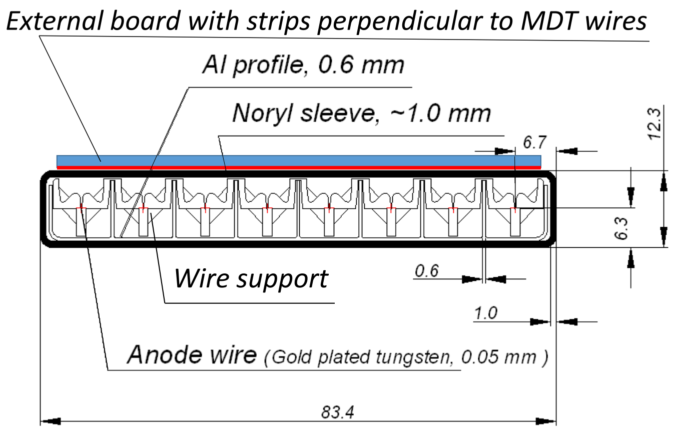

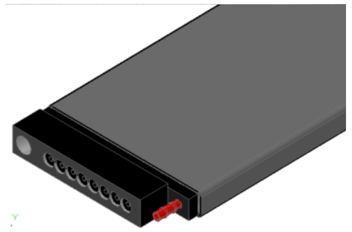

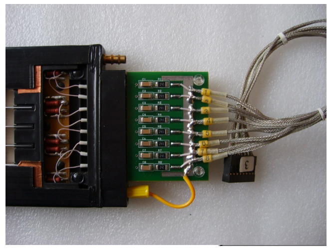

Electromagnetic Calorimeter (ECal)

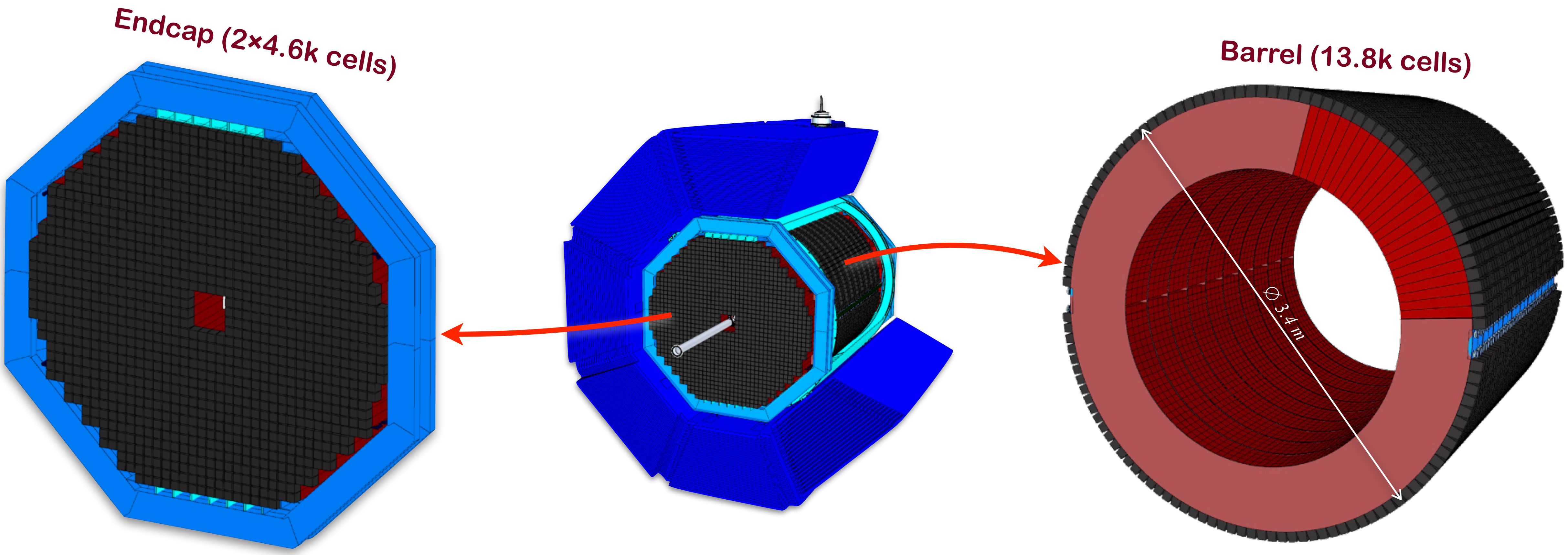

- Purpose: detection of prompt photons and photons from π^0, η and χ_c decays
- Identification of electrons and positrons
- Number of radiation lengths $18.6X_0$
- Total weight is 40t (barrel) + 28t (endcap) = 68t
- Total number of channels is ~23k
- Energy resolution is ~$5\% / \sqrt{E}$
- Low energy threshold is ~50 MeV
- Time resolution is ~0.5 ns

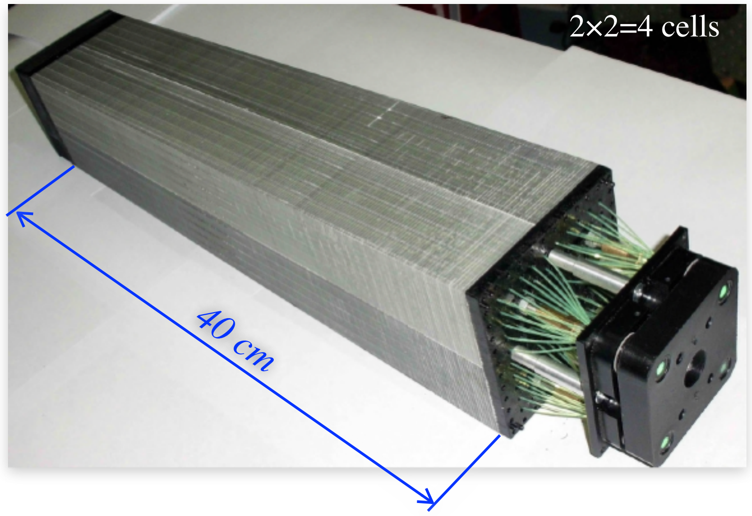

- 200 layers of lead (0.5 mm) and scintillator (1.5mm)
- 36 fibers of one cell transmit light to 6×6 mm² SiPM
- Moliere radius is ~2.4 cm

Test results with cosmic particles

Setup of 4 modules

- Each module consist of 9 cells of 4x4 cm^2
- All 36 cells were fully tested

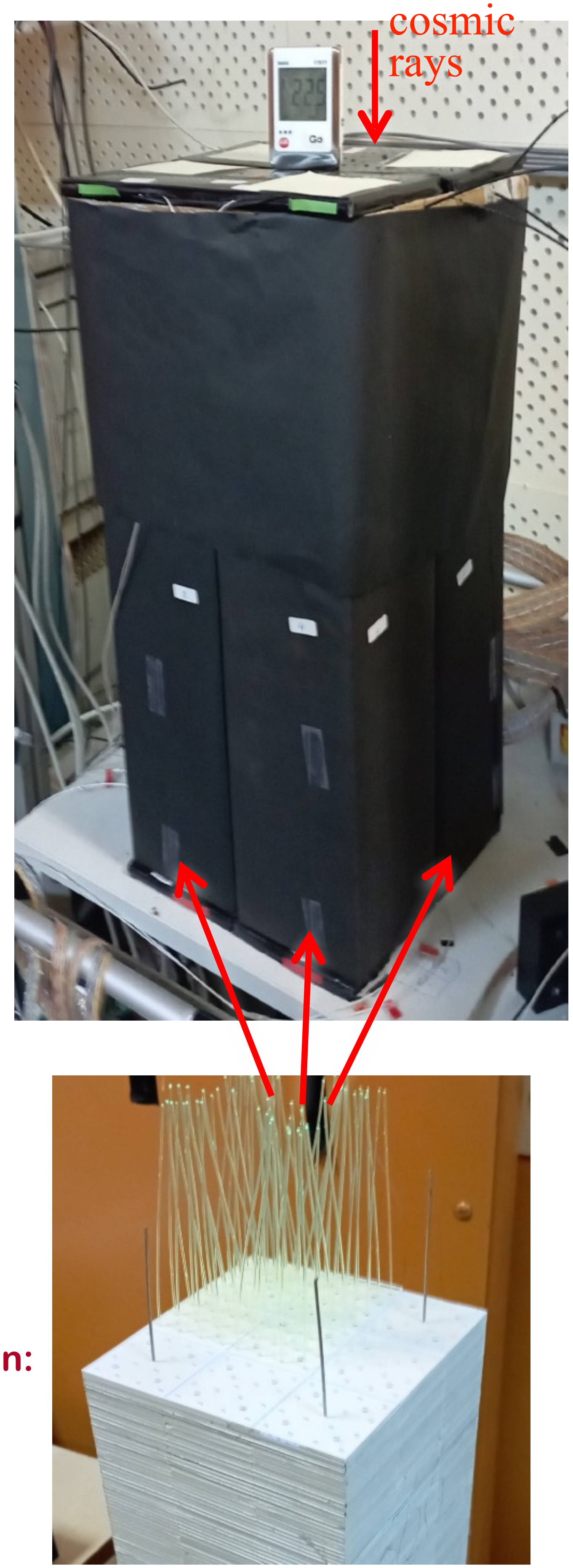

Cell assembled of:

- 1.5 mm Scintillator
- 0.3 mm Lead
- 200 layers

Scintillator composition:

- Polysterene
- 1.5% Paterphenyle
- 0.05% POPOP

- Light detection by new NDL SiPm Series EQR15 (intrinsic epitaxial layer as a quenching resistor (EQR))
- For now, old modules with a cross section of 4×4 cm^2, left over from MPD production, are being used
- A matrix form for new scintillator production (40×40×1.5 mm^3) was ordered. A 4-set mold will produce 4 scintillator plate per minute.
- The relative energy resolution for MIP: dE/E=9.6% which corresponds to 240 MeV of electron signal and consistent with MC prediction
  - Spectra of all 36 cells were tested and give consistent results.

Sum ECAL Energy

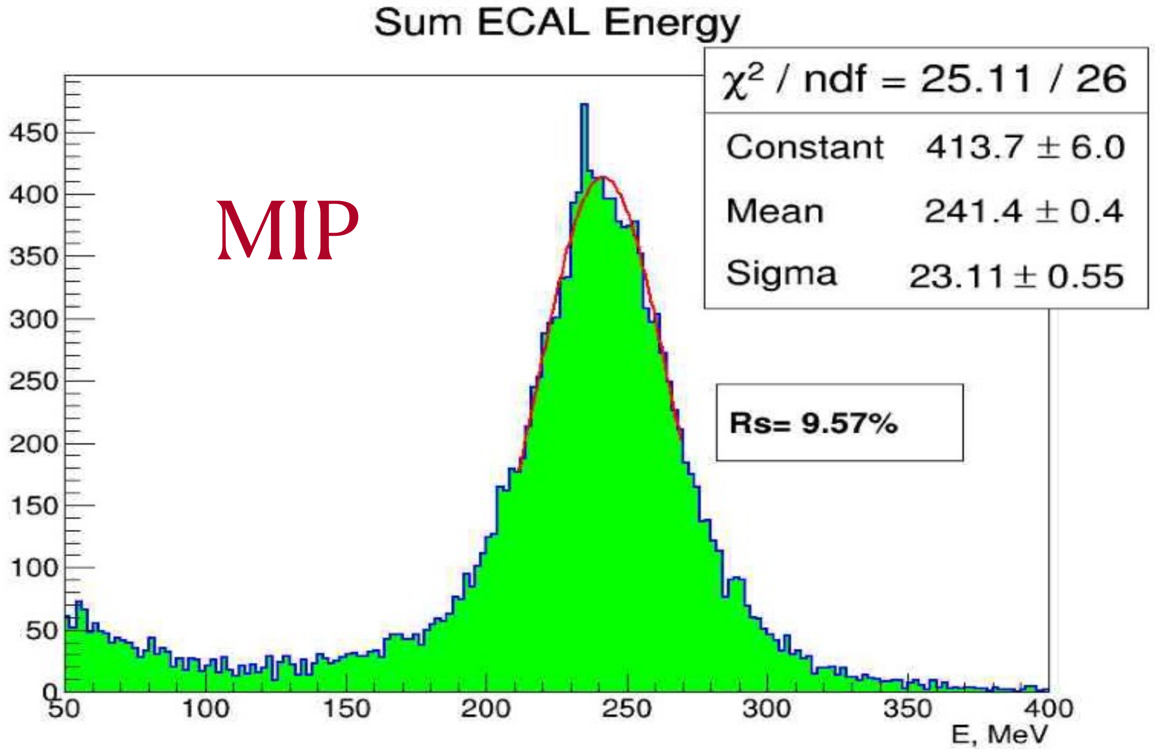

Detectors inside ECal (tracking + PID)

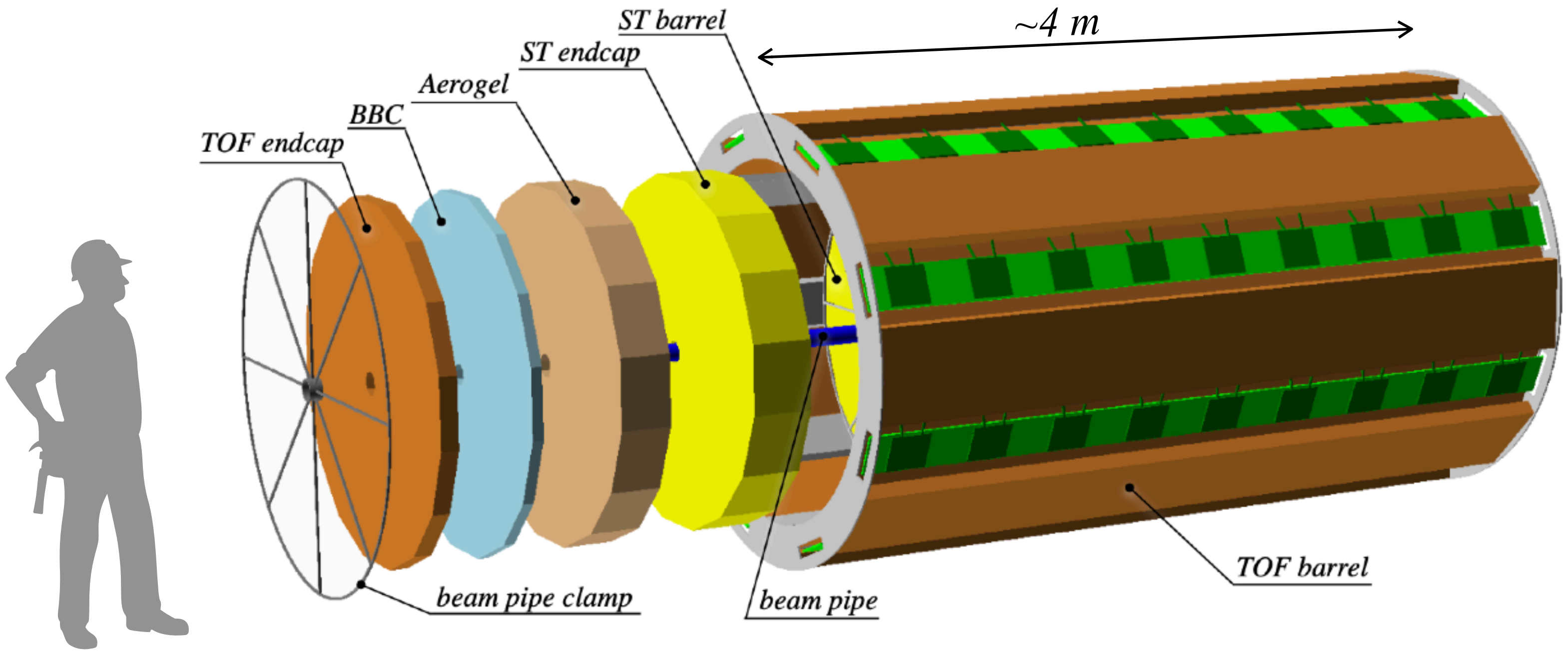

- All endcaps are loaded one-by-one presumably by hand
- No need to divide the endcap detectors into two halves

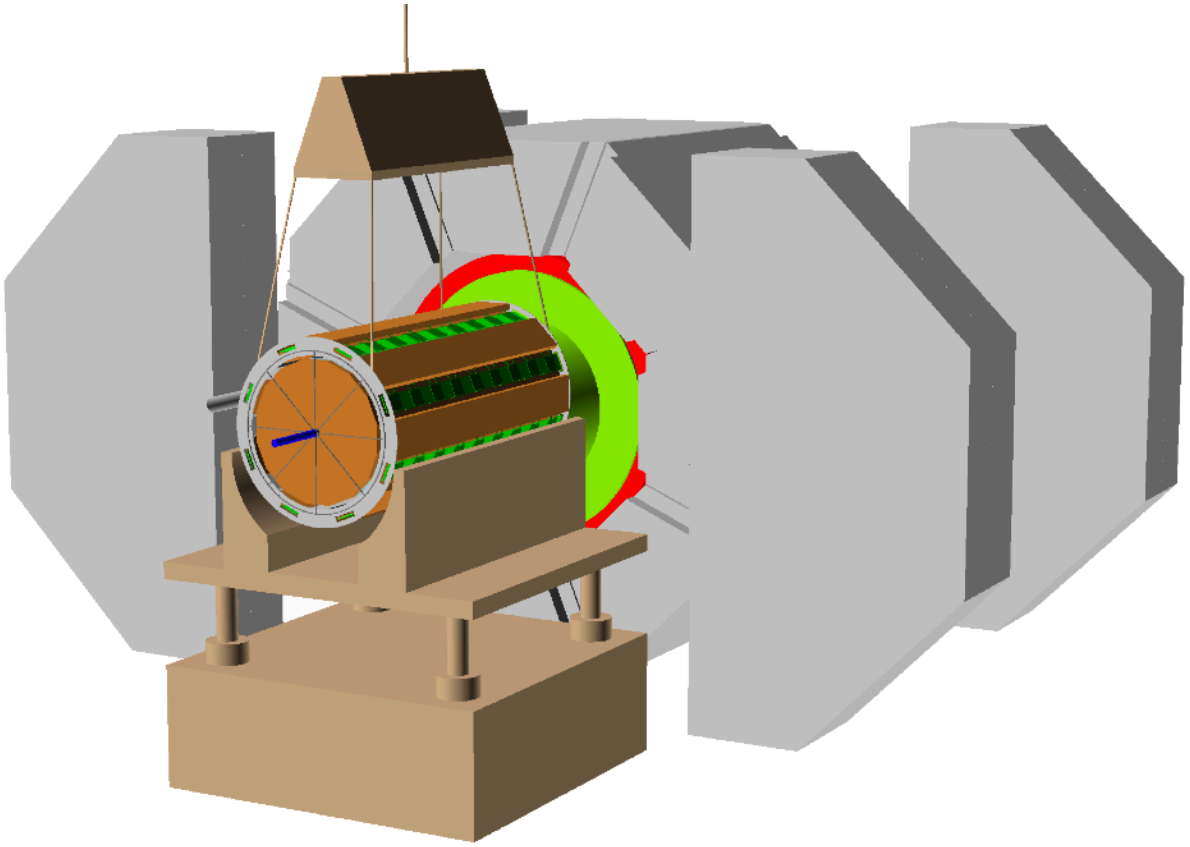

For the case when **assembling will not be allowed** in the experimental hall due to MPD runs, it can be done outside the aria.

T.Enik

Barrel of Straw Tracker (ST)

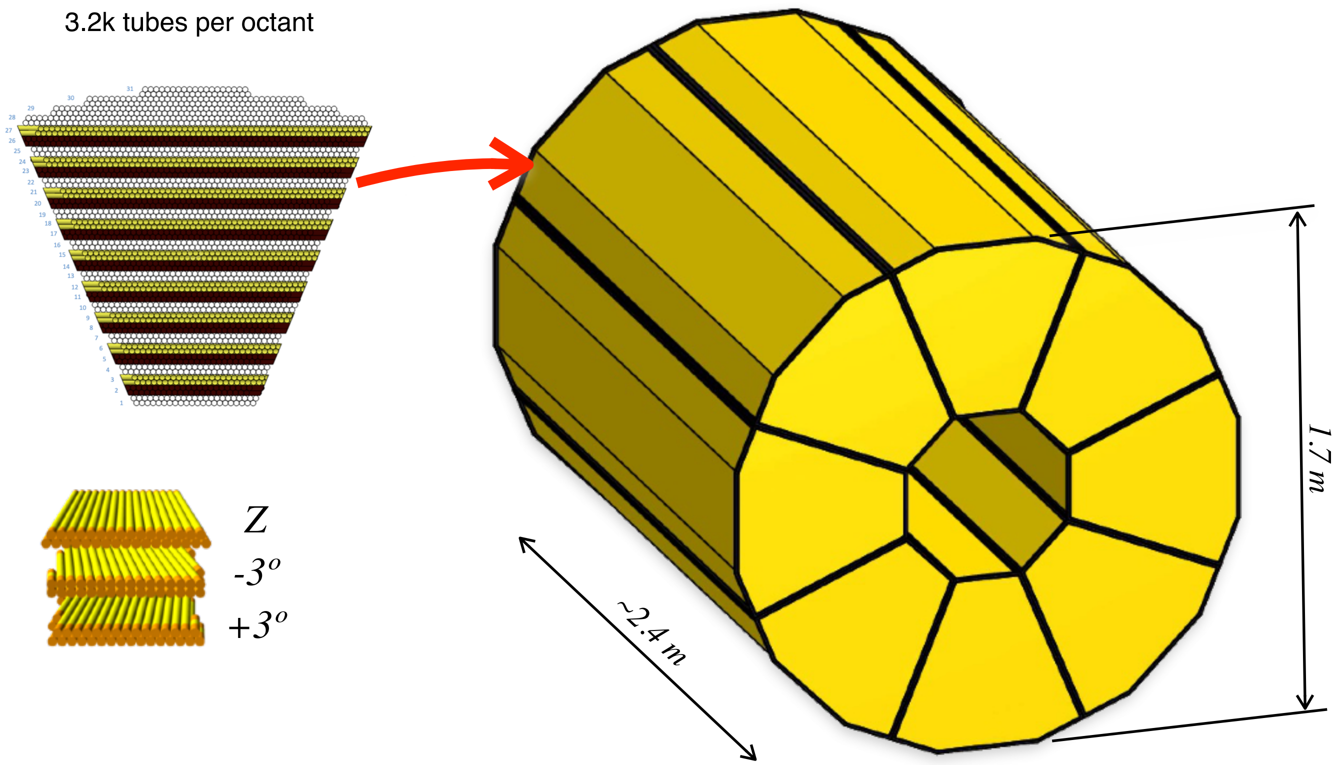

- Main tracker system of SPD
- Barrel is made of 8 modules with 30 double-layers oriented as *z,+3°,-3°*
- Maximum drift time of 120 ns for ∅=10mm straw
- Straw tubes are made of a PET foil that is ultrasonic welded to form a tube
- Spatial resolution of 150 μm
- Expected DAQ rate up to several hundred MHz/tube (electronics is limiting factor)
- Number of readout channels ~26k
- Extensive experience in straw production in JINR for several experiments: ATLAS, NA58, NA62, NA64; prototypes for: COZY-TOF, CREAM, SHiP, COMET, DUNE.

Energy loss in straw tubes

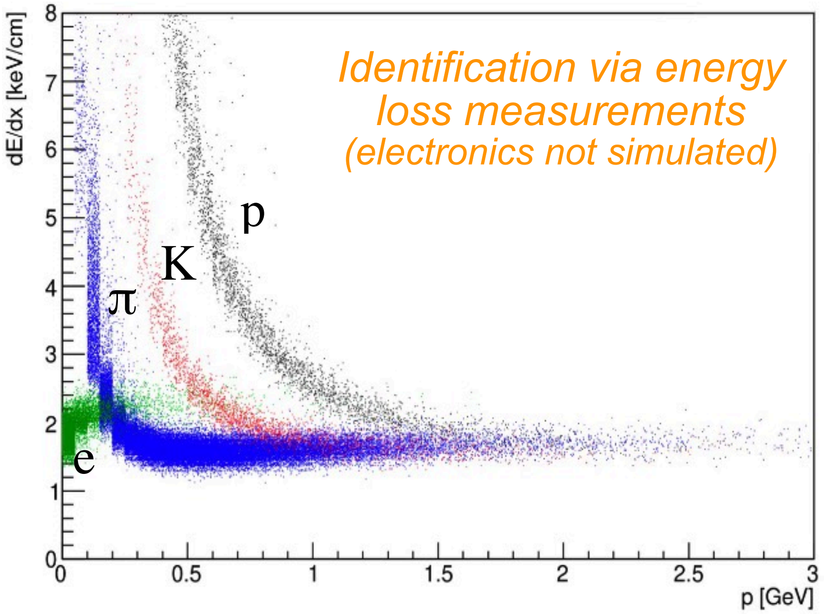

σ_p/p (μ, θ=90°)

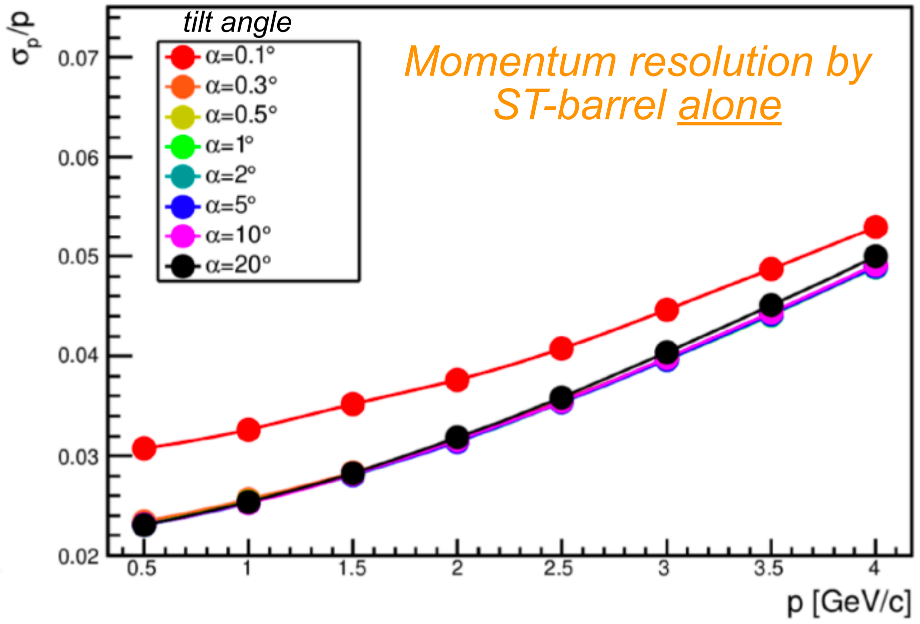

straw production for NA62 (~2010)

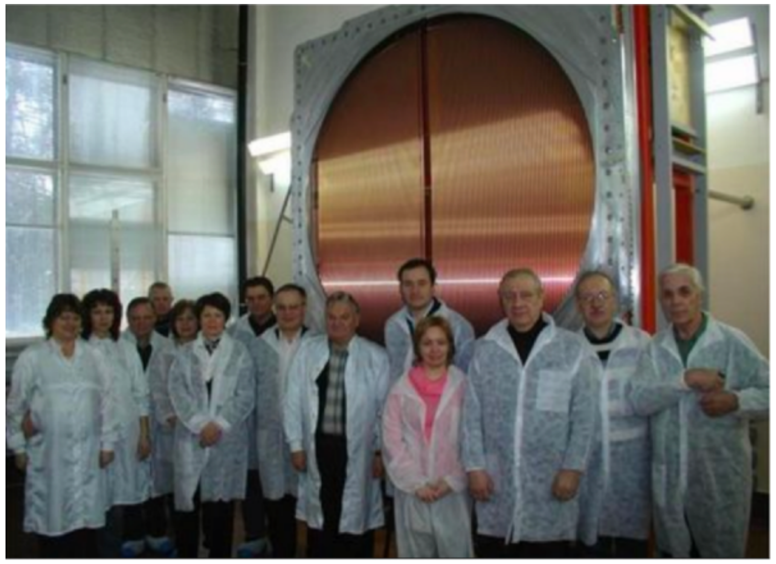

CRISM
Khotkovo

Power frame for the Straw-barrel

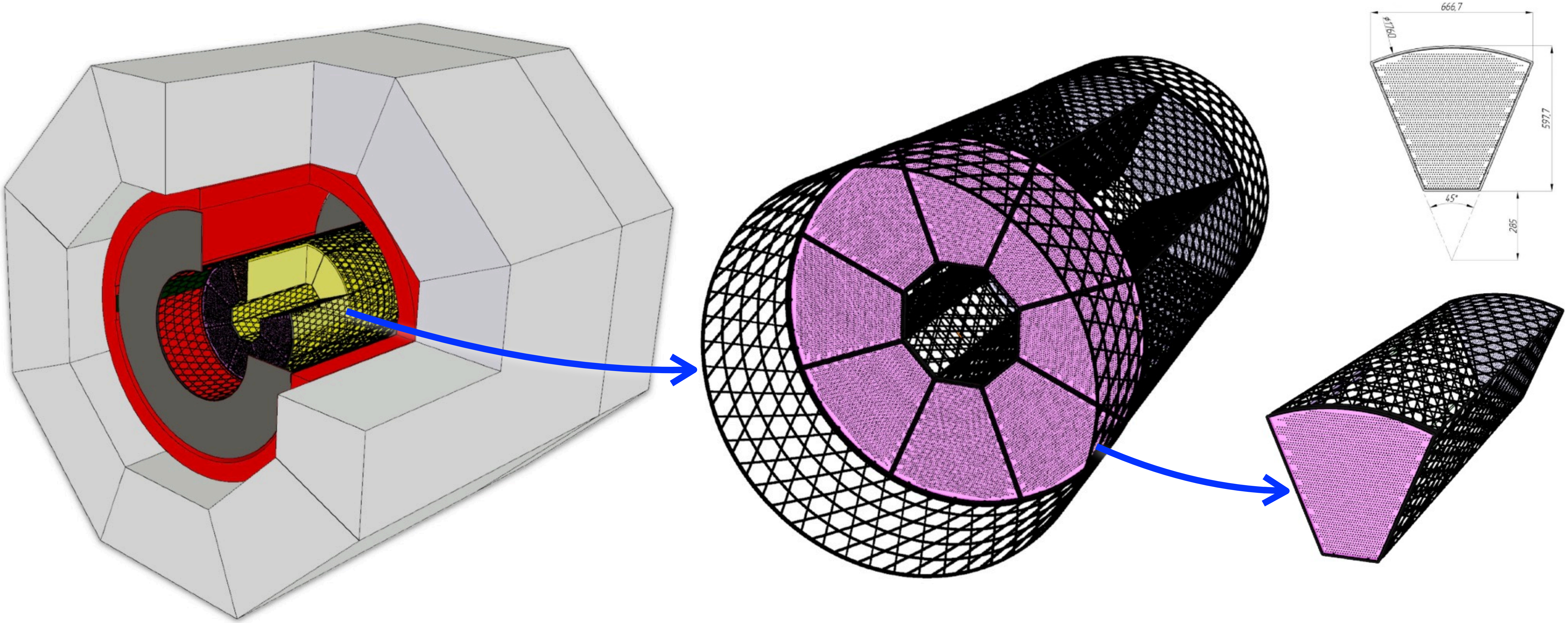

- Contract for the preparation of the conceptual design of the power frame was signed with CRISM earlier this year
- Engineers of CRISM were in charge for the development and production of the ECal power frame in MPD
- The frame will be made of carbon fiber composite material UMT49-12K-EP (Rosatom)
- A preliminary design, which takes into account all the tolerances imposed by the Technical Assignment, was prepared

Endcap of Straw Tracker (ST)

G.Kekelidze
V.Kramorenko

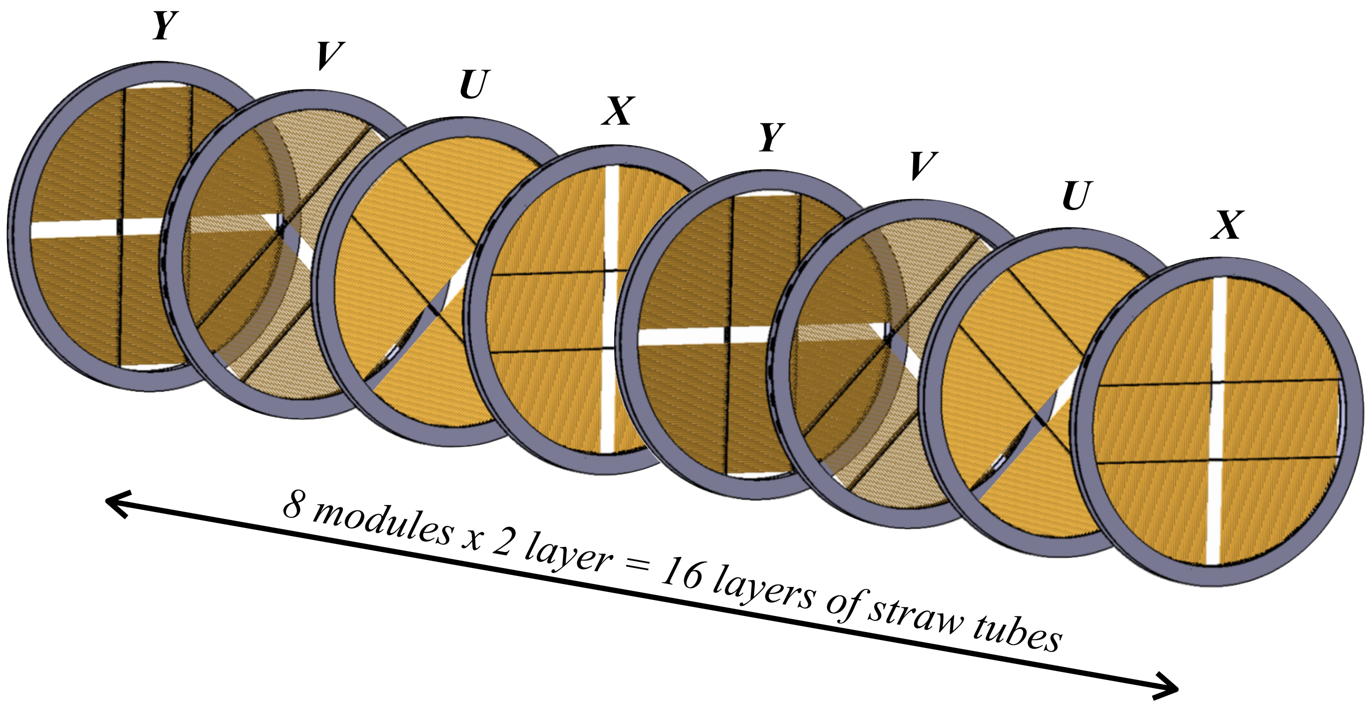

- One ST endcap contains 8 modules: *X, +45º, -45º, Y*
- One module contains 288 tubes in total, which are arranged in two layers shifted by half a tube
- Total number of tubes in two endcaps is

  288 tubes × 16 modules × 2 endcaps = 9216 tubes
- The thickness of one module is 30 mm
- Eight coordinate planes are mounted together on a rigid flat table to form a 240 mm thick rigid block
- One straw is made by winding two ”kapton” tapes forming a tube with ∅ = 9.56 mm

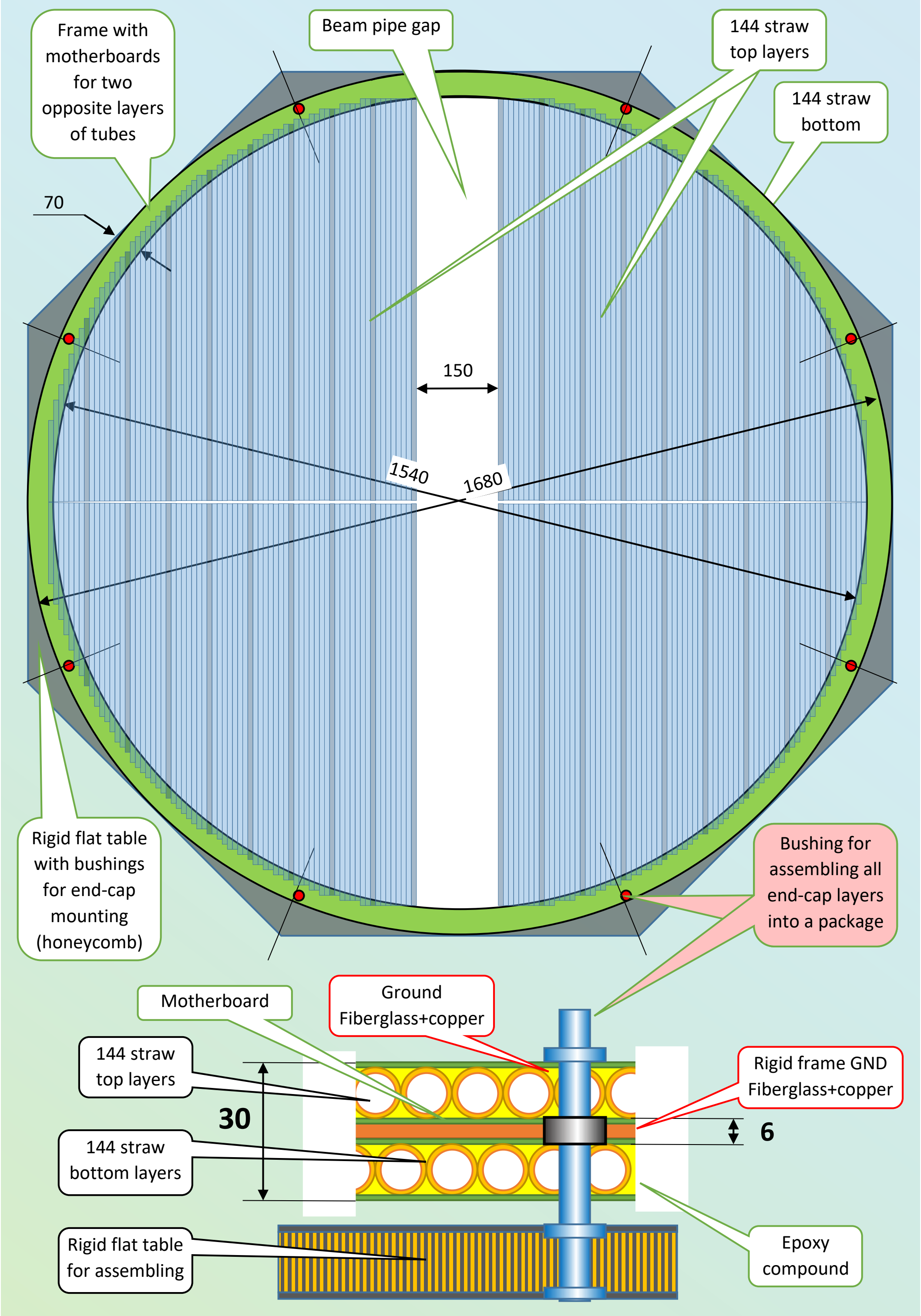

Progress on Straw-endcap prototype

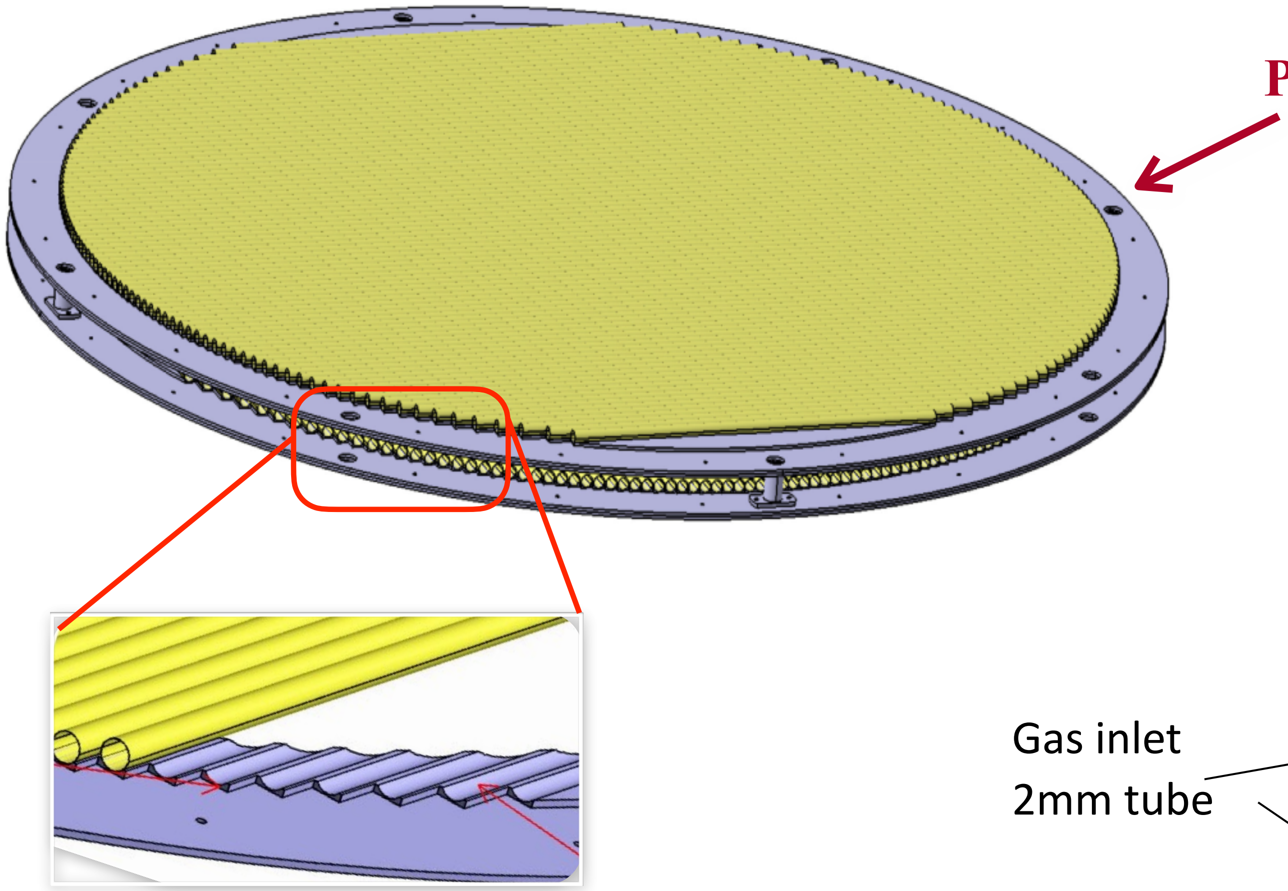

Prototype of ∅=1m with two layers of tubes rotated 90 degrees relative to each other

End-plugs for ∅=9.54 mm tubes were designed and a 400 of them were manufactured using a 3D printer

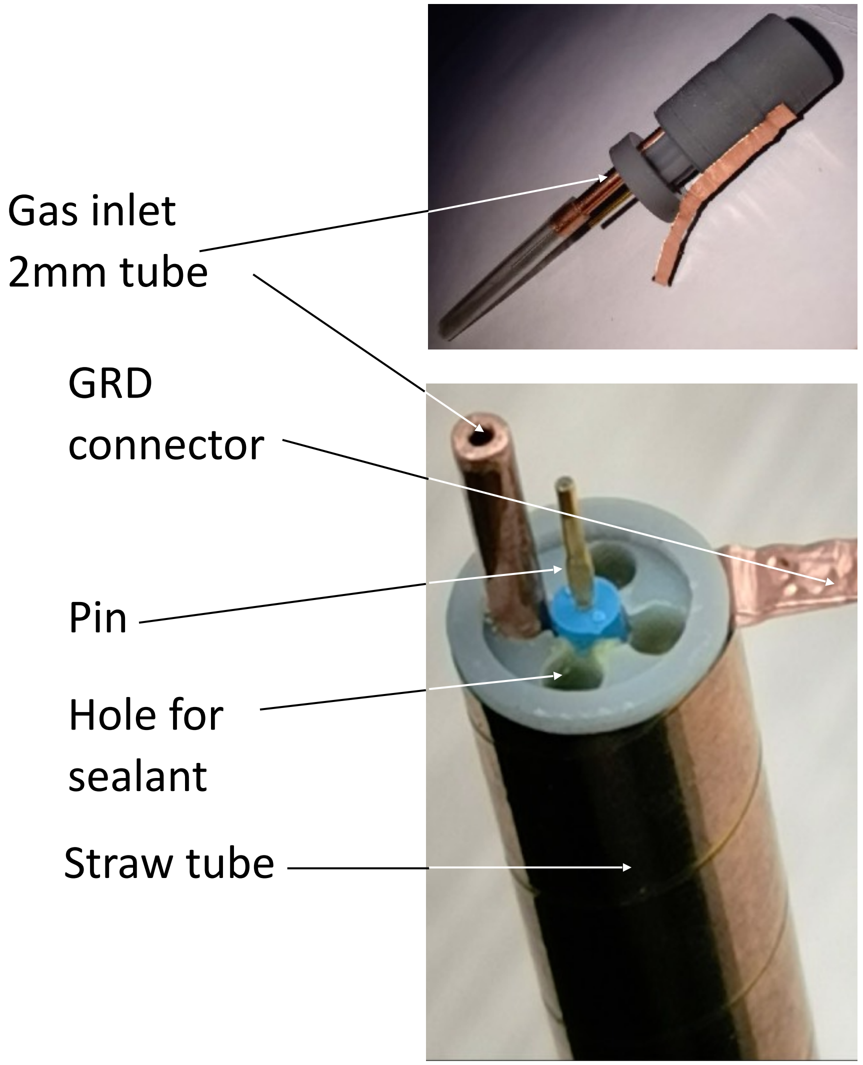

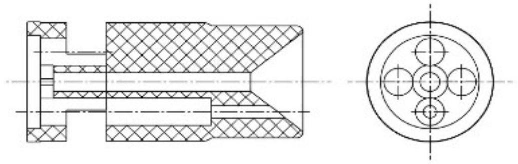

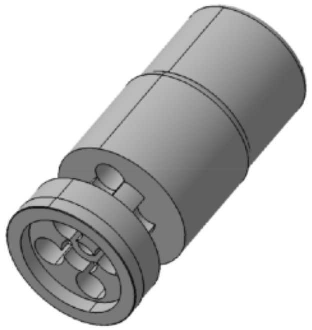

- The purpose of making the prototype is to test the assembly technology (stretching straws before gluing them to the frame)
- Aluminum sheets were purchased in the spring. The frame is being manufactured in LHEP workshop
- Tubes of the required diameter have been manufactured
- The issue of electronics remains open

Application of ST for the dE/dx analysis (PID)

Straw of SPD

- Number of primary ionized e- per straw is about the same as per pad in TPC => similar abilities for identification
- Using TDC+ADC for readout. See VMM3 as an example

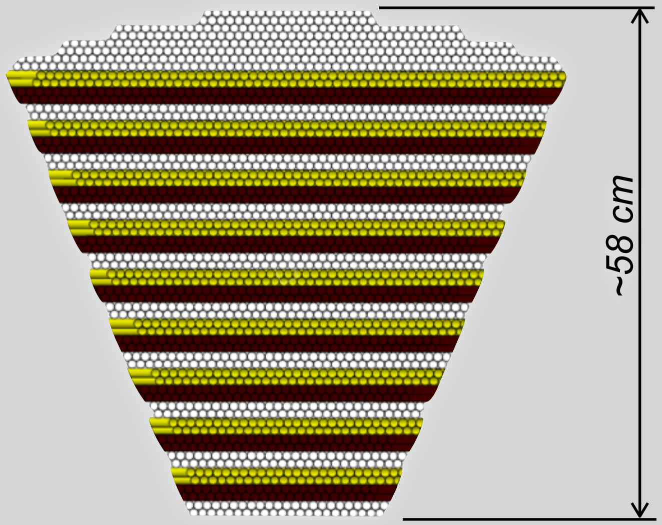

<u>∅=10mm straw</u>: S = **78 mm²**

TPC of MPD (for comparison)

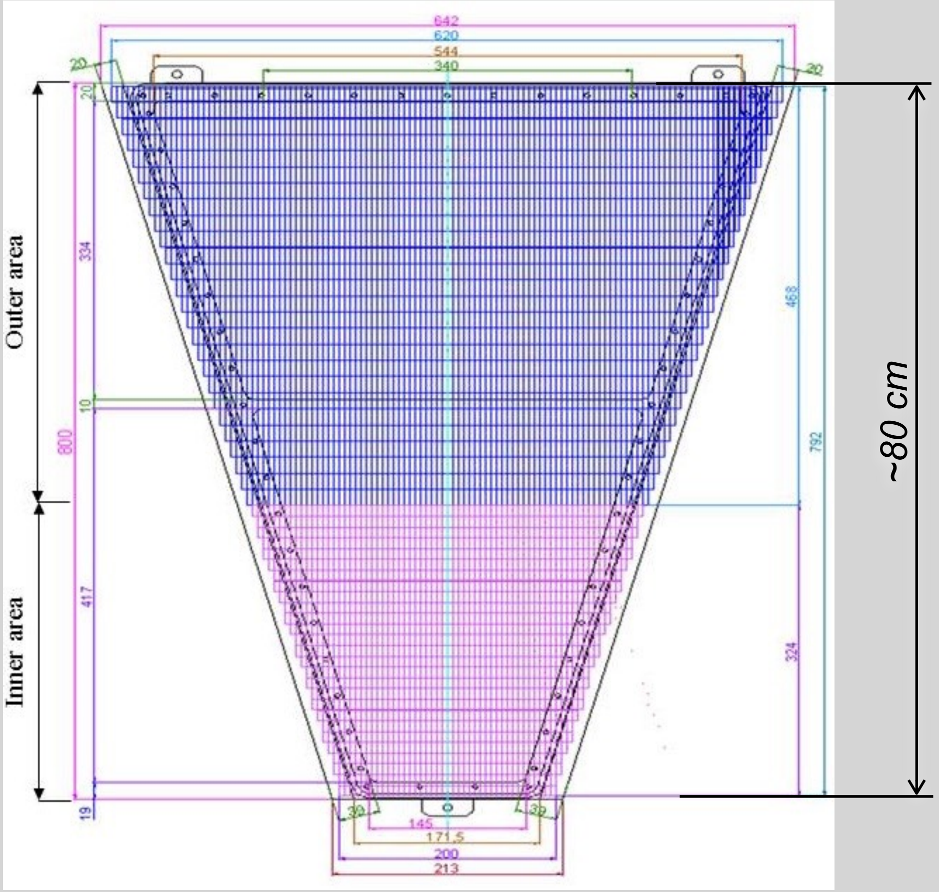

<u>Inner pads</u>: 5mm × 12mm = **60 mm²**, <u>Outer pads</u>: 5mm × 18mm = **90 mm²**

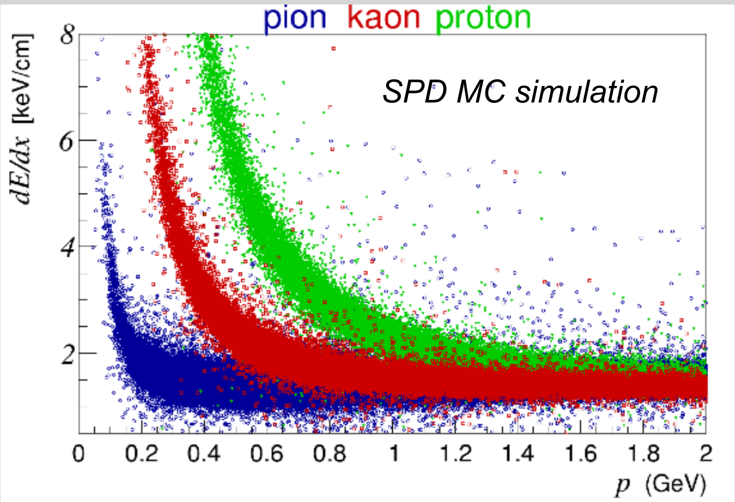

- For the 1-st stage of experiment ST will be the only PID detector in SPD for π/K/p.
- Only the low momentum region

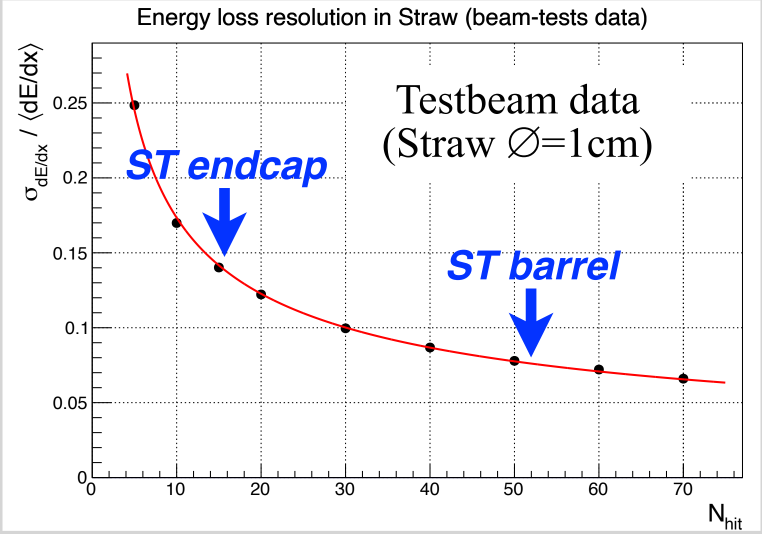

Y.Wang,
V.Chmill

Time-of-flight (TOF) detector

Schematic view of self-sealed MRPC

(B.Wang et al, JINST 15 (2020) 08, C08022)

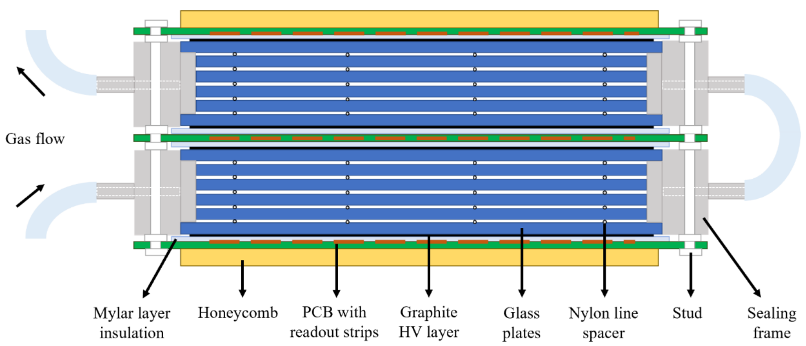

- Purpose: π/K/p discrimination for momenta ≲2 GeV, determination of t_0.
- Time resolution requirement <60 ps.
- Self-sealed Multigap Resistive Plate Chambers (MRPC) are the base option.
- DAQ electronics is under discussion. Analog of NINO chip v1 is in production.
- Number of readout channels is ~12.2k

Reconstruction for pp at √s=27 GeV

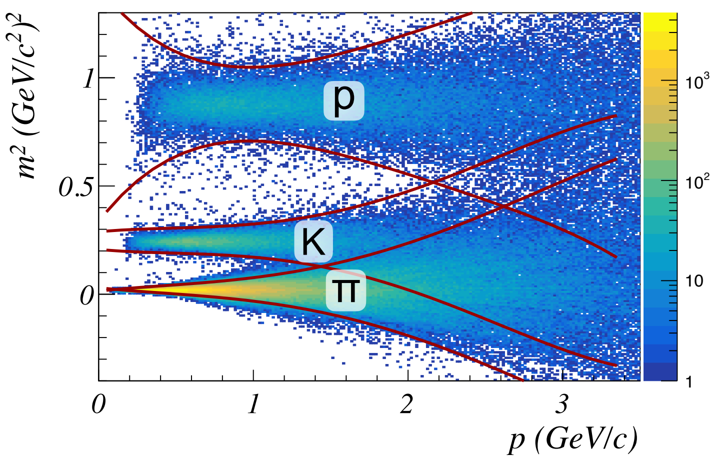

TOF Chambers for Barrel
(overlap in 2 dimensions)

16×9=144 MRPC

TOF Chamder
32 strips

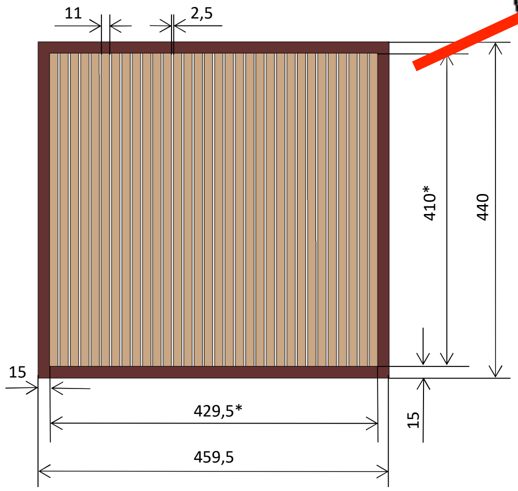

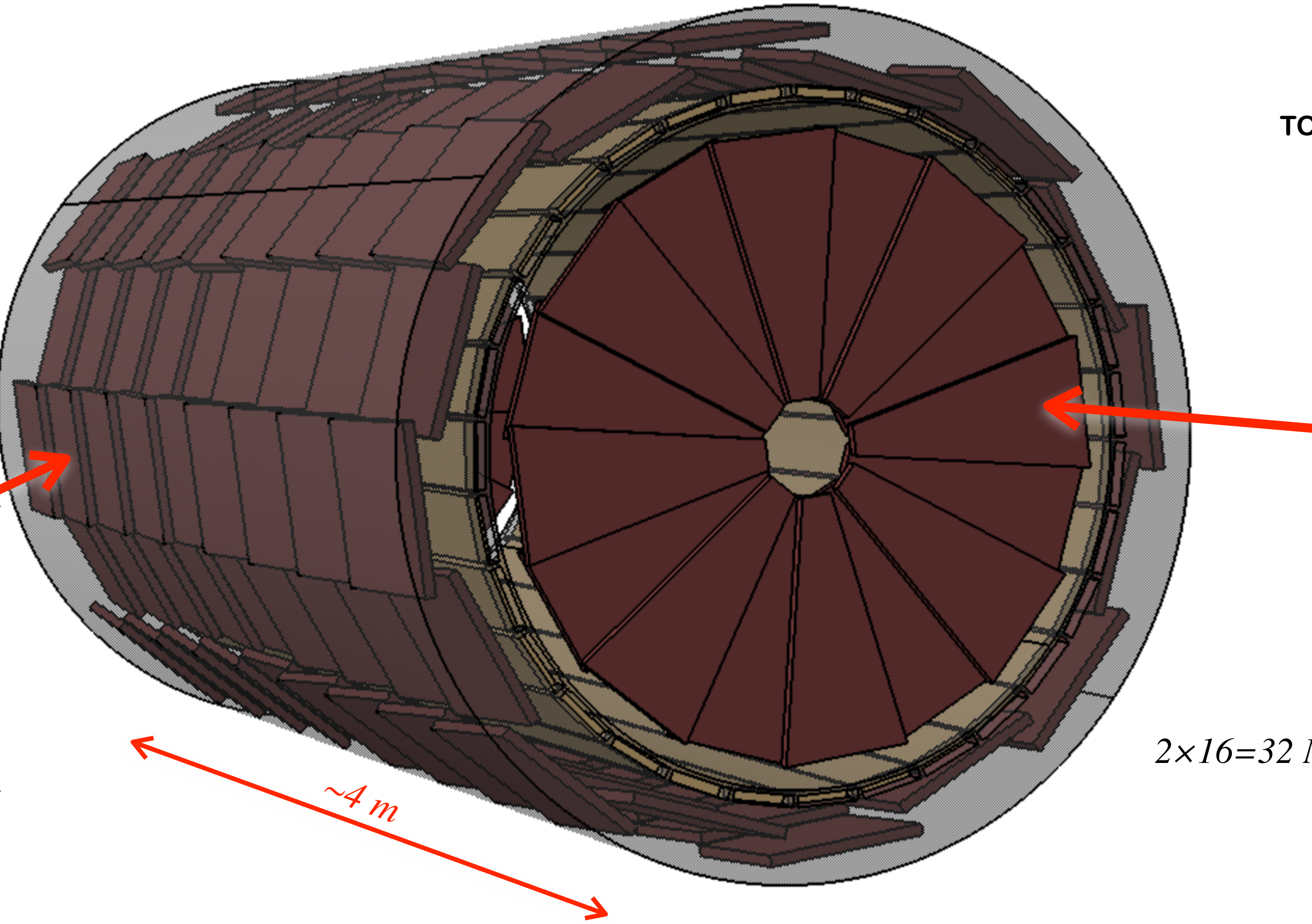

TOF Chambers for Endcap
48 strips

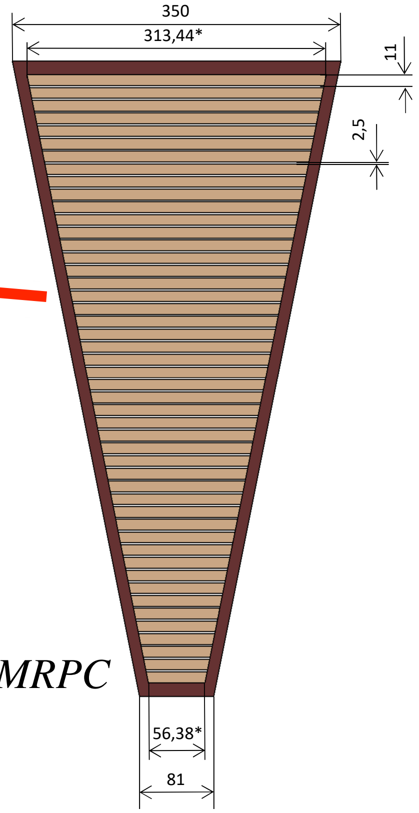

2×16=32 MRPC

A.Barnyakov (BINP)

Focusing Aerogel RICH (FARICH) detector

Principle of detector operation

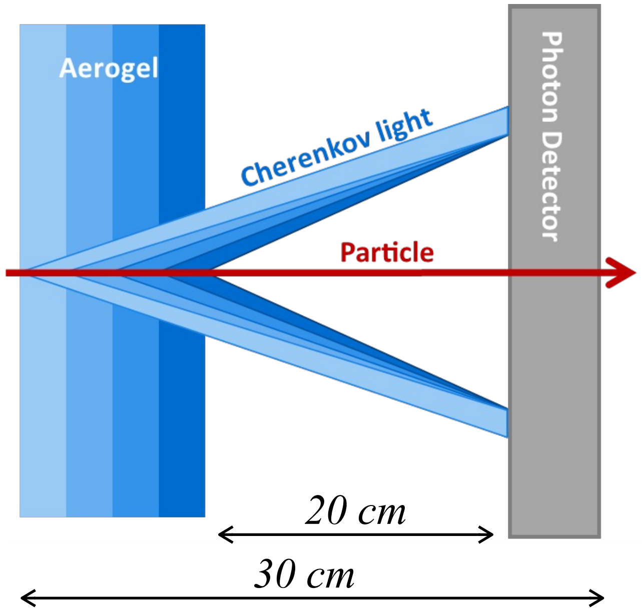

- Purpose: identification of high momentum particles ($p \gtrsim 1.5$ GeV) which cannot be discriminated by TOF
- Requirement: π/K separation at 6 GeV/c up to 3.5σ
- Disk-shaped detector in endcap with an area of 2 m^2
- Multilayer focusing aerogel radiator produced in BINP
- Development of Multi-anode MCP-PMT is ongoing in Russia (so far PMT of Hamamatsu, Photonis, Photek)
- The FARICH concept was published in 2005
- It was realized as a detector in Belle-II (KEK) in 2017

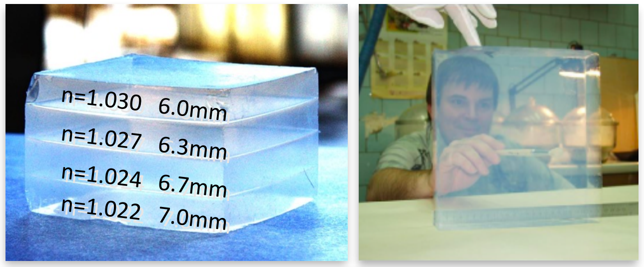

Accumulated *xy* distribution of hits

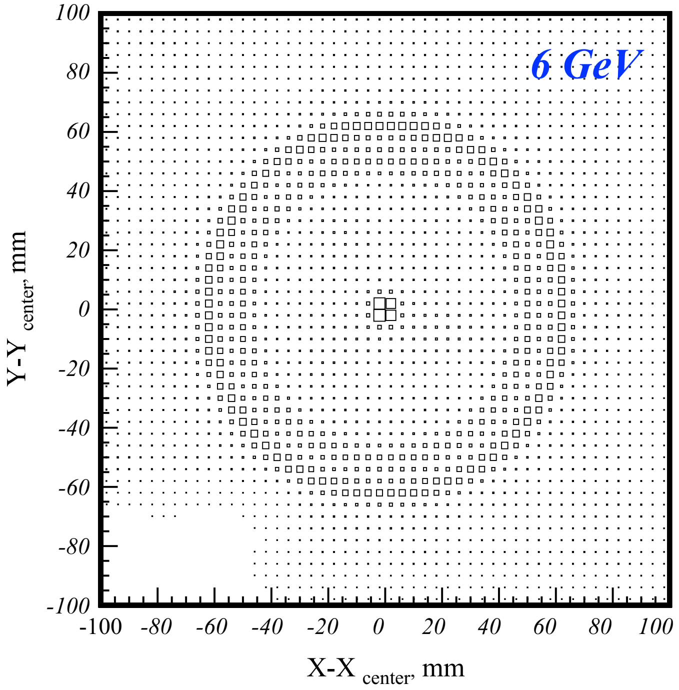

Ring radius distribution of γ

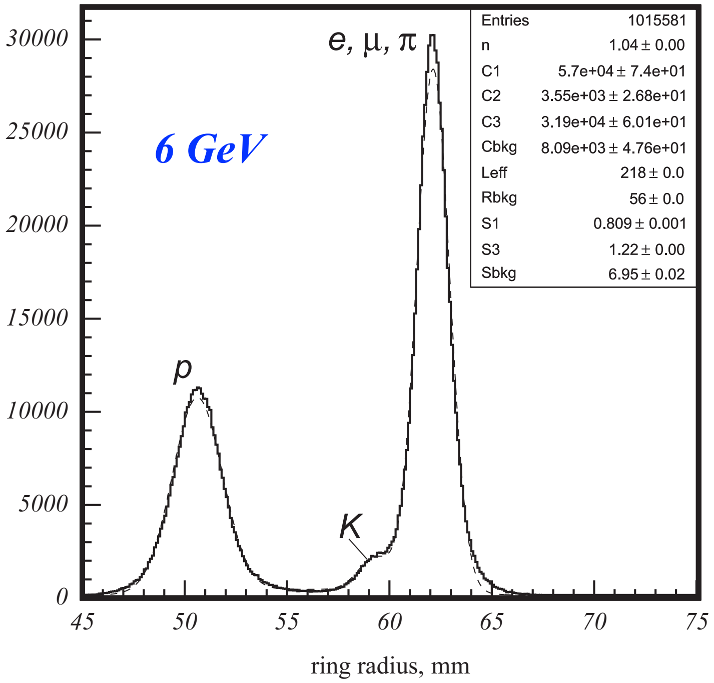

```
Entries           1015581
n             1.04 ± 0.00
C1      5.7e+04 ± 7.4e+01
C2    3.55e+03 ± 2.68e+01
C3    3.19e+04 ± 6.01e+01
Cbkg  8.09e+03 ± 4.76e+01
Leff              218 ± 0.0
Rbkg               56 ± 0.0
S1          0.809 ± 0.001
S3            1.22 ± 0.00
Sbkg          6.95 ± 0.02
```

Ability to distinguish between π and K

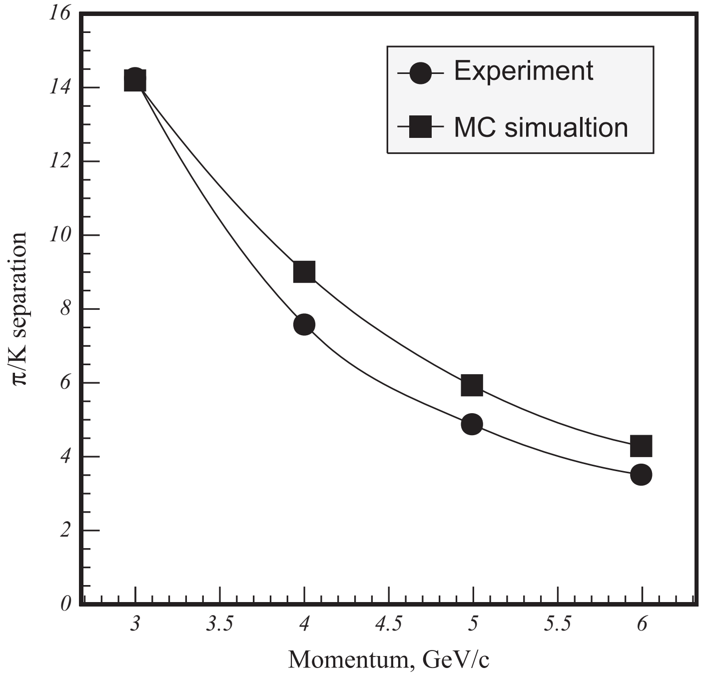

A.Barnyakov et al, NIMA732(2013)352

Inner Tracker System of SPD

Micro pattern gaseous detector for the 1-st phase of SPD

(commissioning by ~2028)

Cylindrical MicroMegas (MM)

Purpose: temporary replacement for SVD, it serves to improve momentum resolution of tracks by about 2 times 3.5% (ST) →1.7% (ST+MM).

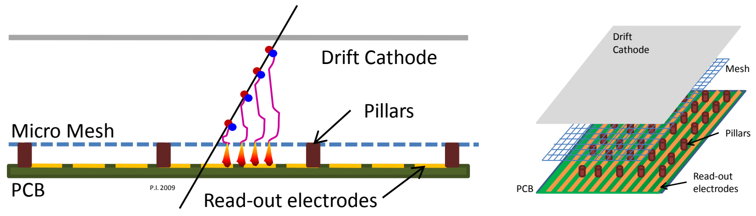

Ionization gap 3 mm, amplification gap 120 μm, gas mixture $Ar:C_4H_{10}$ = 90:10, gas gain 10^4, pitch size 450 μm, will be manufactured in LNP JINR, ***spatial resolution ~150 μm***.

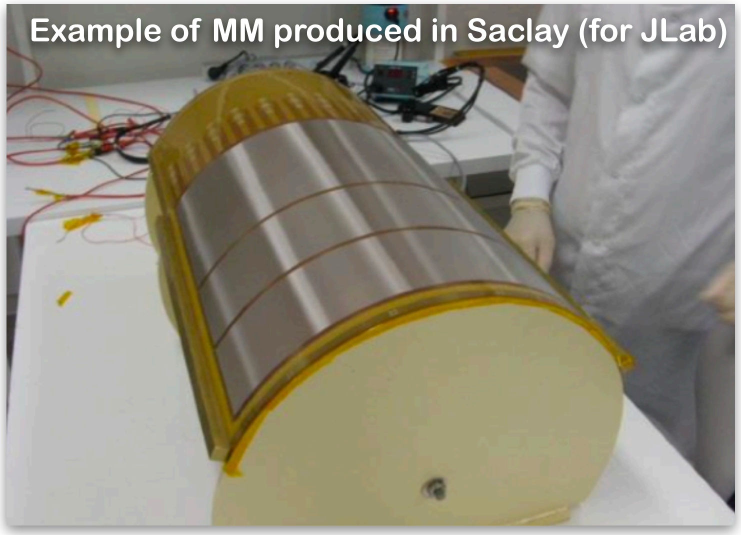

Example of MM produced in Saclay (for JLab)

Bulk technology, cylindrically bent, 1 super-layer at R = 5 cm with strip tilt angles 0º, ±5º and length of 90 cm, readout electronics at two ends, ~5.4k channels.

Silicon Vertex Detectors (SVD) for the 2-nd phase of SPD

(one of two options, commissioning by ~2035)

Double-Sided Silicon Detector (DSSD)

Main purpose of the detector is to reconstruct the position of D-meson decay vertices (σ_z=76 μm).

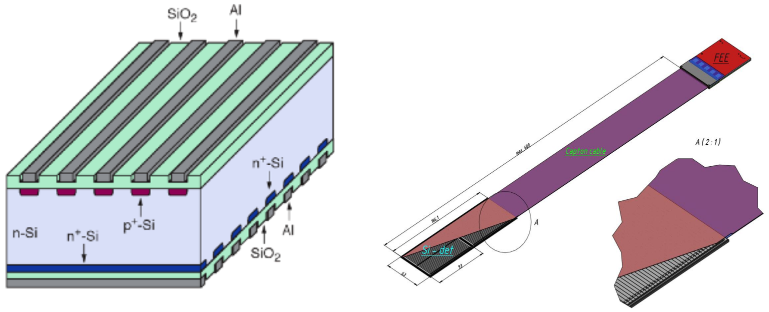

Silicon wafer size 63×93 mm², thickness 300 μm, orthogonal strips on p^+ and n^+ sides, p^+ pitch 95 μm, n^+ pitch 282 μm, produced by ZNTC Russia, ***spatial resolution 27 (81) μm*** for p^+ (n^+) side.

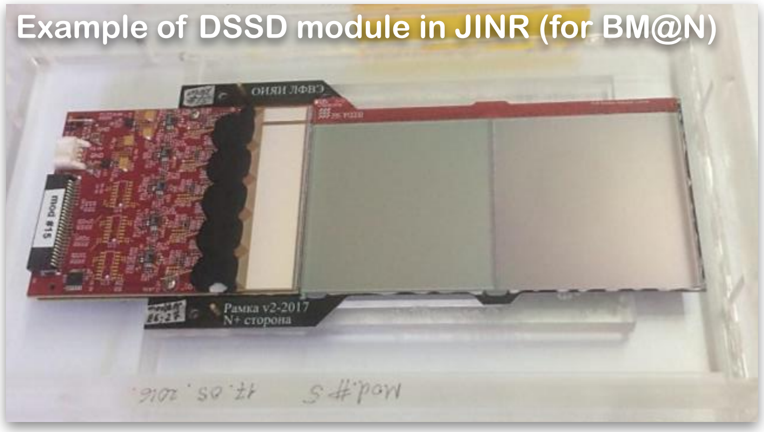

Example of DSSD module in JINR (for BM@N)

DSSD modules are assembled in ladders with carbon fiber support, 3 layers (R=5, 13, 21 cm) in barrel 74 cm long, 3 layers in each endcap, readout electronics at two ends, ~108k channels.

Monolithic Active Pixel Sensors (MAPS)

Main purpose of the detector is to reconstruct the position of D-meson decay vertices (σ_z=51 μm).

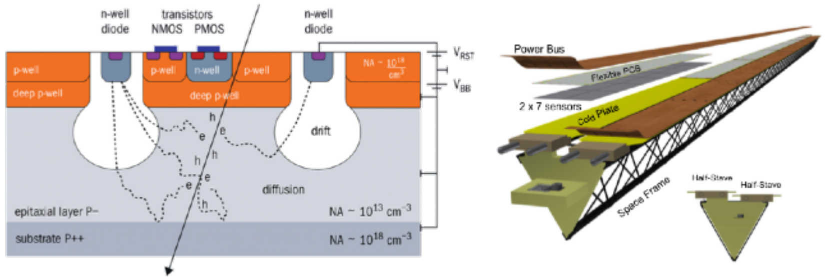

Silicon wafer size 30×15 mm², thickness 50 μm, pitch 28 μm, 512×1024 pixels, sensor and FEE sections are integrated in a single chip, so far is not produced in Russia, ***spatial resolution 5 μm***.

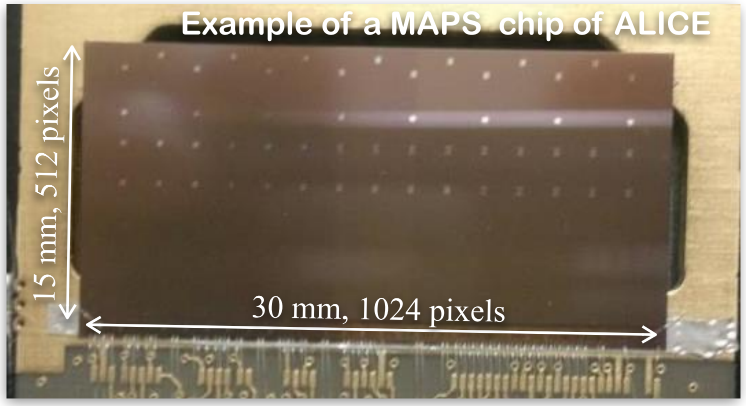

Example of a MAPS chip of ALICE

MAPS chips are assembled in staves with carbon fiber support, 4 layers (R=4, 10, 15, 21 cm) with the external layer 127 cm long, FE electronics is part of the chip, ~10^9 pixels for readout.

DSSD: N.Zamyatin,
O.Tarasov

Silicon Vertex Detector (SVD)

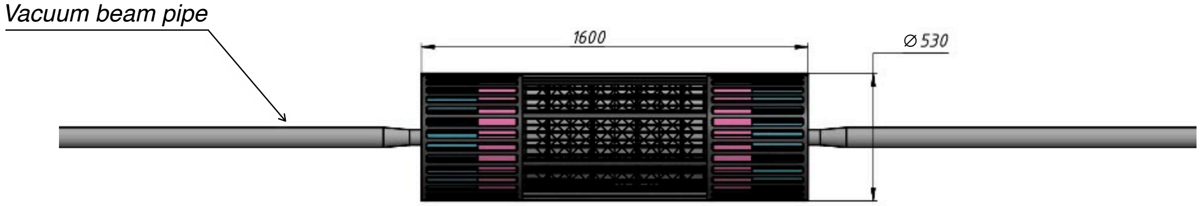

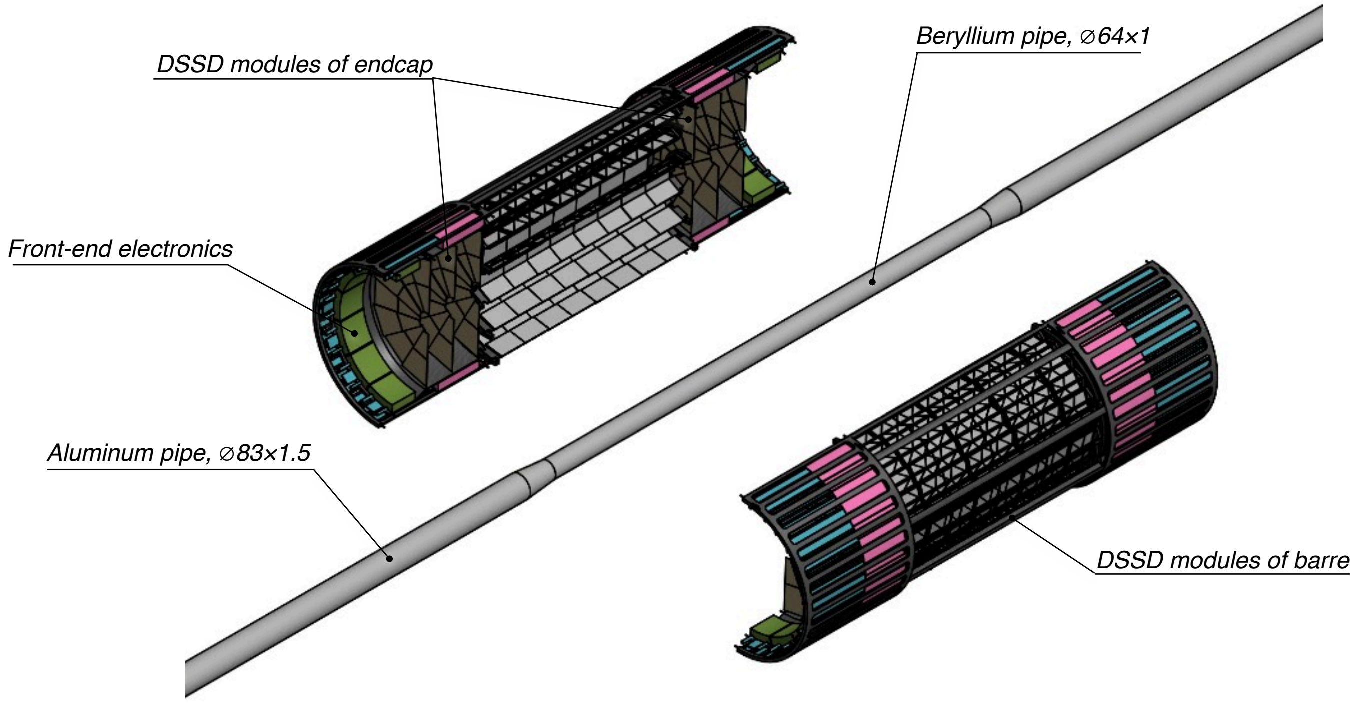

Transverse momentum resolution

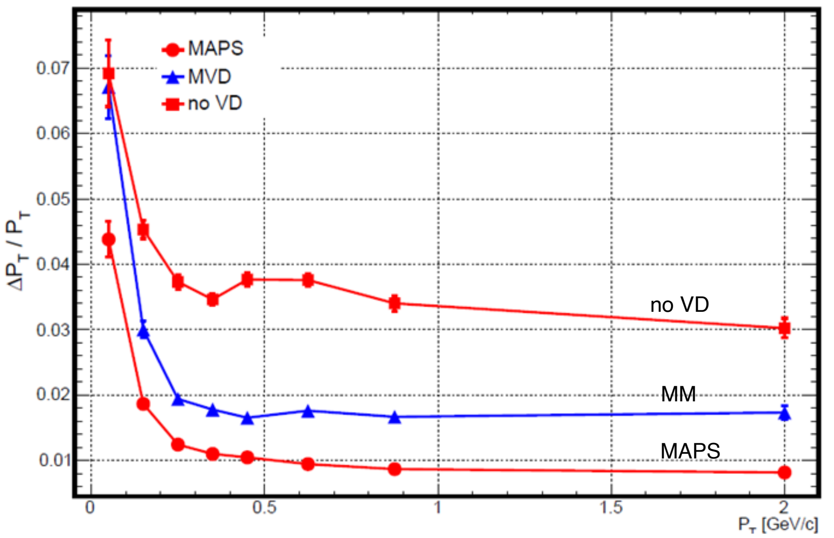

Distance between production and decay vertex

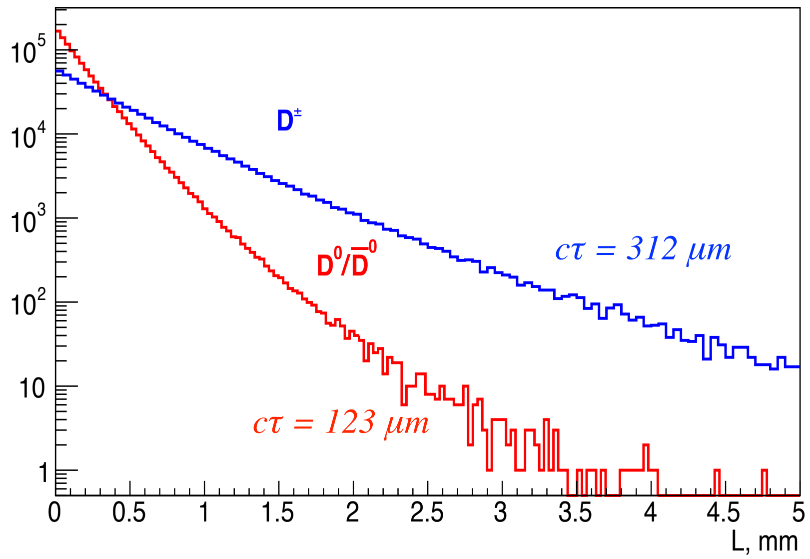

$D0 \to \pi^+ + K^-$: secondary vertex x-resolution

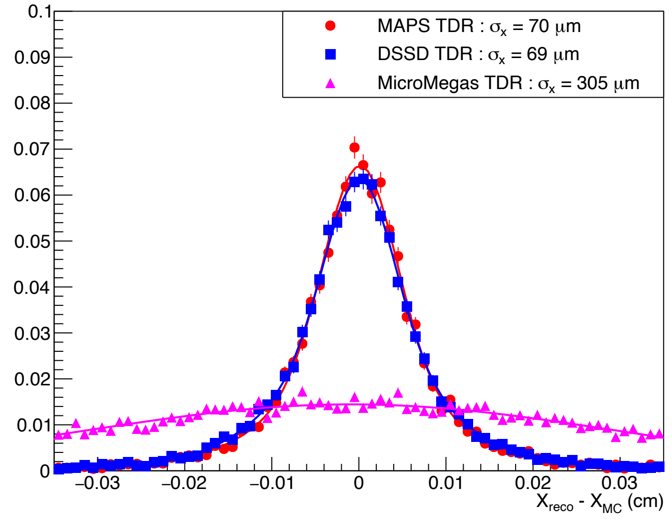

$D0 \to \pi^+ + K^-$: secondary vertex z-resolution

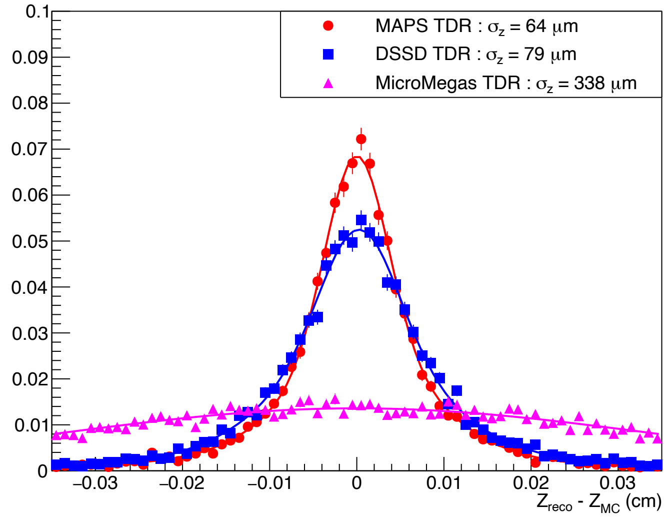

Progress in developing a cylindrical MM prototype in LNP

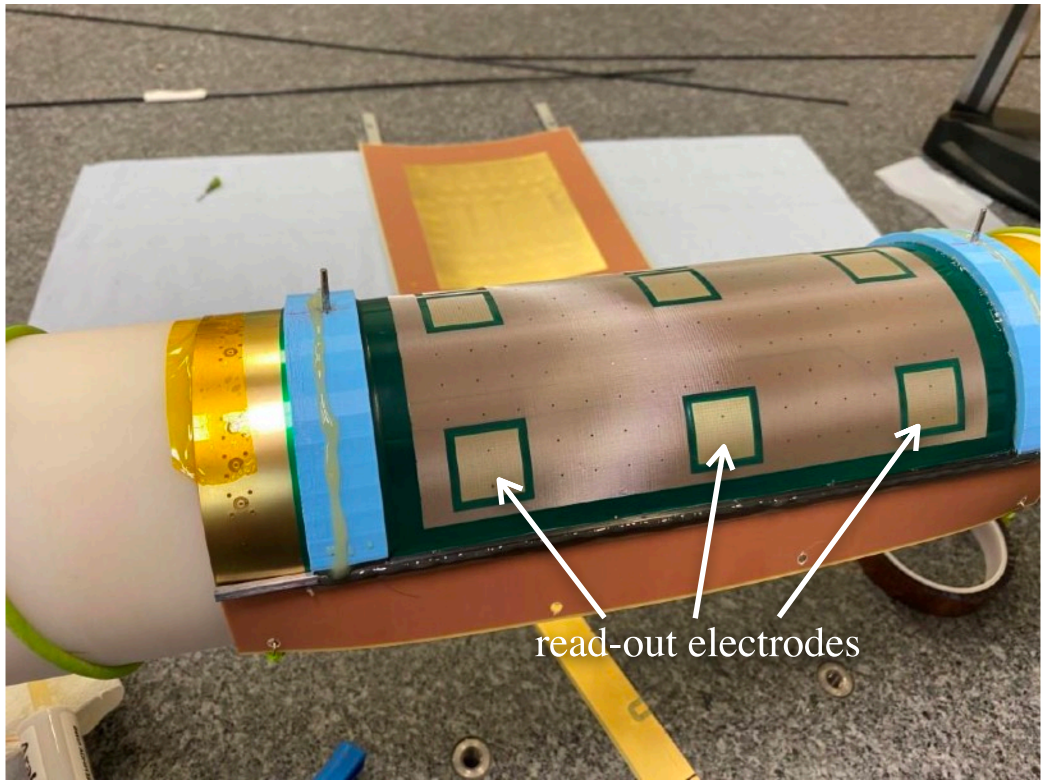

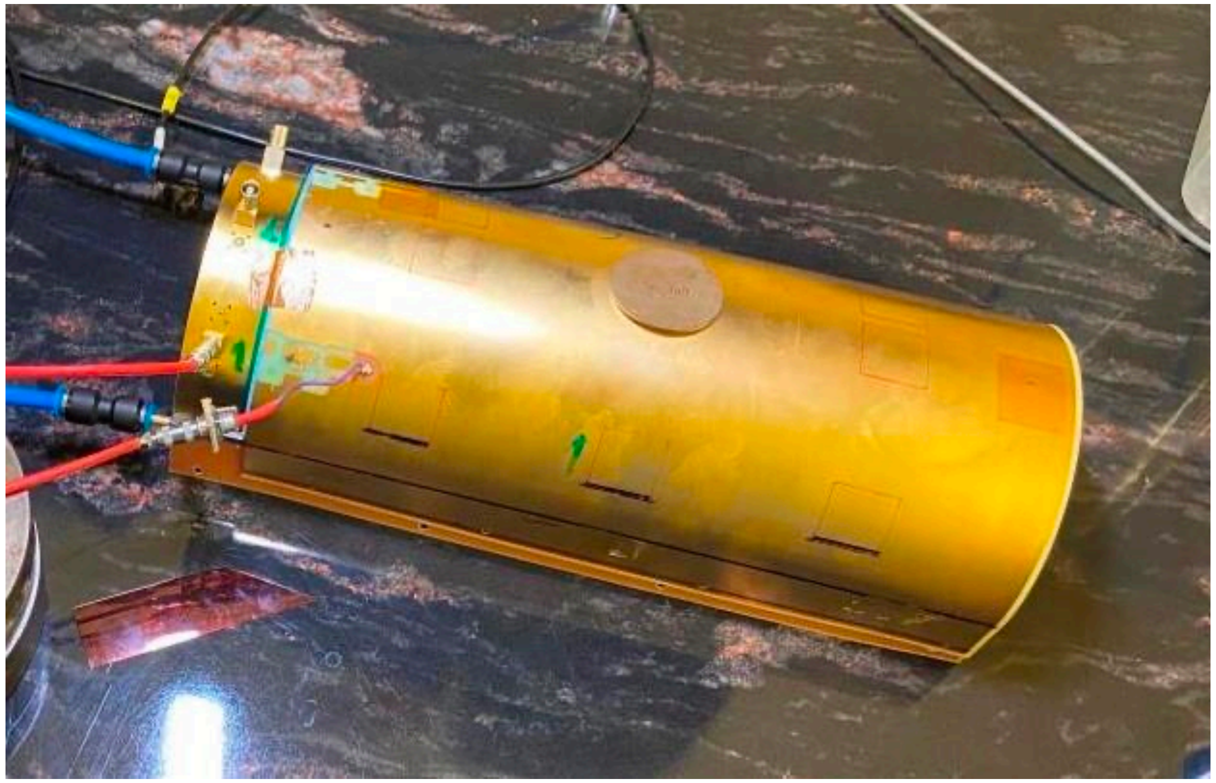

LNP, Desember 2023

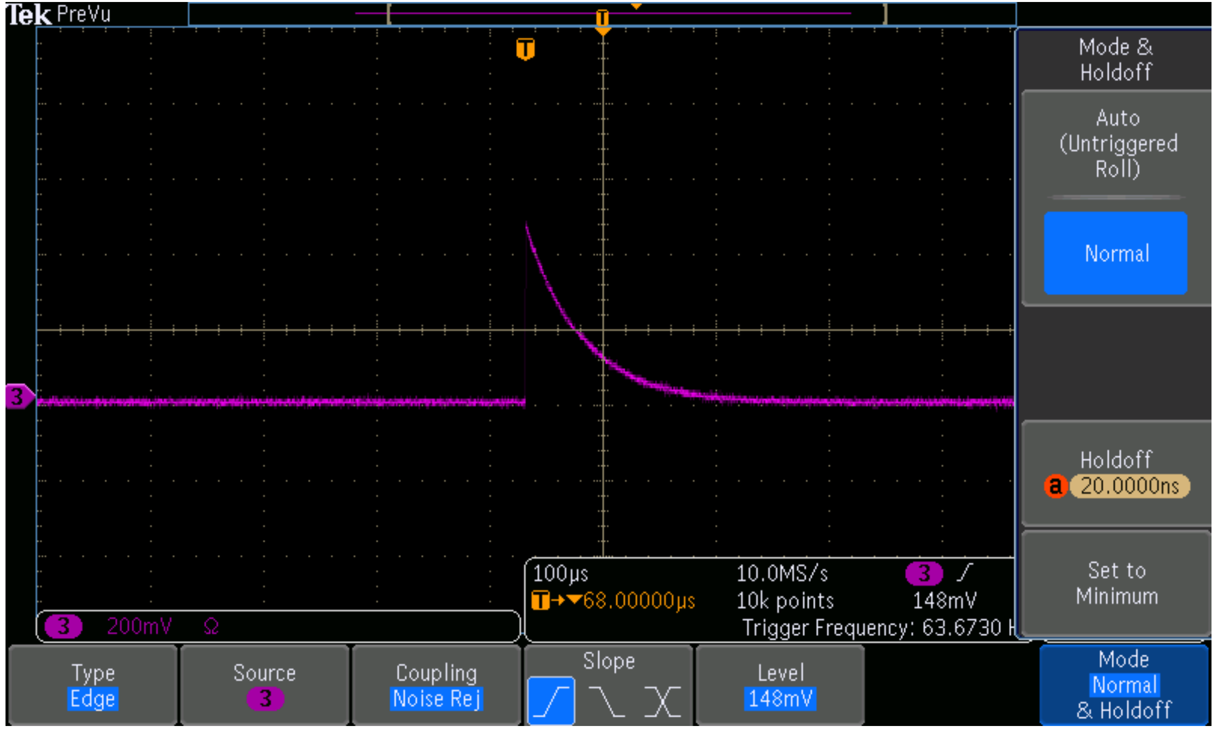
Tek PreVu

Mode & Holdoff

Auto (Untriggered Roll)

Normal

Holdoff a 20.0000ns

Set to Minimum

100µs

T→▾68.00000µs

10.0MS/s

10k points

3 ⌐ 148mV

Trigger Frequency: 63.6730 H

3 200mV Ω

Type Edge

Source 3

Coupling Noise Rej

Slope

Level 148mV

Mode Normal & Holdoff

- Cylindrical MMs have so far been produced only in Saclay for CLASS12, R=10 cm.
- MM production stages for SPD (**R=5 cm**):
  - Photolithography to produce RO board
  - Bending and fixation on template
  - Gluing force elements (longbeams, arcs)
  - Gluing cathode plain and hermetization
  - Finalization (cut-out technological detail, add gas connectors, etc)
- Stable signal (U_{gain}=525V, G=10^4)

Detectors for local polarimetry and luminosity control

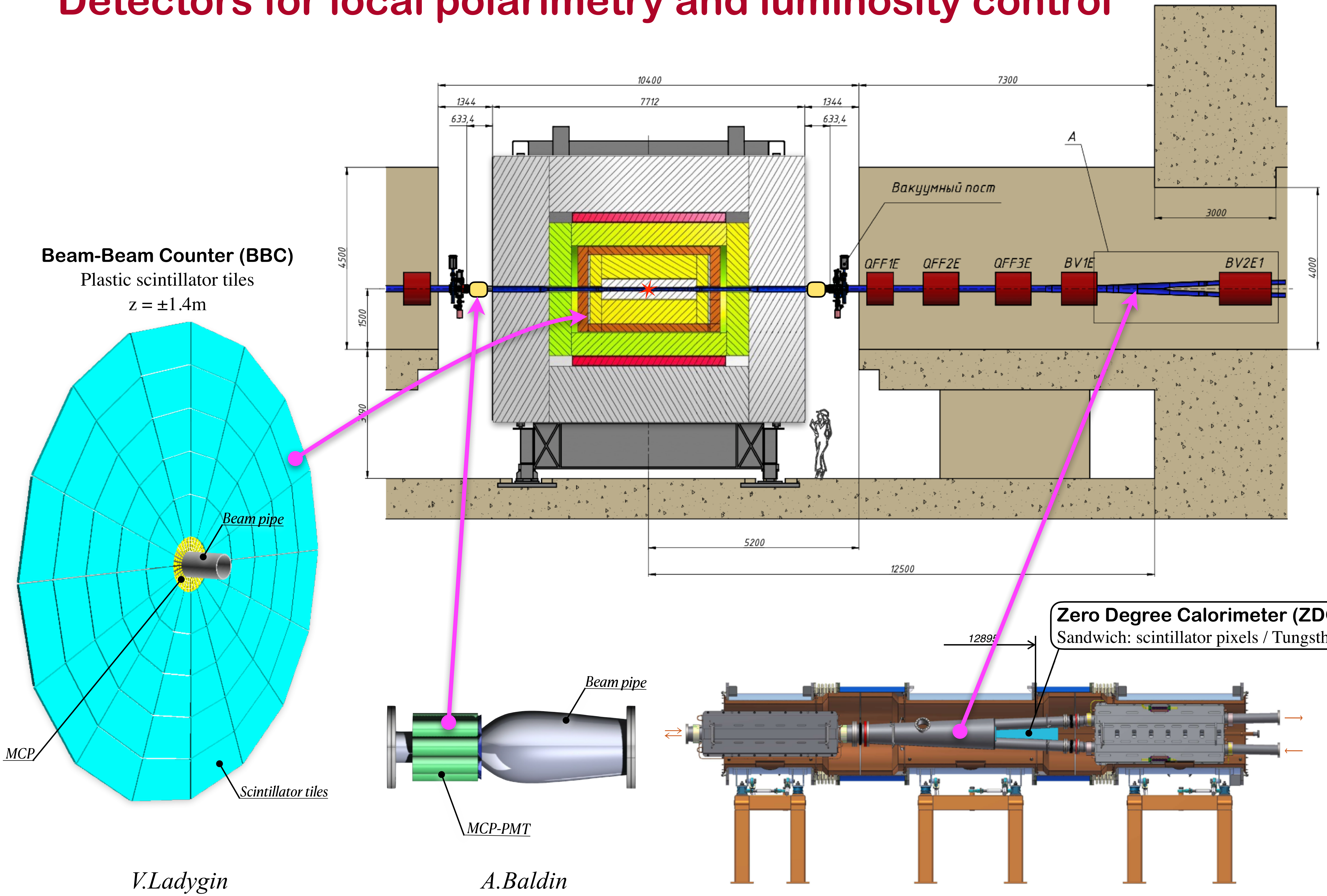

Beam-Beam Counter (BBC)
Plastic scintillator tiles
z = ±1.4m

Zero Degree Calorimeter (ZDC)
Sandwich: scintillator pixels / Tungsthen

V.Ladygin

A.Baldin

I.Alekseev (ITEP)

Progress on Beam-Beam-Counter (BBC)

Tile height 55.7 mm
25 tiles in sector (similar to STAR EPD)

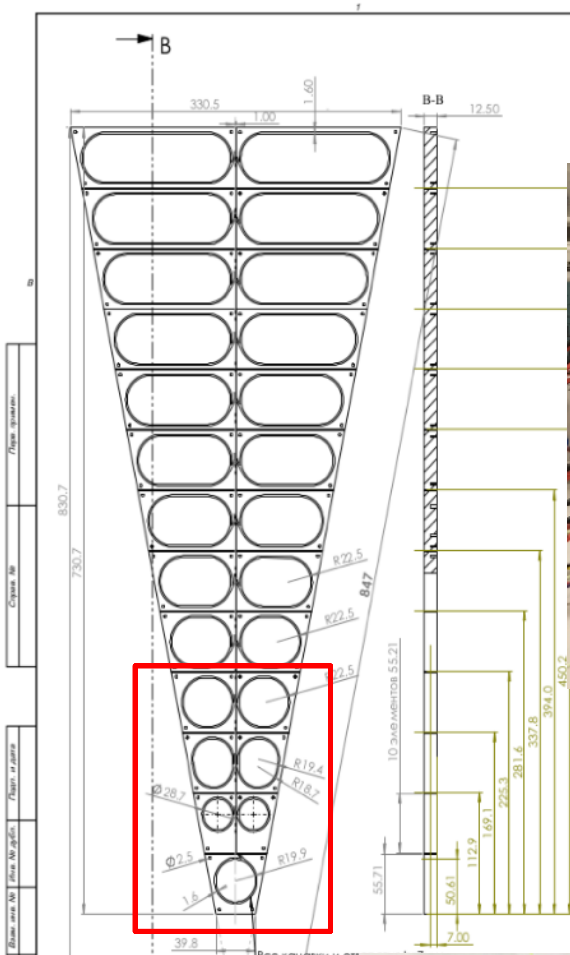

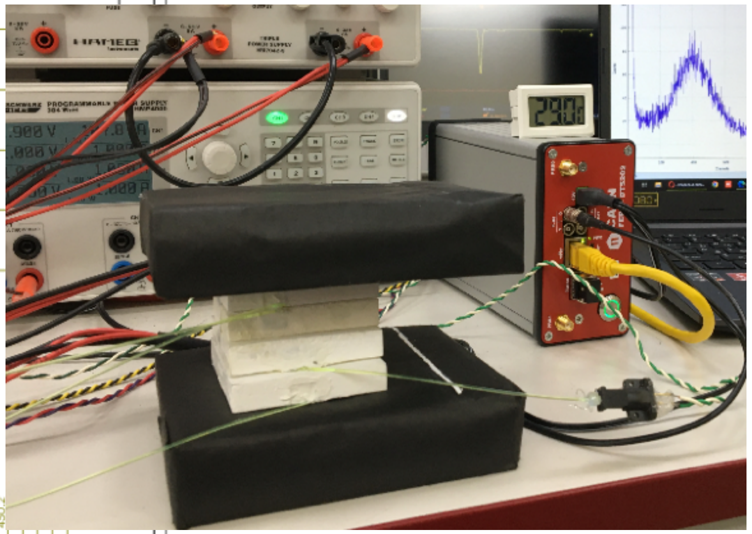

The BBC prototype options:

- ➢**CAEN FERS-5200 readout system**
- ➢scintillator prototype tiles (thickness 10 mm)
  - Tyvek covered vs **chemical mating**
- ➢scintillation optical fibers (WLS and clear)
  - KURARAY vs Saint-Gobain Crystals
- ➢optical cement
  - CKTN Med vs OK-72
- ➢SENSL SiPMs (MicroFC-x0035-SMT)
  - 3x3 mm^2 (for tests) vs **1x1 mm^2**

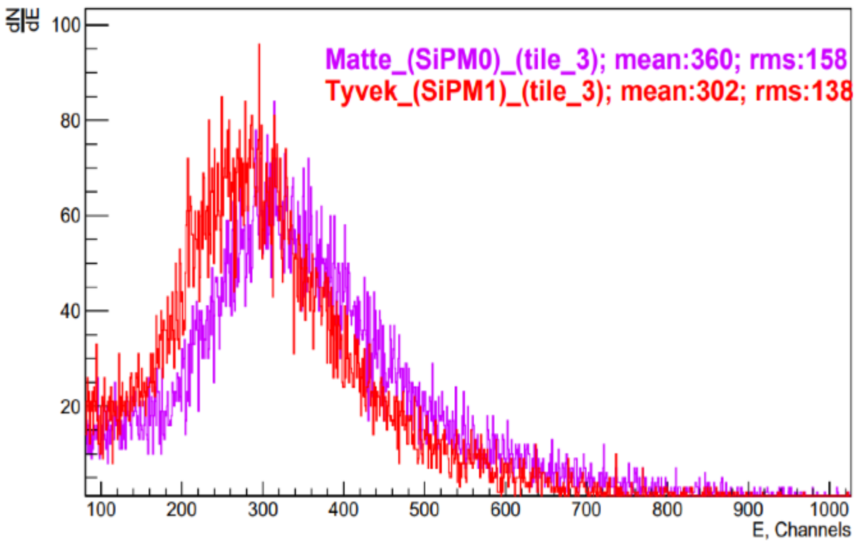

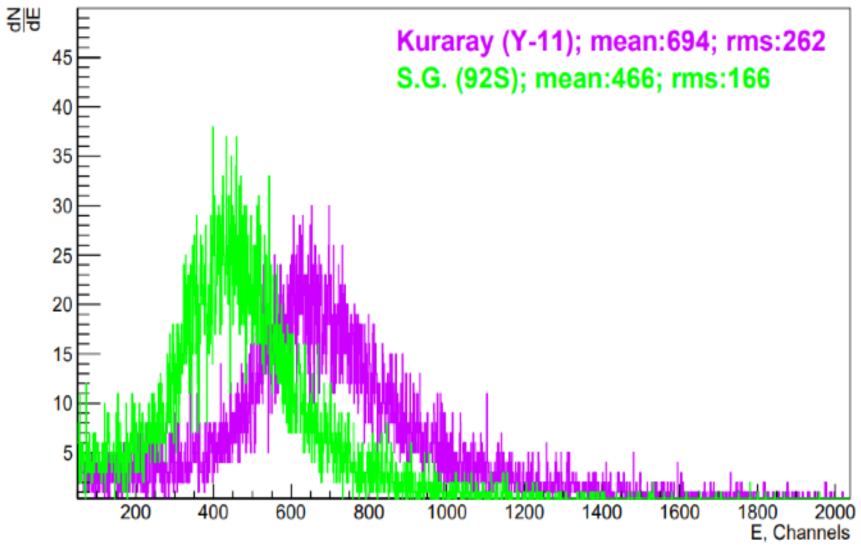

Currently, the selection of materials for the build of 7 detector prototype sector tiles is underway

V.Ladygin, A.Tishevsky

I.Alekseev (ITEP),
S.Shimanskiy

Progress on Zero Degree Calorimeter (ZDC)

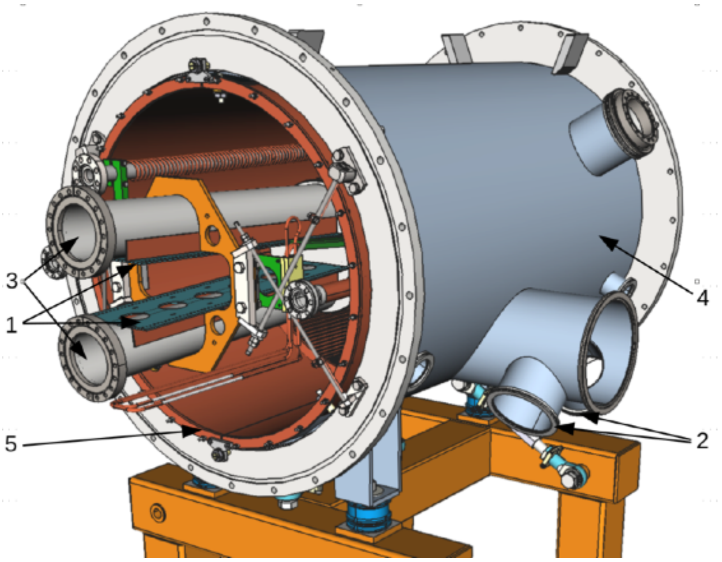

One plane of ZDC
(for initial tests)

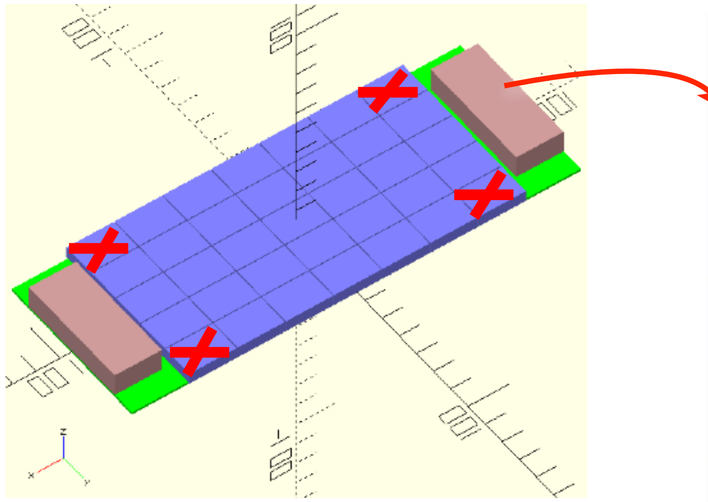

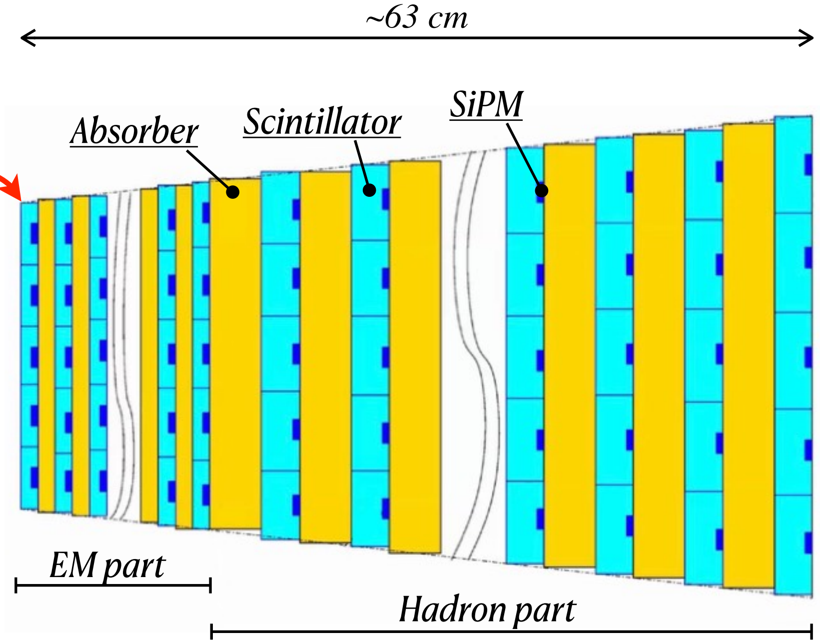

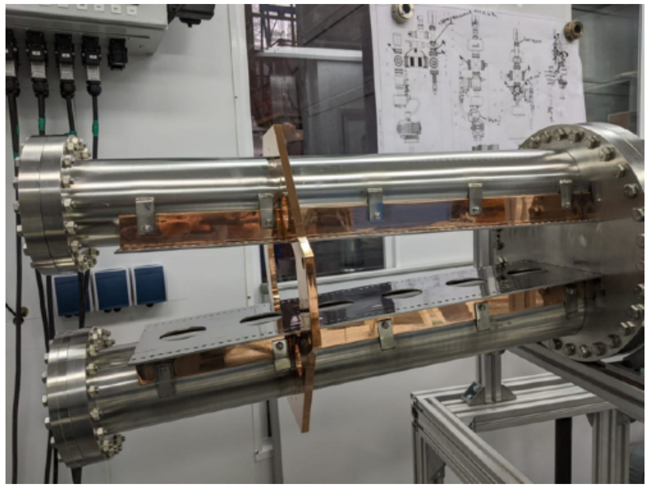

- Energy resolution for neutrons (50 ÷ 60)% / $\sqrt{E}$ ⊕ (8 ÷ 10)%. Time resolution 150 ÷ 200 ps. Neutron entry point spatial resolution 10 mm.
- Beam pipe sections for the ZDC cite are received in JINR October. Now under tests by vacuum group. The place for ZDC is fine and well acceptable for installation.
- For the initial test a single ZDC plane with 31 scintillator tile (no tiles in the corners) is being developed.
- DAQ electronics: A5202 based on Citiroc-1A chip produced by WeeROC. It has 64 channels which provide SiPM bias, amplification and readout.

L.Afanasyev

Data Acquisition System (DAQ)

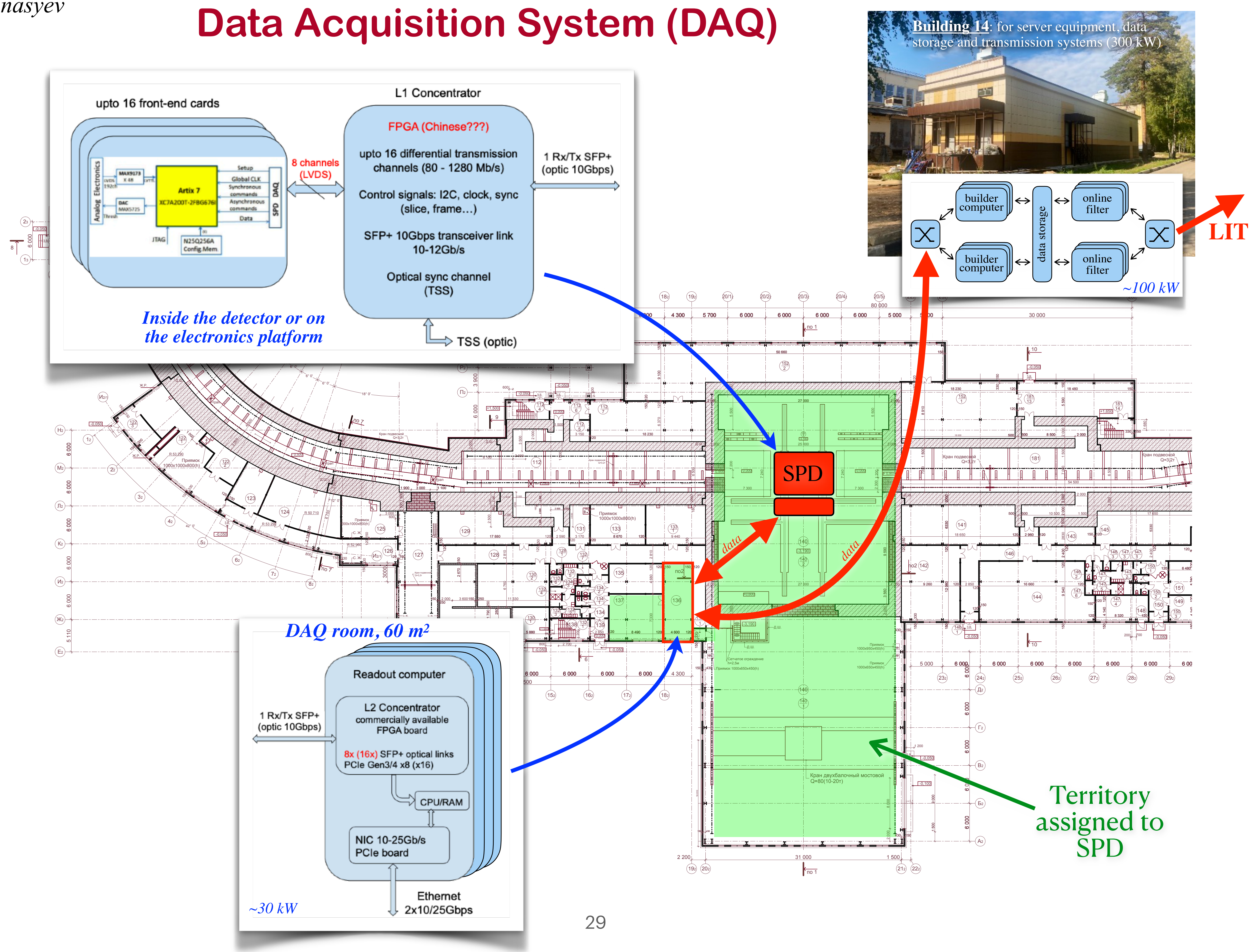

Building 14: for server equipment, data storage and transmission systems (300 kW)

upto 16 front-end cards

8 channels (LVDS)

L1 Concentrator

FPGA (Chinese???)

upto 16 differential transmission channels (80 - 1280 Mb/s)

Control signals: I2C, clock, sync (slice, frame…)

SFP+ 10Gbps transceiver link 10-12Gb/s

Optical sync channel (TSS)

1 Rx/Tx SFP+ (optic 10Gbps)

TSS (optic)

Inside the detector or on the electronics platform

~100 kW

LIT

SPD

DAQ room, 60 m²

Readout computer

1 Rx/Tx SFP+ (optic 10Gbps)

L2 Concentrator commercially available FPGA board

8x (16x) SFP+ optical links PCIe Gen3/4 x8 (x16)

CPU/RAM

NIC 10-25Gb/s PCIe board

Ethernet 2x10/25Gbps

~30 kW

Territory assigned to SPD

Data Acquisition System (DAQ)

- Bunch crossing every 76 ns → crossing rate 12.5 MHz
- At maximum luminosity of 10^{32} cm^{-2}s^{-1} the interaction rate is 4 MHz
- No hardware trigger to avoid possible biases
- Raw data stream 20 GB/s or 200 PB/year
- Online filter to reduce data by oder of magnitude to ~10 PB/year

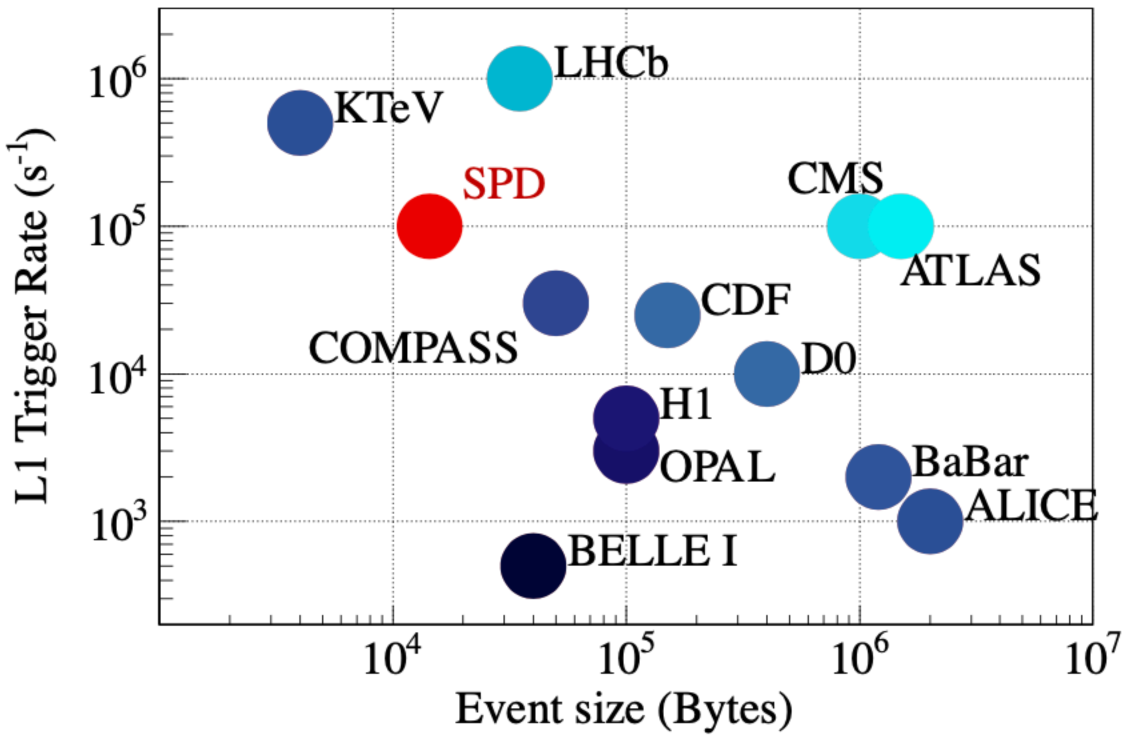

Data volume vs time

- ***Preparation for the experiment.*** Monte Carlo simulation from 2024 to 2028 will provide 2 PB per year. Total per stage: ***10 PB***.
- ***Stage I:*** running at low luminosity of the NICA collider. Monte Carlo simulation and real data taking from 2028 to 2030 will provide 4 PB per year. Reprocessing: 2 PB per year. Total per stage: ***18 PB***.
- ***Upgrade of the setup*** for operation at high luminosity. Monte Carlo simulation from 2031 to 2032 will provide 2 PB per year. Reprocessing: 2 PB per year. Total per stage: ***8 PB***.
- ***Stage II:*** running at maximum design luminosity of the NICA collider. Monte Carlo simulation and real data taking from 2033 to 2036 will provide 20 PB per year. Reprocessing: 10 PB per year. Total per stage: ***120 PB***.

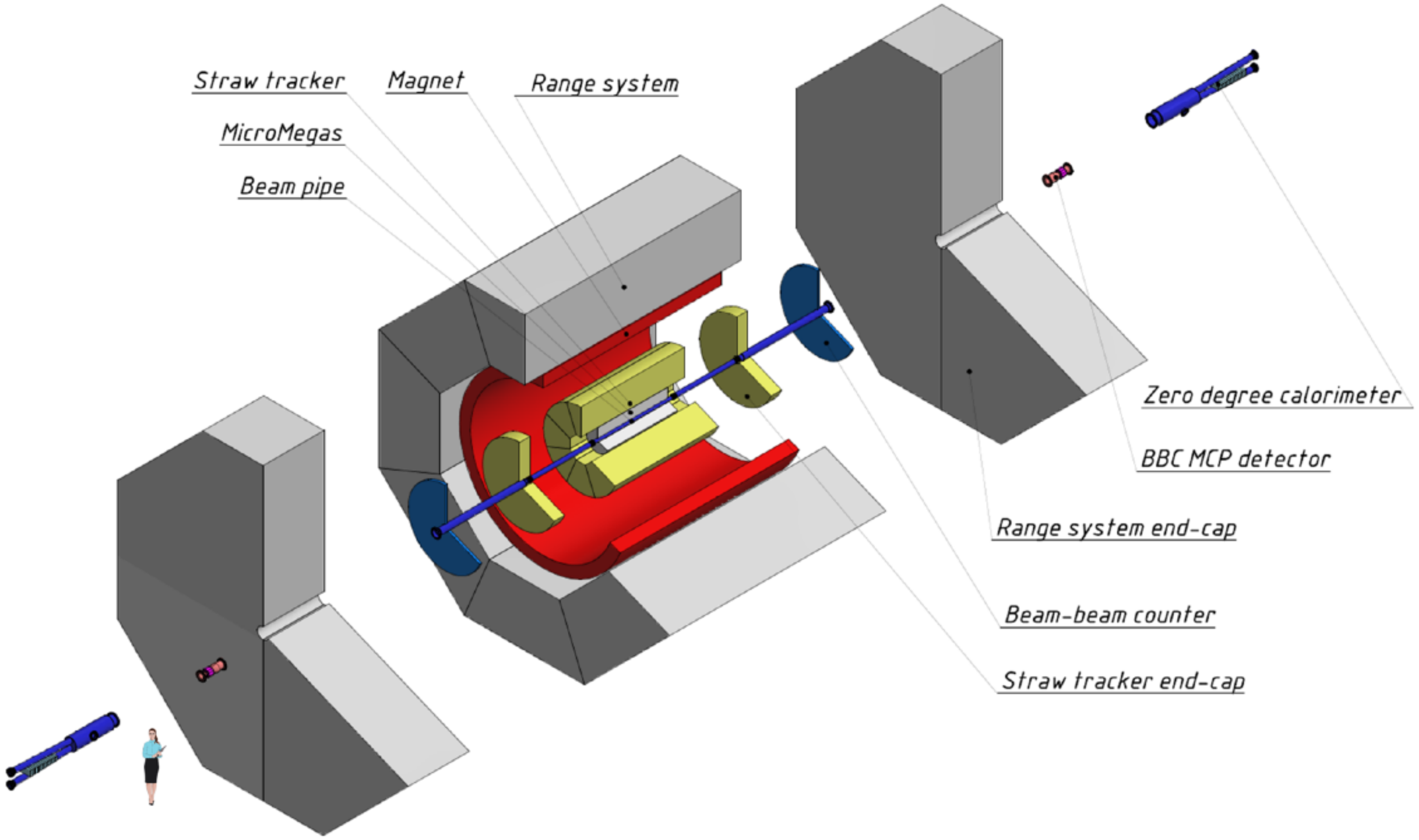

Stage I of experiment

- Basic set of subsystems
  - Magnet, RS, Straw
  - MM, BBC, MCP, ZDC
- No PID detector (TOF, FARICH), no ECal, no SVD
- p-beam: $\sqrt{s} \lesssim 15$ GeV, $\mathcal{L} \lesssim 10^{30}$ $s^{-1}cm^{-2}$

Stage II: Fully assembled setup

- p-beam: $\sqrt{s}=27$ GeV, $\mathcal{L}=10^{32}$ $s^{-1}cm^{-2}$ with interaction rate of ~4 MHz

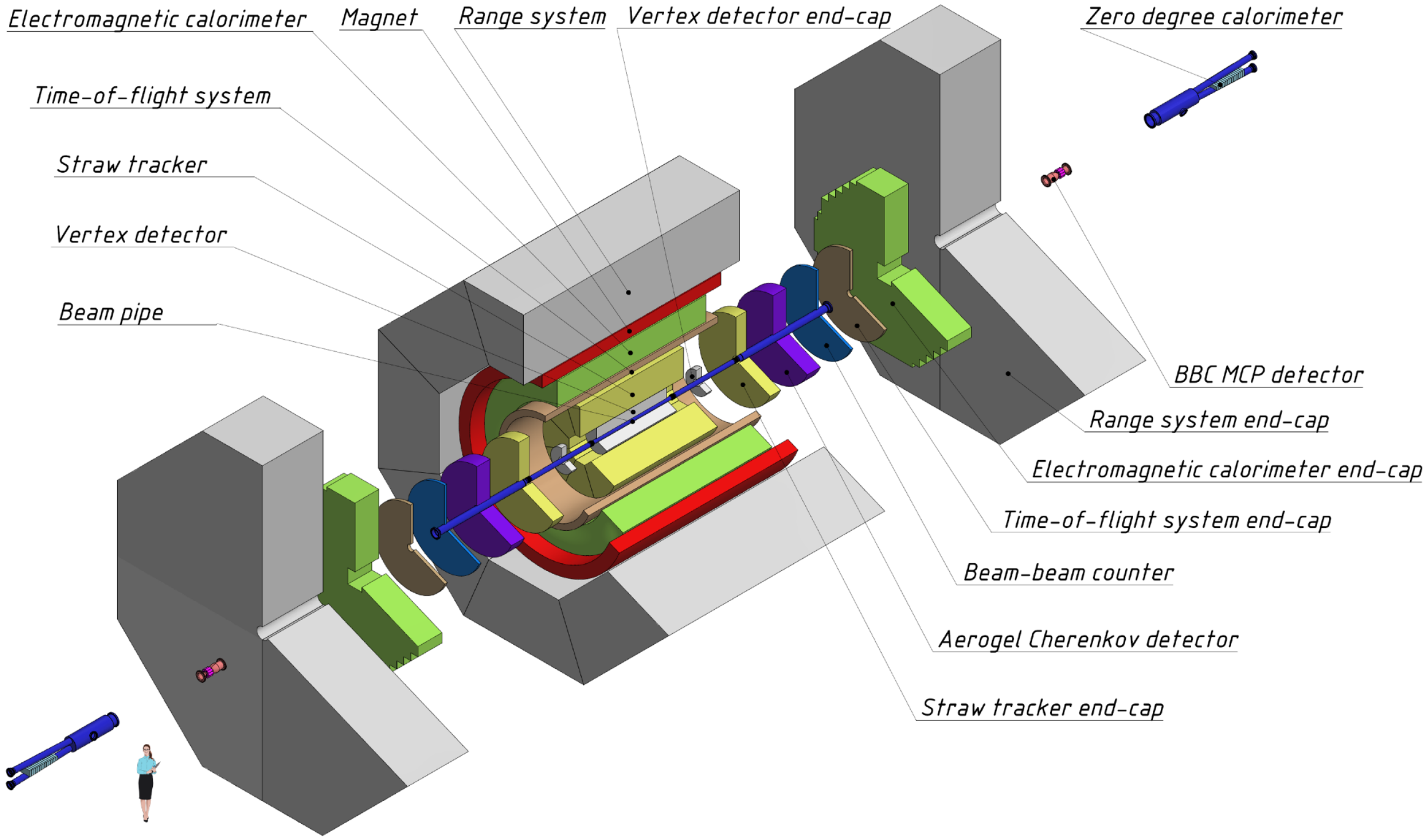

Conclusions

- NICA collider will start operation in heavy ion mode in early 2025
- Possibility of running (polarized) proton beams in NICA is currently being studied
- SPD (Spin Physics Detector) is a universal facility with the primary goal to study unpolarized and polarized gluon content of *p* and *d*
  - 4π detector will be equipped with silicon detector, straw tracker, TOF and FARICH for PID, calorimetry, muon system and monitoring detectors
- SPD Technical Design Report was released at the beginning of 2023
- More information could be found at http://spd.jinr.ru

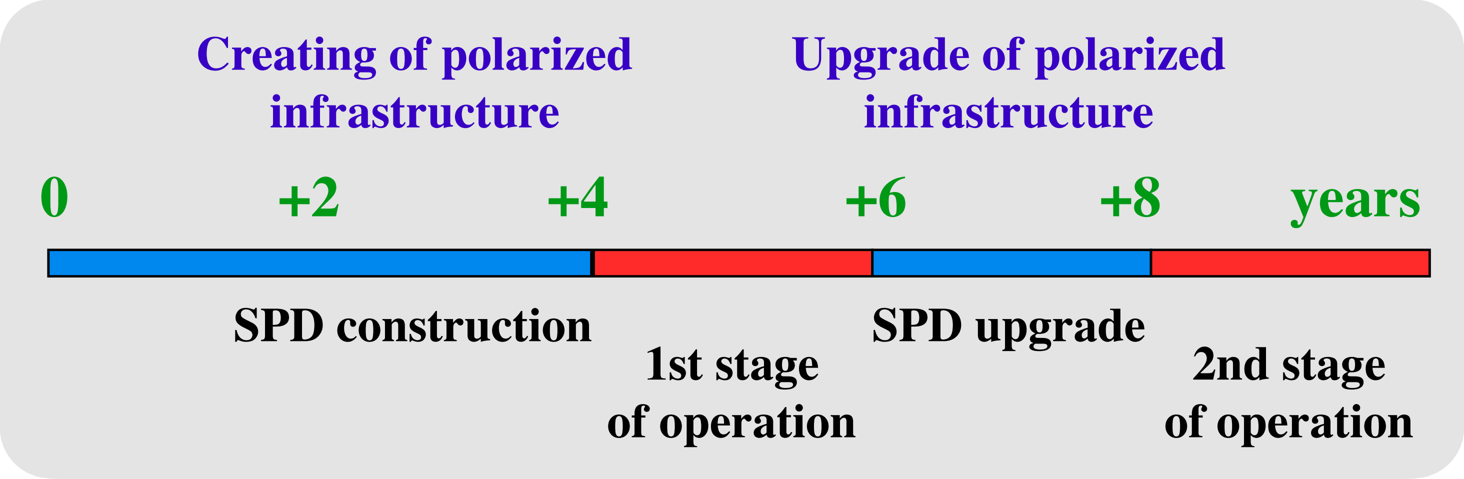

Creating of polarized infrastructure

Upgrade of polarized infrastructure

0 +2 +4 +6 +8 years

SPD construction

1st stage of operation

SPD upgrade

2nd stage of operation

backup

MoU signed

1 A.I. Alikhanyan National Science Laboratory (Yerevan Physics Institute), Yerevan
2 NRC “Kurchatov Institute” - PNPI, Gatchina
3 Samara National Research University (Samara University), Samara
4 Saint Petersburg Polytechnic University St. Petersburg
5 Saint Petersburg State University, St. Petersburg
6 Skobeltsyn Institute of Nuclear Physics, Moscow State University, Moscow
7 Tomsk State University, Tomsk
8 Belgorod State University, Belgorod
9 Lebedev Physical Institute of RAS, Moscow
10 Institute for Nuclear Research of the RAS, Moscow
11 National Research Nuclear University MEPhI, Moscow
12 Institute of Nuclear Physics (INP RK), Almaty
13 Institute for Nuclear Problems of BSU, Minsk

14 NRC “Kurchatov Institute”, Moscow (NRC KI)
15 Higher Institute of Technologies and Applied Sciences, Havana

SPD compared to other spin experiments

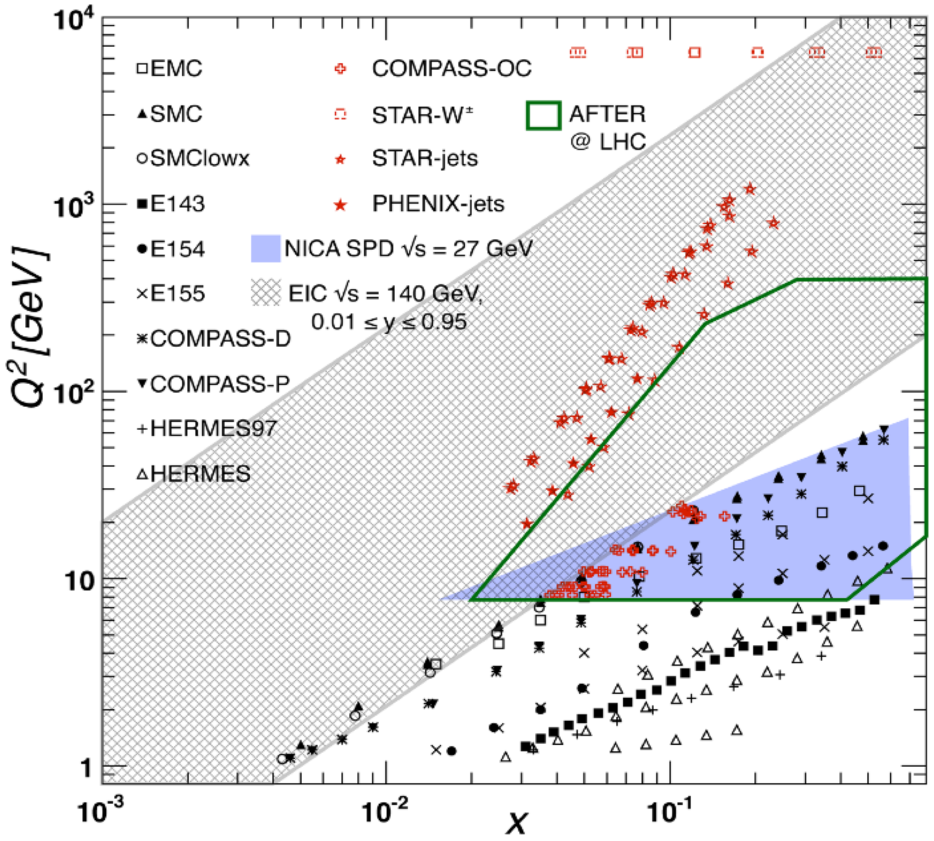

Main present and future gluon-spin-physics experiments

Experimental facility	SPD @NICA	RHIC	EIC	AFTER @LHC	LHCspin
Scientific center	JINR	BNL	BNL	CERN	CERN
Operation mode	collider	collider	collider	fixed target	fixed target
Colliding particles & polarization	$p^{\uparrow}$-$p^{\uparrow}$ $d^{\uparrow}$-$d^{\uparrow}$ $p^{\uparrow}$-d, p-$d^{\uparrow}$	$p^{\uparrow}$-$p^{\uparrow}$	$e^{\uparrow}$-$p^{\uparrow}$, $d^{\uparrow}$,$^3\mathrm{He}^{\uparrow}$	p-$p^{\uparrow}$,$d^{\uparrow}$	p-$p^{\uparrow}$
Center-of-mass energy $\sqrt{s_{NN}}$, GeV	≤27 (p-p) ≤13.5 (d-d) ≤19 (p-d)	63, 200, 500	20-140 (ep)	115	115
Max. luminosity, 10^{32} cm^{-2} s^{-1}	~1 (p-p) ~0.1 (d-d)	2	1000	up to ~10 (p-p)	4.7
Physics run	>2025	running	>2030	>2025	>2025

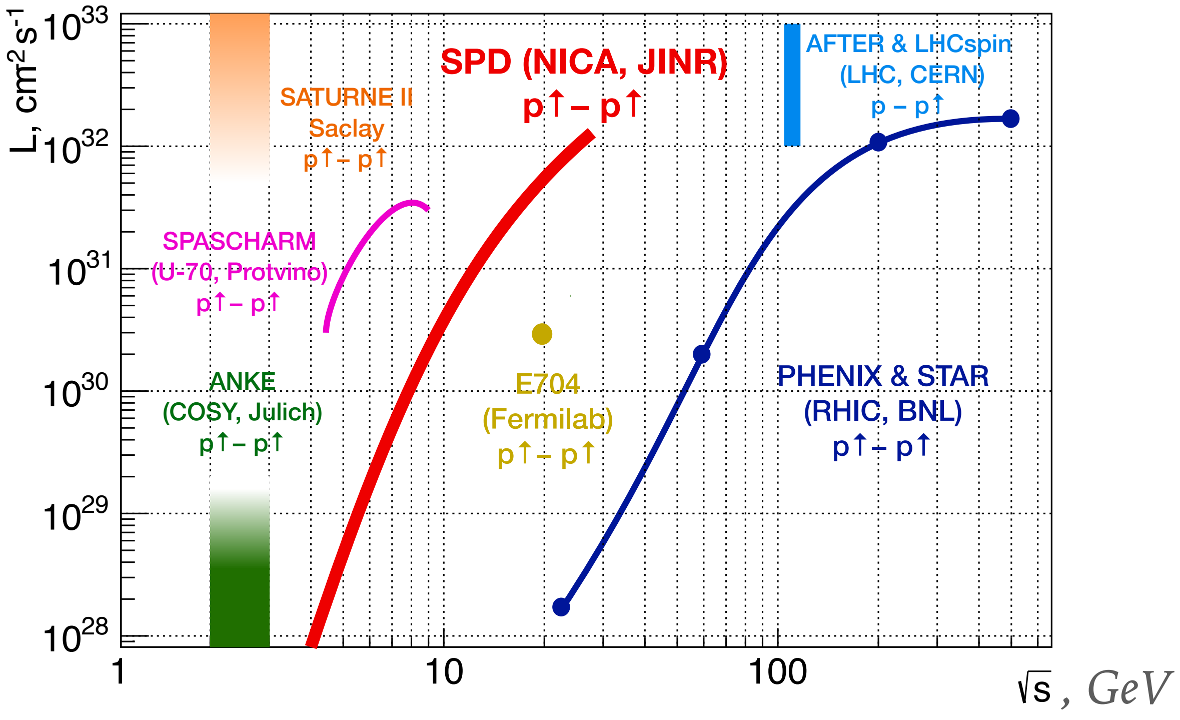

- Access to intermediate and high values of x
- Low energy but collider experiment (compared to fixed target). Nearly 4π coverage
- Two injector complexes available ⇒ mixed combinations p↑-d and p-d↑ are possible

Yu.Filatov 28.04.2021

Spin dynamics in the SPD solenoidal field 1T

Δz is a displacement of IP from the SPD center

Ψ is a spin deviation angle

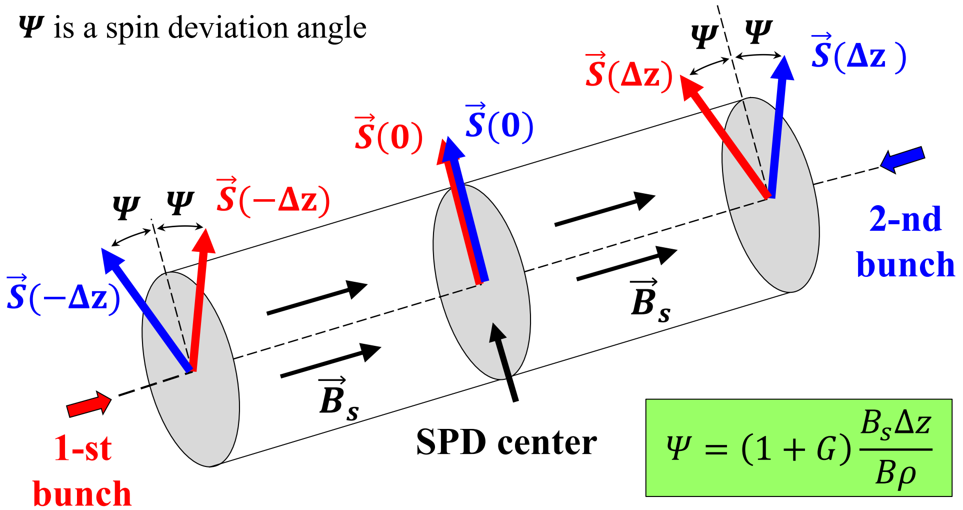

$$\Psi = (1+G)\frac{B_s \Delta z}{B\rho}$$

$B\rho$ is a magnetic rigidity

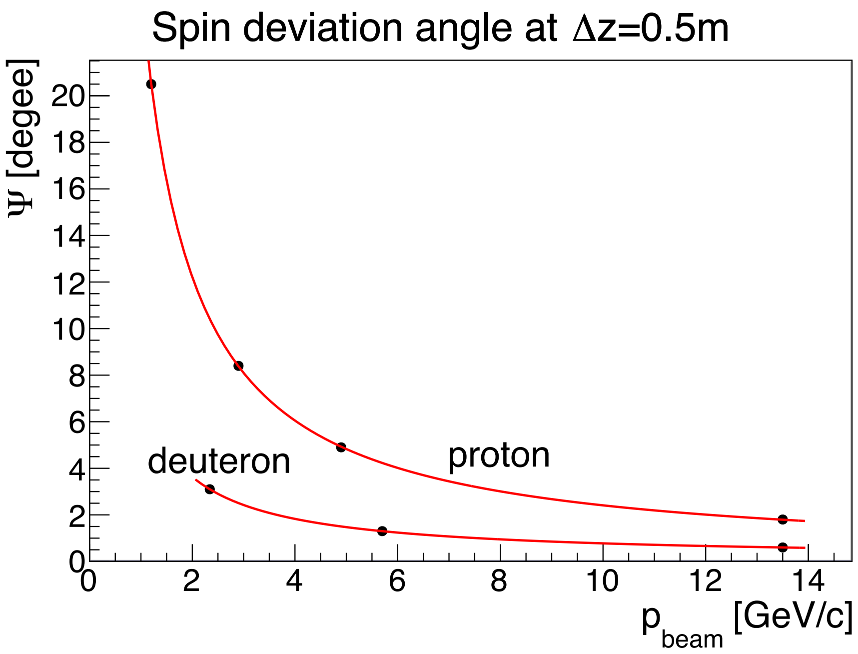

Luminosity reduction due to displacement of IP from the SPD center

IP is displaced from the SPD center

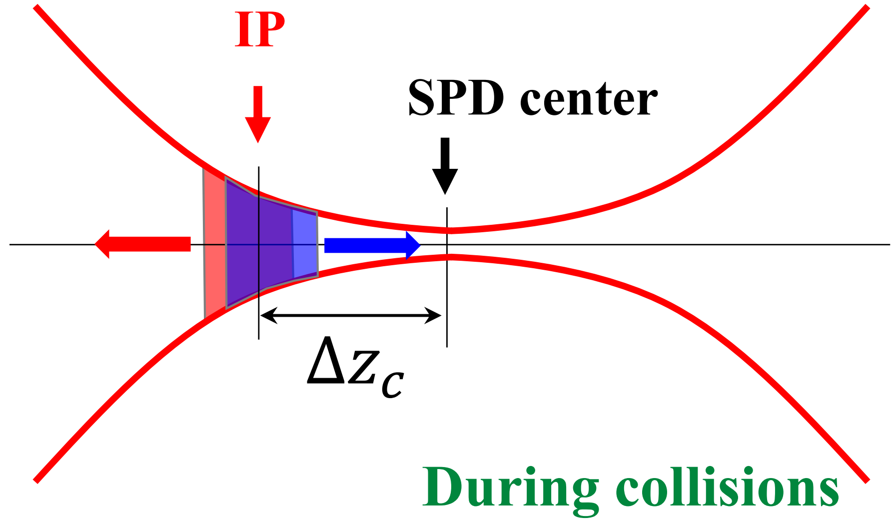

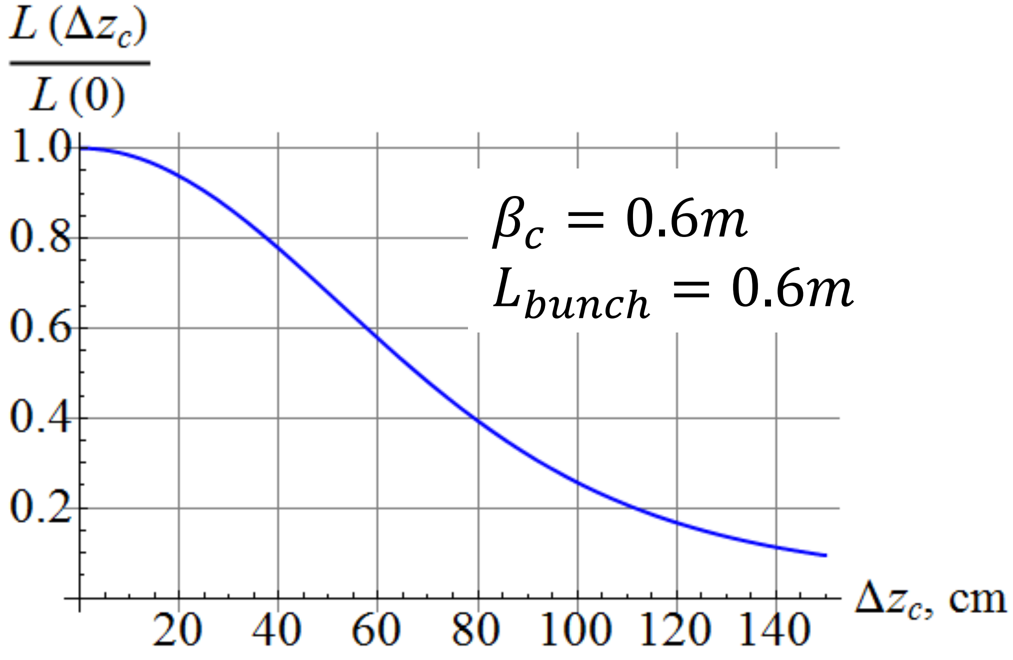

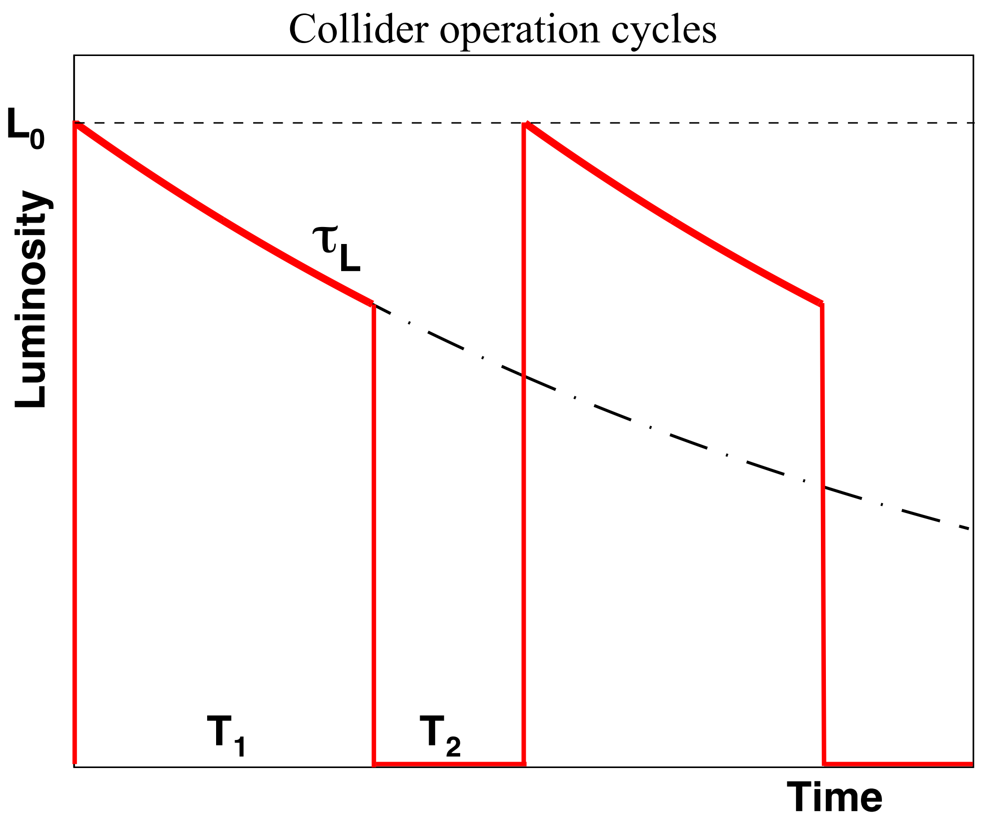
Collider operation cycles

- Formation of polarized proton beams in the NICA collider is presently under study
  - $T_1 \approx 2$h, $T_2 \approx 1$h, $\tau_L \approx 6$h, $\tau_P \approx 3$day
  - Effective luminosity $L_{eff} \approx 0.6L_0$, maximum luminosity $L_0 \approx 10^{23}$ cm^{-2}s^{-1}

- All bunches in one ring will have the same polarization (~70%)
- Spin navigator (SN) is based on weak solenoids with $BL \leq 0.6$Tm
- It takes ~1s for Spin-Flipper based on SN to reverse the polarization

Operation mode with spin flippers

1st ring +++… |xxx| - - -… | | - - -… |xxx| +++ …| | +++…

2nd ring +++… | | +++…|xxx| - - -… | | - - - … |xxx| +++…

(+ +) (- +) (- -) (+ -) (+ +)

|xxx| - spin-flipper switching-on, no data taking

| | - spin-flipper switching-off, no data taking

Calorimeter suspension scheme in CMS/LHC

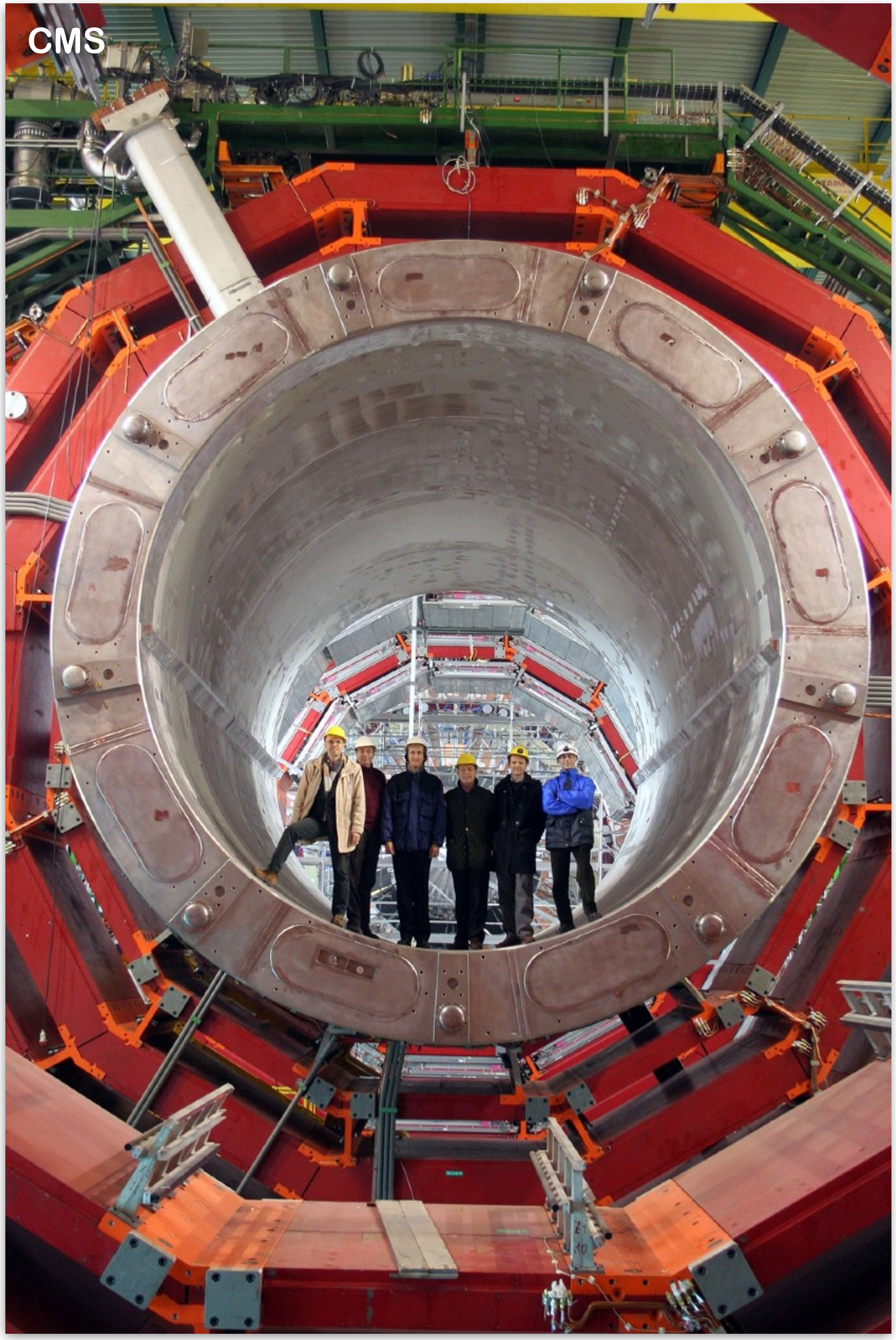

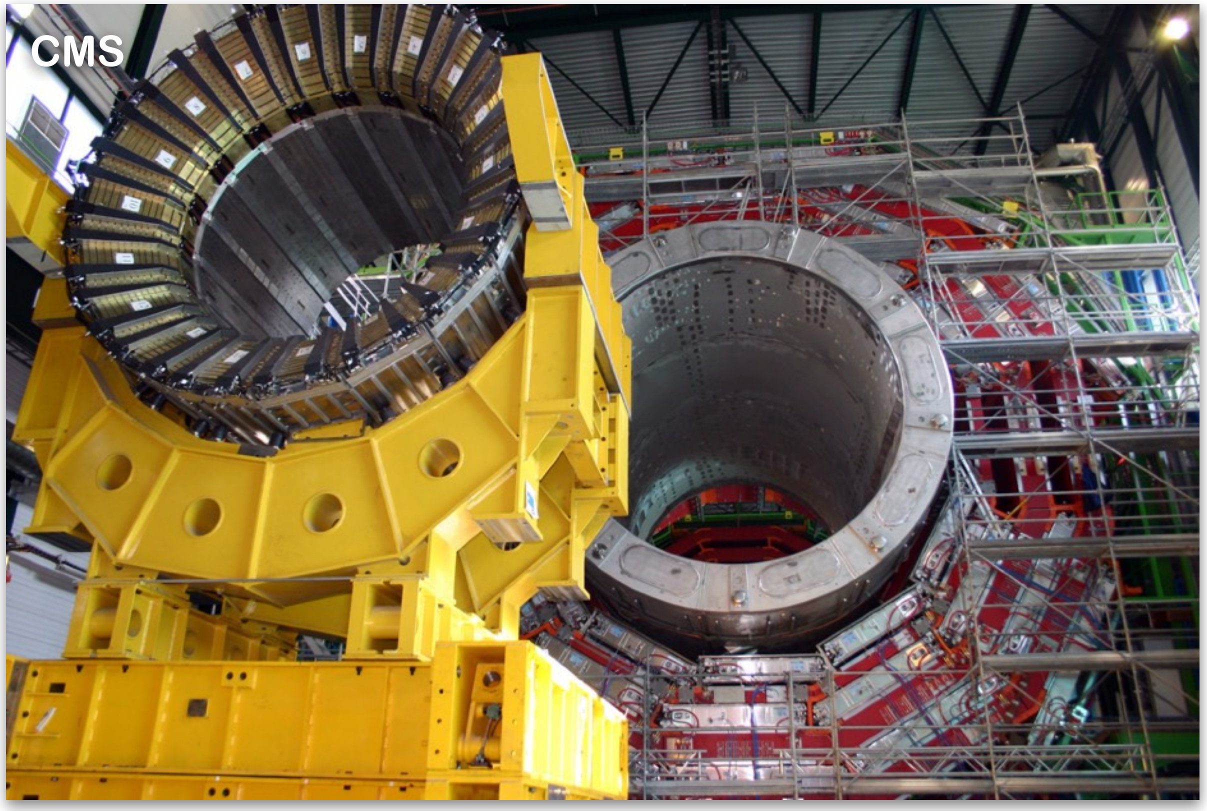

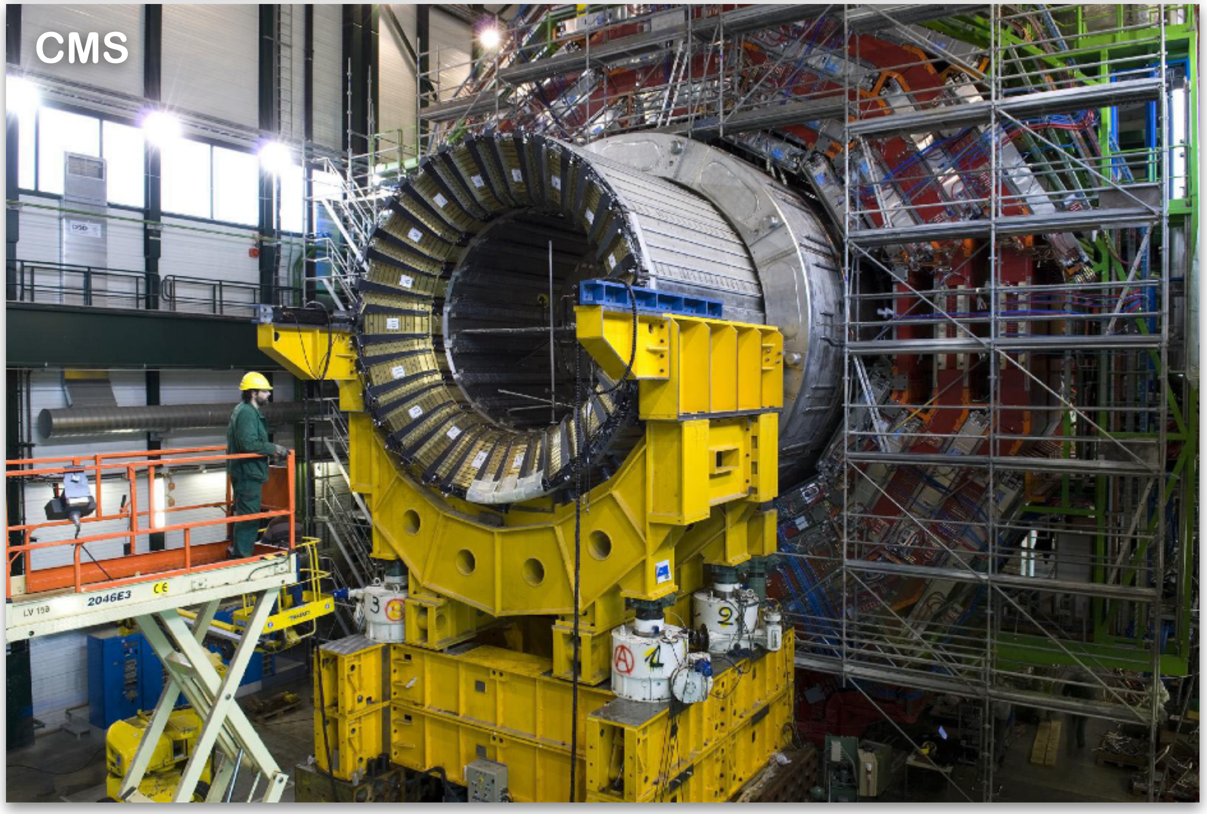

Model calculation of quark orbital angular momentum

$$L_z^q = \int dx\, d^2\vec{k}_T\, d\vec{b}_\perp\, (\vec{b}_\perp \times \vec{k}_T)_z\, \rho_{LU}(\vec{b}_\perp, \vec{k}_T, x)$$

Wigner distribution of unpolarized (U) quark in a longitudinally (L) polarized nucleon

Light-cone constituent quark model (LCCQM)
C.Lorce, B.Pasquini, X.Xiong, F.Yuan, arXiv:1111.4827

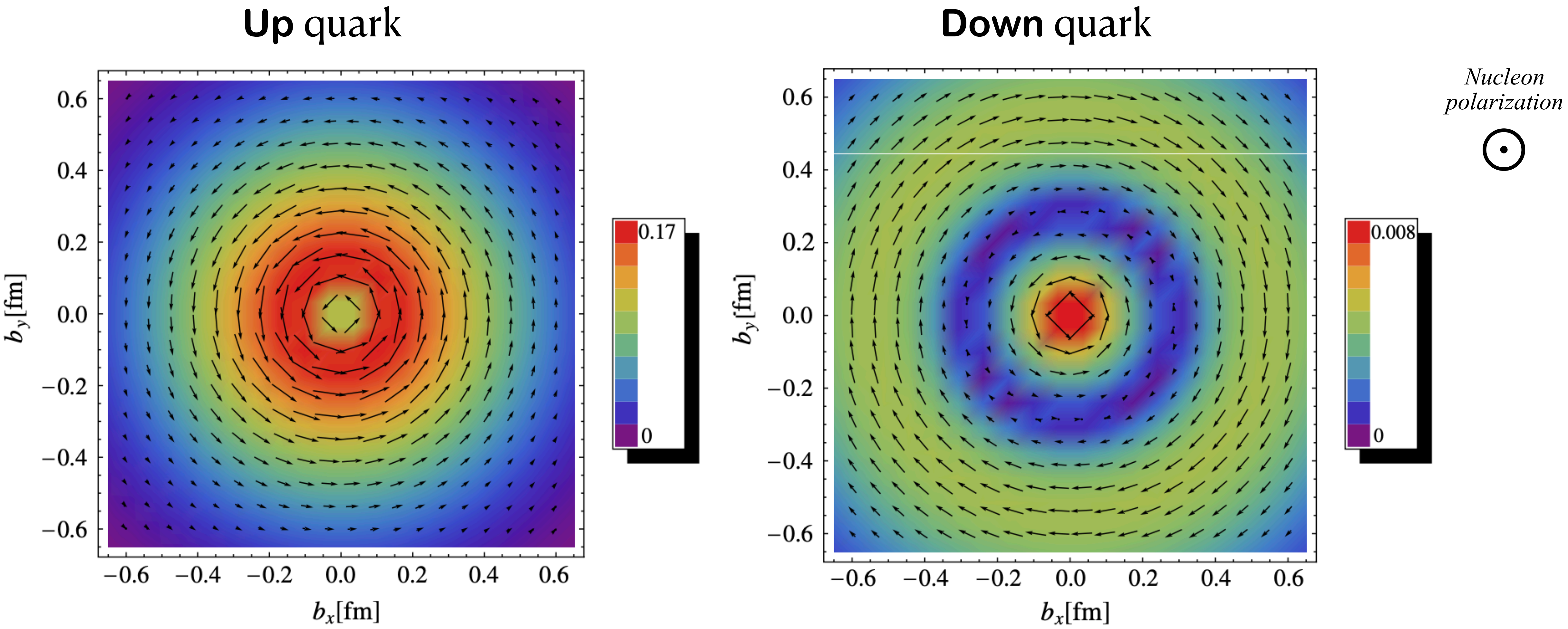

Functions describing the nucleon structure

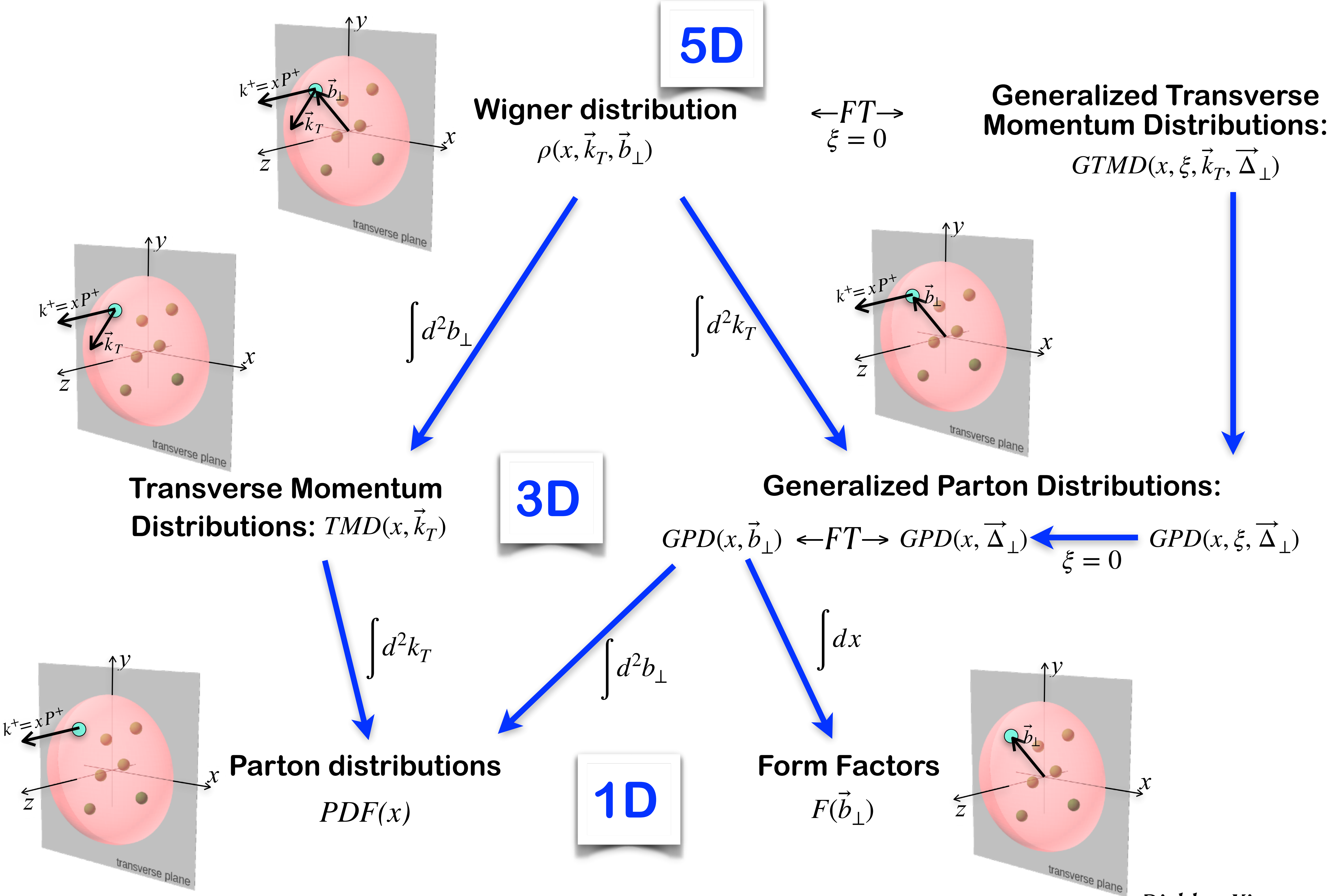

5D

Wigner distribution
$\rho(x, \vec{k}_T, \vec{b}_\perp)$

$\xleftrightarrow{FT}$
$\xi = 0$

Generalized Transverse Momentum Distributions:
$GTMD(x, \xi, \vec{k}_T, \vec{\Delta}_\perp)$

$\int d^2 b_\perp$

$\int d^2 k_T$

3D

Transverse Momentum Distributions: $TMD(x, \vec{k}_T)$

Generalized Parton Distributions:

$GPD(x, \vec{b}_\perp) \xleftrightarrow{FT} GPD(x, \vec{\Delta}_\perp) \xleftarrow[\xi = 0]{} GPD(x, \xi, \vec{\Delta}_\perp)$

$\int d^2 k_T$

$\int d^2 b_\perp$

$\int dx$

Parton distributions
$PDF(x)$

1D

Form Factors
$F(\vec{b}_\perp)$

Diehl, arXiv:1512.01328

Transverse momentum-dependent (TMD) distributions

- 3D partonic structure of hadron in momentum space (coordinate position of partons is obtained from GPD)
- Transverse motion of quarks results in correlations between the orbital angular momentum and the spin of quarks for nucleons at different polarization states
- TMDs give rise to spin and azimuthal asymmetries

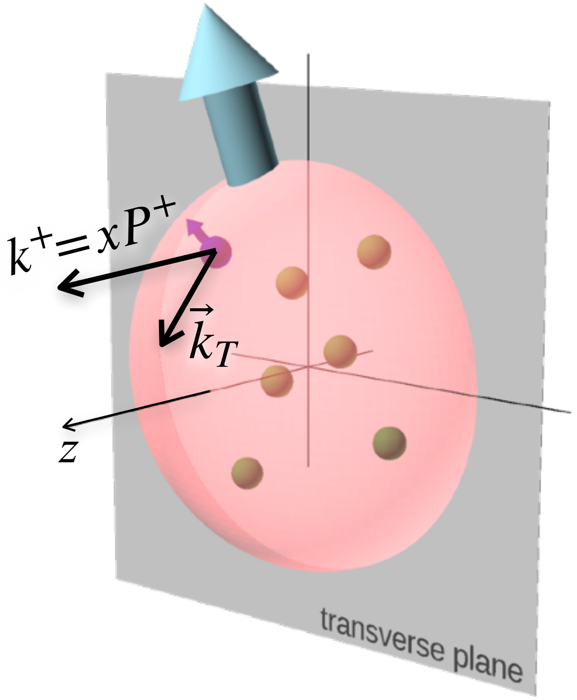

$\vec{k}_\perp$ and $\hat{z}$ are vectors

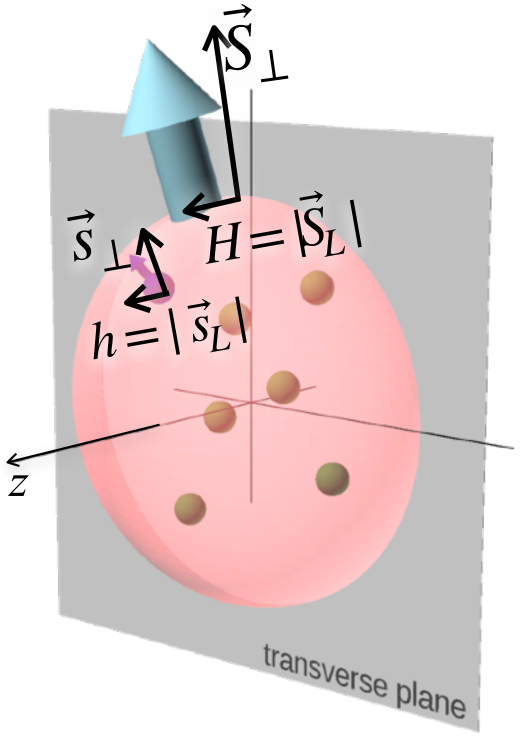

h and H are pseudoscalars
$\vec{S}_\perp$ and $\vec{s}_\perp$ are axial vectors

- Hadronic tensor is decomposed into a set of basis tensors multiplied by *scalar* structure functions (TMDs)
- One needs to find out the basis tensors assuming hermiticity, parity and time-reversal invariances.
- Only 8 independent combinations to construct a *scalar* up to terms quadratic in k_T => Leading twist distributions (densities) in the context of parton model

Transverse momentum-dependent (TMD) parton distributions

Independent of $\vec{k}_\perp$

Number density	**Helicity**	**Transversity**
$\mathbb{1}$	hH	$\vec{s}_\perp \cdot \vec{S}_\perp$
$\times\, f_1(x, k_T^2)$	$\times\, g_{1L}(x, k_T^2)$	$\times\, h_1(x, k_T^2)$

Product of pseudo-scalar and axial vector

Worm gear T	**Worm gear L**
$h\,(\vec{k}_\perp \cdot \vec{S}_\perp)$	$H\,(\vec{k}_\perp \cdot \vec{s}_\perp)$
$\times\, g_{1T}(x, k_T^2)$	$\times\, h_{1L}^{\perp}(x, k_T^2)$

(h and H are pseudoscalars) + ($\vec{k}_\perp$ and $\hat{z}$ are vectors) +
($\vec{S}_\perp$ and $\vec{s}_\perp$ are axial vectors) + hermiticity, parity, time-reversal invariances.
Only 8 independent combinations up to terms quadratic in $\vec{k}_\perp$

Triple product (T-odd)

Sivers function	**Boer-Mulders function**
$\vec{S}_\perp\,(\vec{k}_\perp \times \hat{z})$	$\vec{s}_\perp\,(\vec{k}_\perp \times \hat{z})$
$\times\, f_{1T}^{\perp}(x, k_T^2)$	$\times\, h_1^{\perp}(x, k_T^2)$

2-nd power in $\vec{k}_\perp$

Pretzelosity

$$2\,(\vec{S}_\perp \cdot \vec{k}_\perp)(\vec{s}_\perp \cdot \vec{k}_\perp) - \vec{k}_\perp^2(\vec{S}_\perp \cdot \vec{s}_\perp)$$

$$\times\, h_{1T}^{\perp}(x, k_T^2)$$

Transverse momentum-dependent (TMD) parton distributions

		Quark polarization		
		Unpolarized, *f*	**L**ongitudinal, *g*	**T**ransvers, *h*
Nucleon polarization	**U**npolarized	Number density 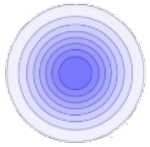 $\sim\mathbb{1}$		Boer-Mulders 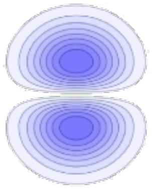 $\sim h\,(\vec{k}_\perp\cdot\vec{S}_\perp)$
	Longitudinal		Helicity 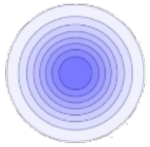 $\sim hH$	Worm-Gear L 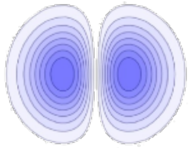 $\sim H\,(\vec{k}_\perp\cdot\vec{s}_\perp)$
	Transvers	Sivers 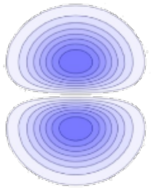 $\sim\vec{S}_\perp\,(\vec{k}_\perp\times\hat{z})$	Worm-Gear T 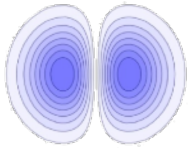 $\sim\vec{s}_\perp\,(\vec{k}_\perp\times\hat{z})$	Transversity 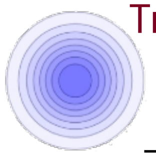 $\sim(\vec{s}_\perp\cdot\vec{S}_\perp)$ Pretzelocity 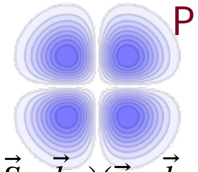 $\sim 2\,(\vec{S}_\perp\cdot\vec{k}_\perp)(\vec{s}_\perp\cdot\vec{k}_\perp)-\vec{k}_\perp^2(\vec{S}_\perp\cdot\vec{s}_\perp)$

- Can be presented as multipoles in momentum space (k_x, k_y)

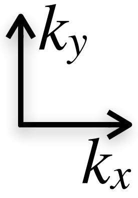

Transverse momentum-dependent (TMD) parton distributions

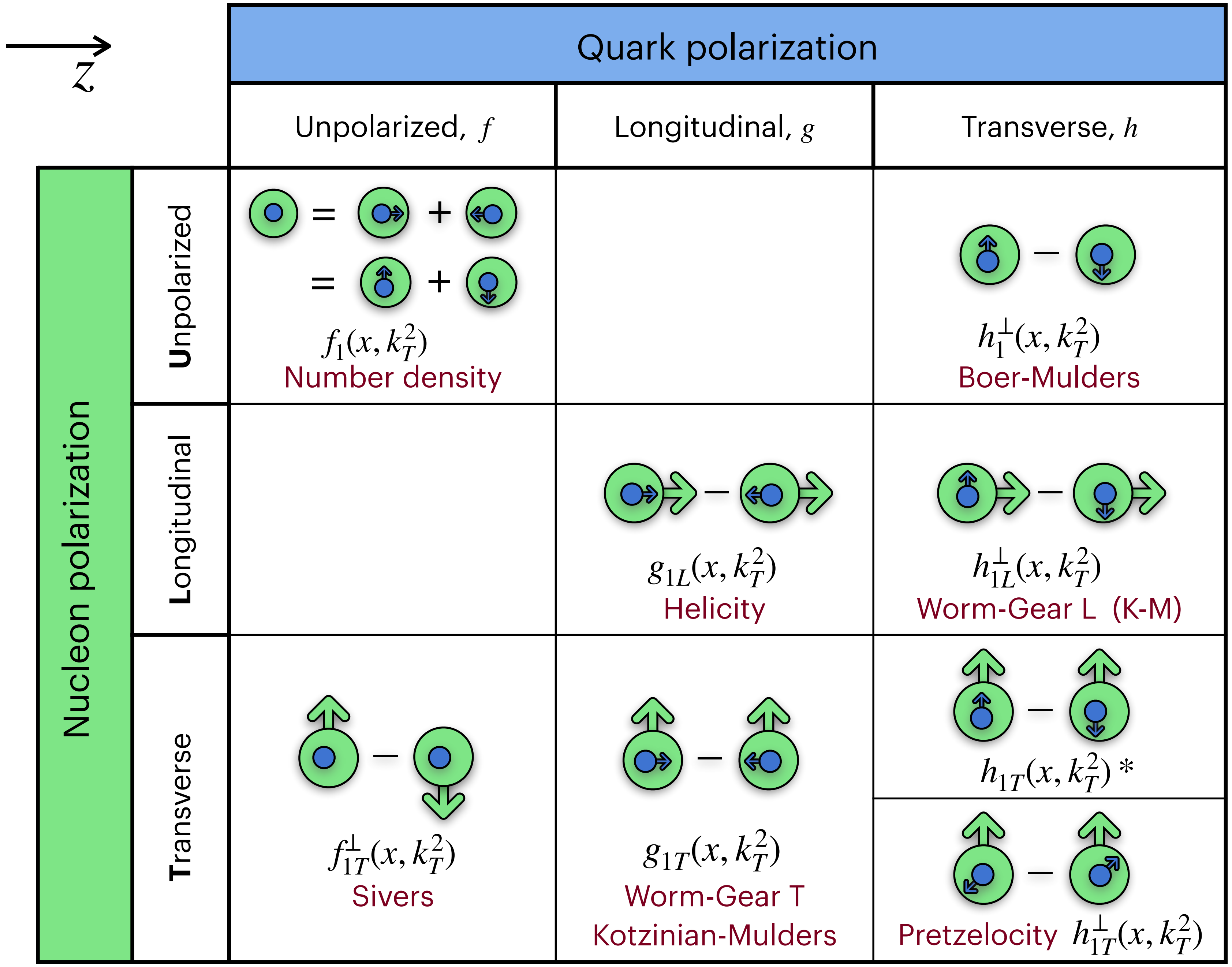

		Quark polarization		
		Unpolarized, f	Longitudinal, g	Transverse, h
Nucleon polarization	Unpolarized	$f_1(x, k_T^2)$ Number density		$h_1^\perp(x, k_T^2)$ Boer-Mulders
	Longitudinal		$g_{1L}(x, k_T^2)$ Helicity	$h_{1L}^\perp(x, k_T^2)$ Worm-Gear L (K-M)
	Transverse	$f_{1T}^\perp(x, k_T^2)$ Sivers	$g_{1T}(x, k_T^2)$ Worm-Gear T Kotzinian-Mulders	$h_{1T}(x, k_T^2)$ * Pretzelocity $h_{1T}^\perp(x, k_T^2)$

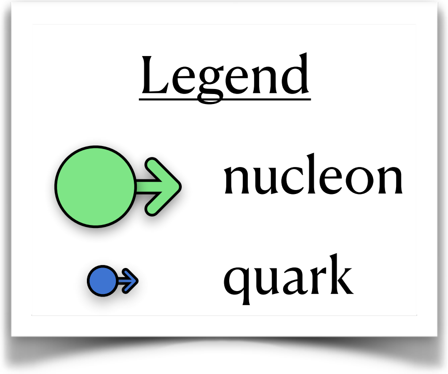

Legend

- 🟢 nucleon
- 🔵 quark

- Subindex "$_1$" indicates the leading twist (twist-2)
- Subindices "$_L$" and "$_T$" indicate polarization of nucleon
- Superscript "$^\perp$" indicates the presence of transverse momenta with uncontracted Lorentz indices
- All 8 twist-2 functions can be interpreted as densities
- 16 functions in twist-3. No more probabilistic interpretation

* Transversity: $h_1 = h_{1T} + \dfrac{k_T^2}{2M^2} h_{1T}^\perp$

Sivers effect

Large single-spin asymmetries (SSA) in $p^{\uparrow}p \rightarrow \pi X$ processes

- Large SSA observed in many inclusive pion production experiments: $p^{\uparrow}p \rightarrow \pi X$

$$\boxed{A_N = \frac{d\sigma^{\uparrow} - d\sigma^{\downarrow}}{d\sigma^{\uparrow} + d\sigma^{\downarrow}}}$$

- Effect is almost independent of energy
- Sivers effect explains the asymmetry assuming opposite contribution of *u* and *d* quarks: $sgn(f_{1T}^{\perp u}) = -\, sgn(f_{1T}^{\perp d})$
  Anselmino et al, hep-ph/9503290, hep-ph/0509035
- Even though effect is large, its description is complicated

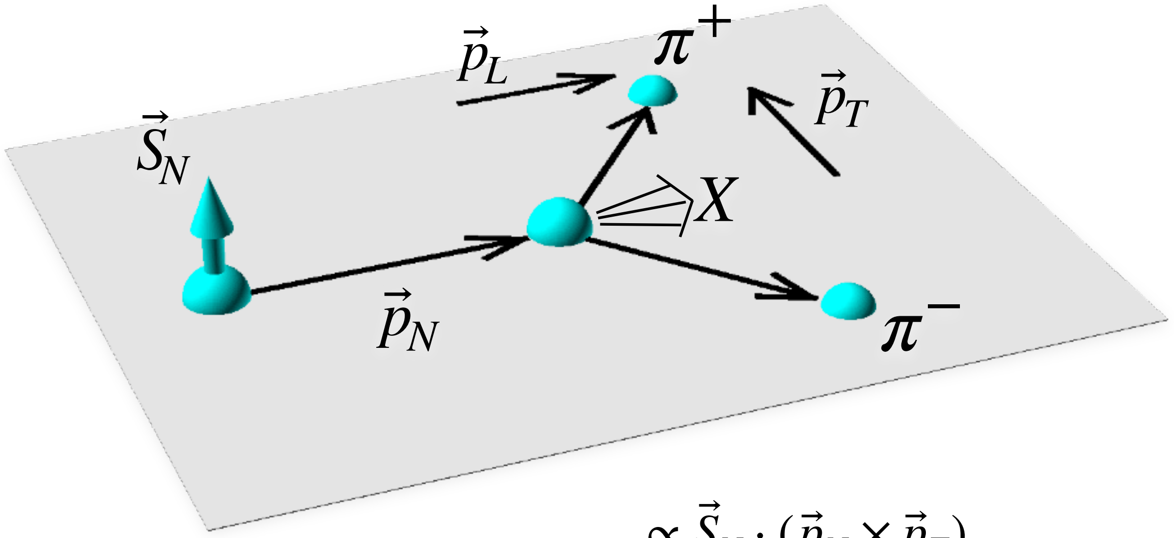

$\propto \vec{S}_N \cdot (\vec{p}_N \times \vec{p}_T)$

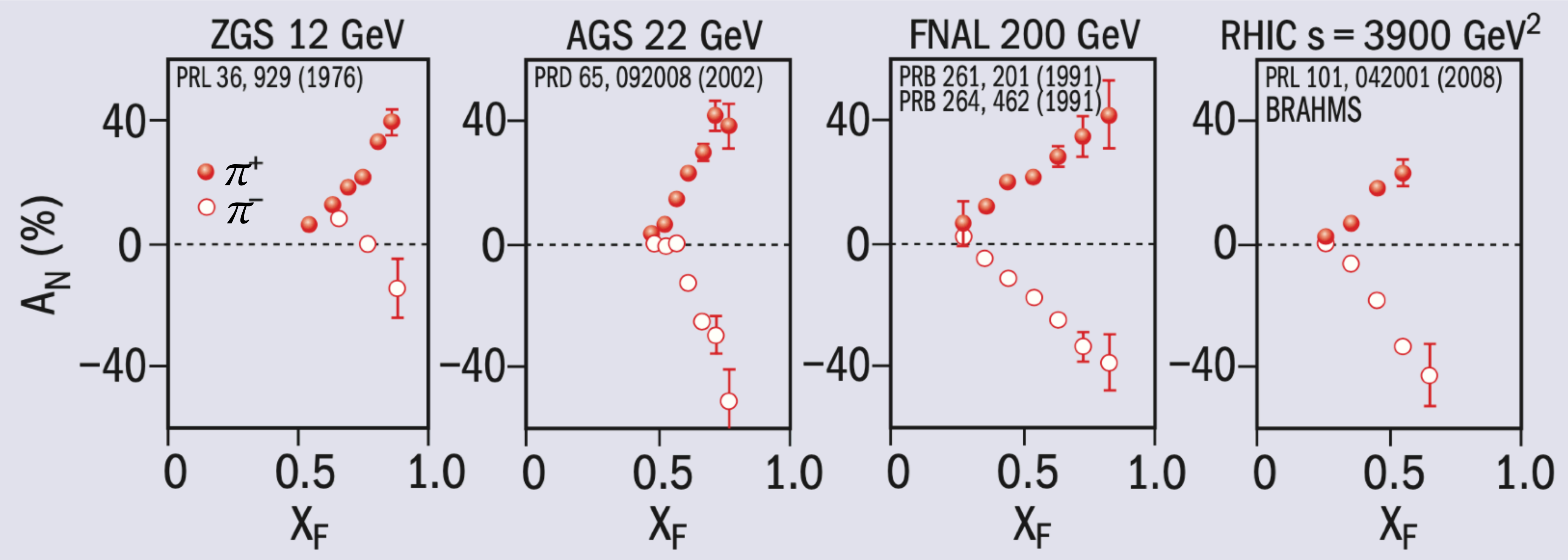

$x_F = 2p_L/\sqrt{s}$

CERN Courier, June 2009

Phenomenological description of SSA of p$^\uparrow$p$\to\pi$X processes

- Generalized parton model (GPM) can be considered as a natural phenomenological extension of the usual collinear factorization scheme, with the inclusion of spin and k_T effects through the TMDs

$$\hat{f}_{q/p^\uparrow}(x,k_T) = f_{q/p}(x,k_T) + \frac{1}{2}\Delta^N f_{q/p^\uparrow}(x,k_T)\ \mathbf{S}\cdot(\hat{\mathbf{P}}\times\hat{\mathbf{k}}_\mathbf{T})$$

- Both Sivers (partonic distributions) and Collins (fragmentation processes) effects contribute to A_N

$$A_N = \frac{[d\sigma^\uparrow - d\sigma^\downarrow]_{Sivers} + [d\sigma^\uparrow - d\sigma^\downarrow]_{Collins}}{d\sigma^\uparrow + d\sigma^\downarrow}$$

Fit of the data on A_N

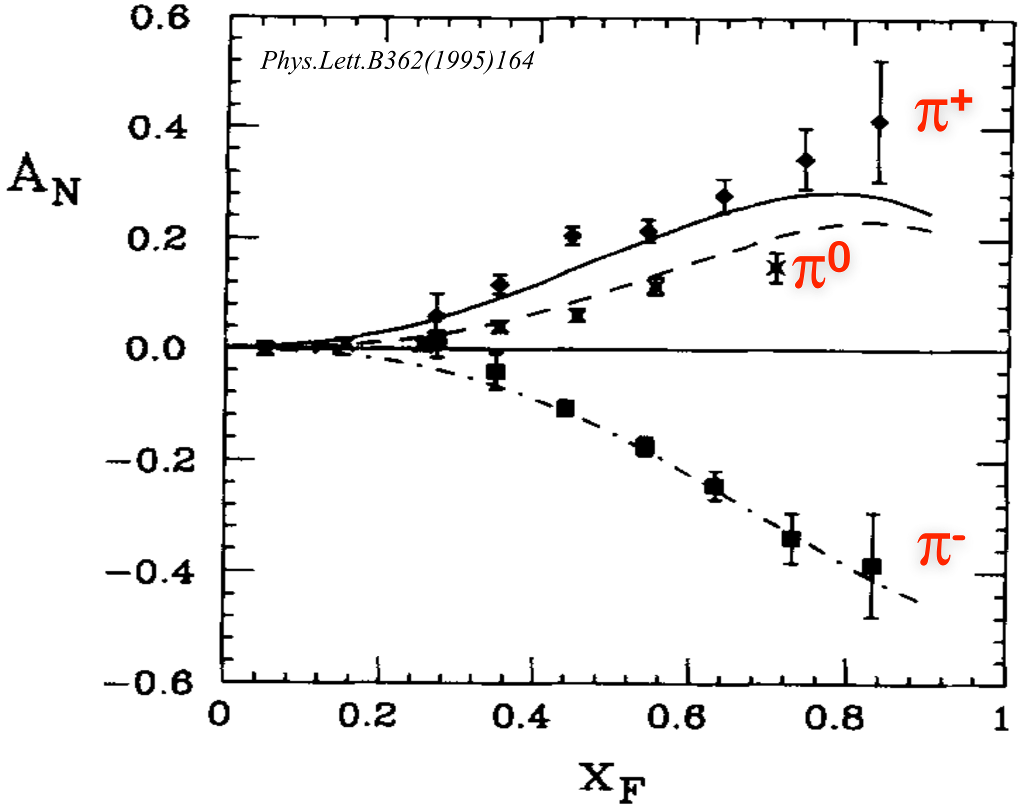

Contributions to A_N

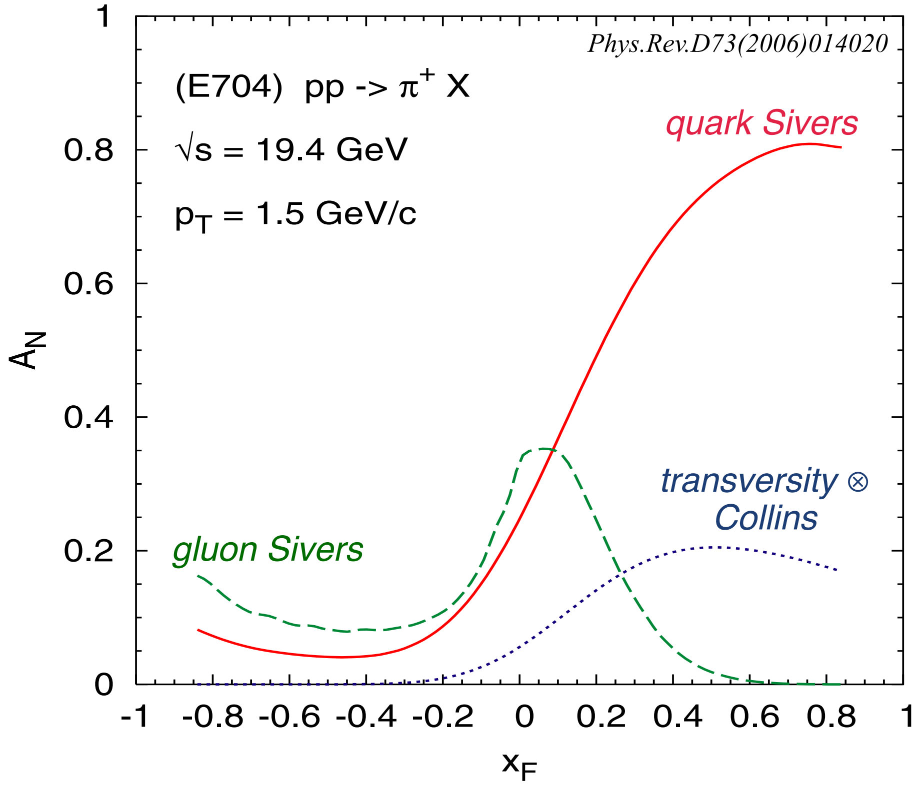

- There is no consistent description (global fit) of all p$^\uparrow$p$\to\pi$X data available so far
- Contribution of Sivers mechanism for quarks is largely dominant in the forward region
- Opposite sign of π+ and π- asymmetries can indicate an opposite sign of Sivers function of u and d quarks
- Gluons can be studied in the central and backward regions of x_F
- New data of SPD over a wide rage of p_T and x_F will provide better constrains for the fit

Fixed target experiments (Eur.Phys.J.C14(2000)427)

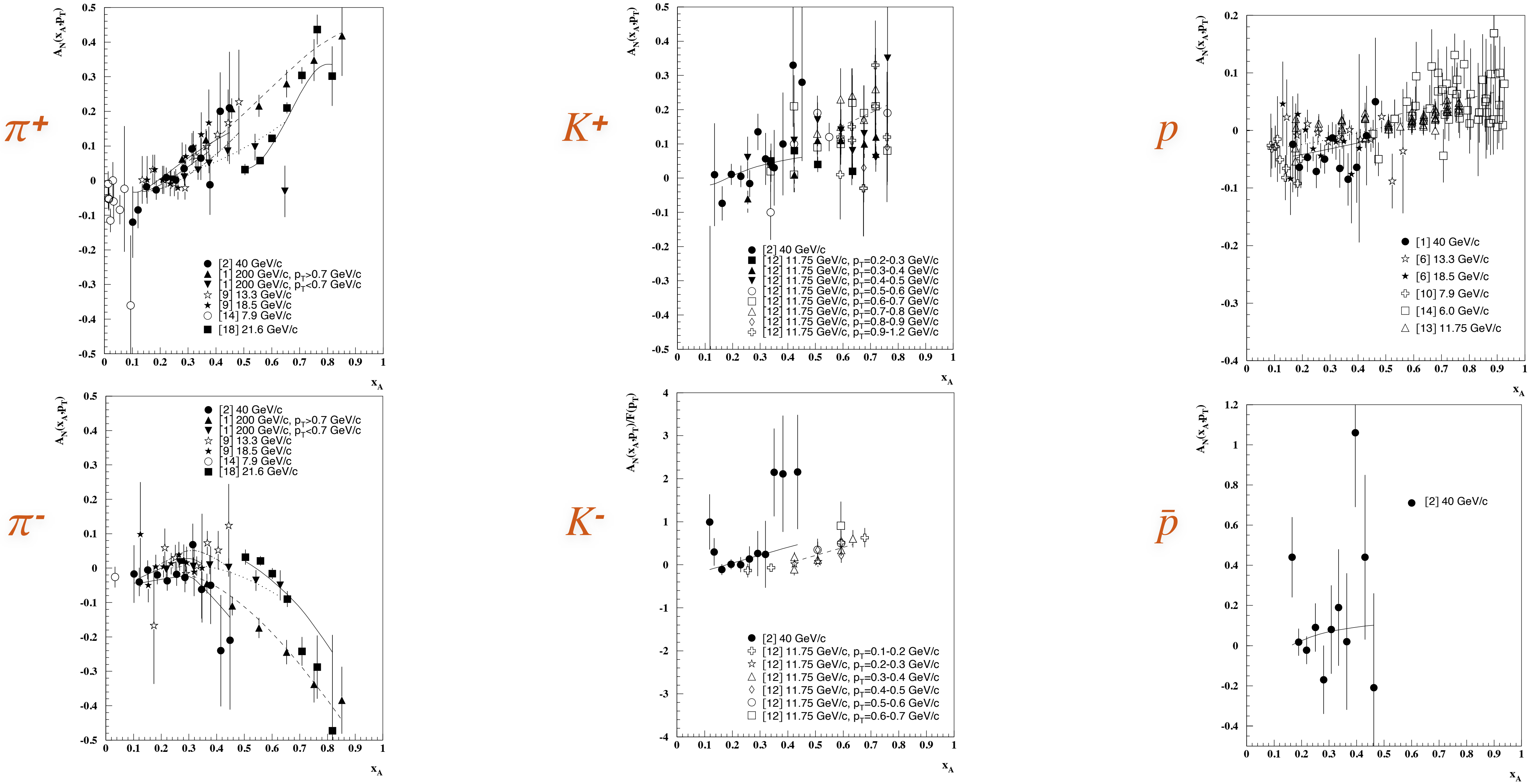

Collider experiment BRAHMS (Phys.Rev.Lett.101(2008)042001)

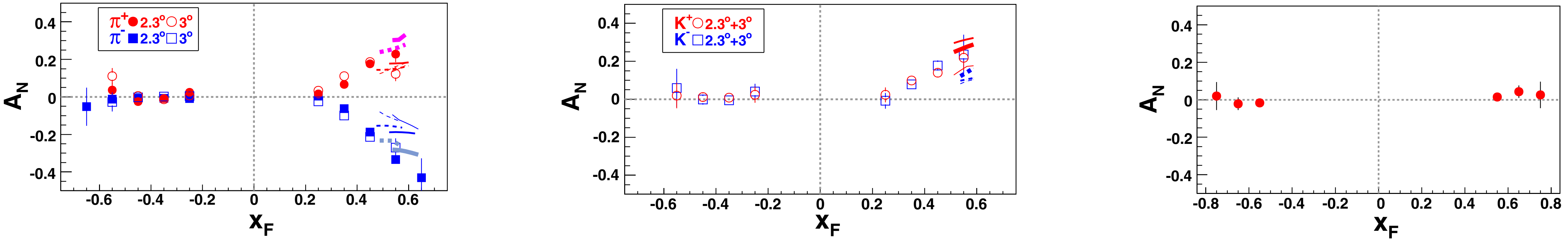

Generalized Transverse Momentum Distribution (GTMD)

- Average momentum *P* and momentum transfer to nucleon *Δ*

$$P = \frac{p+p'}{2}, \qquad \Delta = p' - p$$

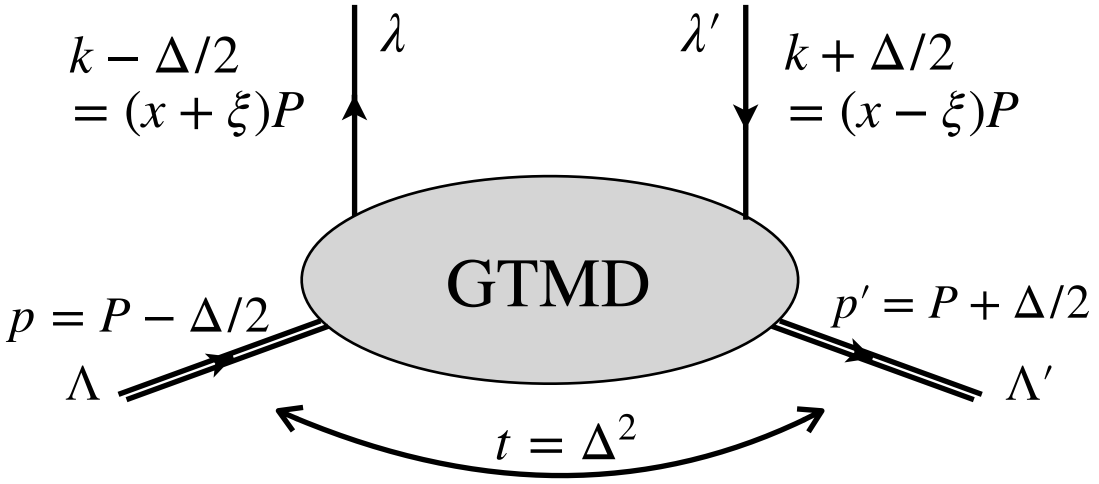

- Average momentum fraction of quark: $x = k^+/P^+$

- Fraction of longitudinal momentum transfer to nucleon (skewness)

$$\xi = \frac{p^+ - p'^+}{p^+ + p'^+} = -\frac{\Delta^+}{2P^+}$$

$$\Delta^2 = -\frac{4\xi^2 m^2 + \vec{\Delta}_\perp^2}{1-\xi^2}$$

- Generalized quark-quark correlator for a spin-1/2 hadron

$$W^{q[\Gamma]}_{\Lambda,\Lambda'} = \frac{1}{2}\int \frac{dz^- d^2\vec{z}_\perp}{(2\pi)^3}\, e^{i\,k\cdot z}\,\langle p',\Lambda'|\,\bar{\psi}^q(-\frac{z}{2})\,\Gamma\,\mathscr{W}(-\frac{z}{2},\frac{z}{2})\,\psi^q(\frac{z}{2})\,|p,\Lambda\rangle\Big|_{z^+=0}$$

nucleon polarization

quark polarization (Dirac matrices)

Wilson gauge link

- Complete parametrization using 16 complex-valued twist-2 GTMDs

$$X(x,\xi,\vec{k}_\perp^2,\vec{k}_\perp\cdot\vec{\Delta}_\perp,\vec{\Delta}_\perp^2;\eta)$$

Meissner, Metz, Schlegel, arXiv:0906.5323

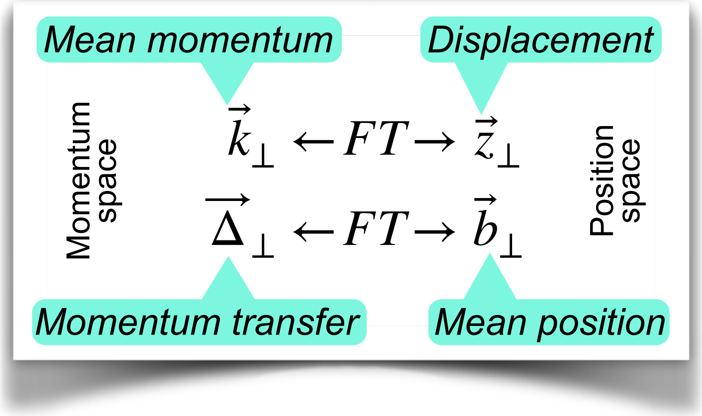

Definitions of OAM kinetic vs canonical

$$L_z^{can} = -\int dx\, d^2k_T\, \frac{\vec{k}^2}{M^2}\, F_{1,4}^{\perp}(x,0,\vec{k}^2,\vec{0}^2)$$

$GTMD(x,\xi,\vec{k}_T,\vec{\Delta}_\perp)$

Nucleon polarization	Quark polarization: U	L	T
U	$F_{1,1}$	$G_{1,1}$	$H_{1,1}\ H_{1,2}$
L	$F_{1,4}$	$G_{1,4}$	$H_{1,7}\ H_{1,8}$
T	$F_{1,2}\ F_{1,3}$	$G_{1,2}\ G_{1,3}$	$H_{1,3}\ H_{1,4}$ $H_{1,5}\ H_{1,6}$

16 in twist-2
32 in twist-3
16 in twist-4

$\xi = 0,\ \vec{\Delta}_\perp = 0$

$\xi = 0,\ \int d^2k_T$

$TMD(x,\vec{k})$

Nucleon polarization	Quark polarization: U	L	T
U	f_1		$h_1^{\perp}$
L		g_{1L}	$h_{1L}^{\perp}$
T	$f_{1T}^{\perp}$	g_{1T}	$h_1\ h_{1T}^{\perp}$

8 in twist-2
16 in twist-3
8 in twist-4

$GPD(x,\vec{\Delta}_\perp)$

Nucleon polarization	Quark polarization: U	L	T
U	H		E_T
L		$\tilde{H}$	$\tilde{E}_T$
T	E	$\tilde{E}$	$H_T\ \tilde{H}_T$

8 in twist-2
16 in twist-3
8 in twist-4

$$L_z^{can} = -\int dx\, d^2k_T\, \frac{\vec{k}^2}{2M^2}\, h_{1T}^{\perp}(x\vec{k}^2)$$

$$L_z^{kin} = \frac{1}{2}\int dx\, x[H(x{,}0{,}0) + E(x{,}0{,}0)] - \frac{1}{2}\int dx\, \tilde{H}(x{,}0{,}0)$$

Example of TMD and GPD processes

TMD

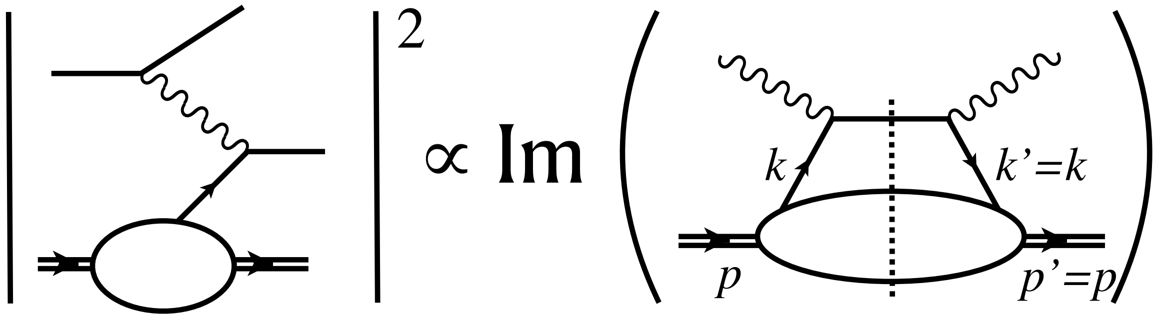

$\gamma^*(q) + p(p) \rightarrow \gamma^*(q) + p(p)$

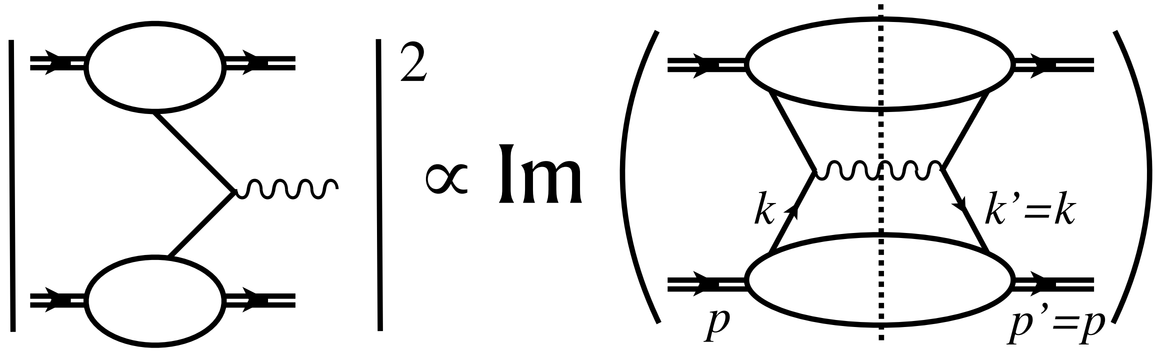

$p(p_1) + p(p_2) \rightarrow p(p_1) + p(p_2)$

4-momentum transferred from probe to nucleon

$\Delta = (p'-p)/2 = 0$ *(forward limit)*

Diagonal matrix element of quark-quark operator

$$\langle p,\Lambda|\bar{\psi}^q(-\frac{z}{2})\Gamma\mathscr{W}(-\frac{z}{2},\frac{z}{2})\psi^q(\frac{z}{2})|p,\Lambda\rangle$$

GPD

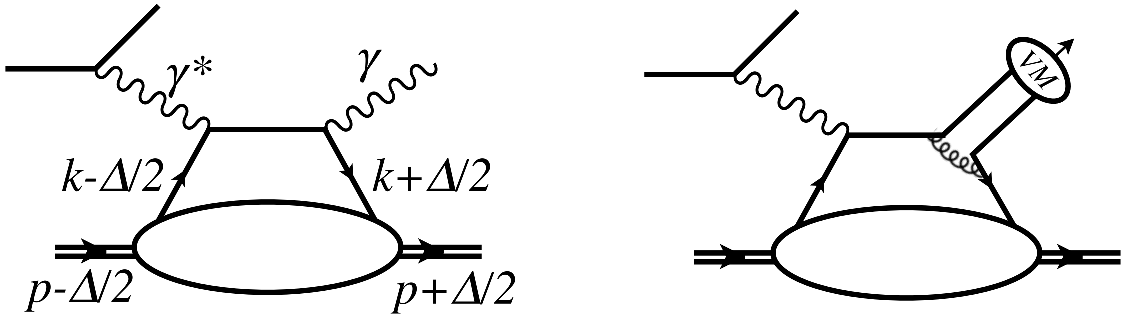

$\gamma^*(q) + p(p) \rightarrow \gamma(q') + p(p')$

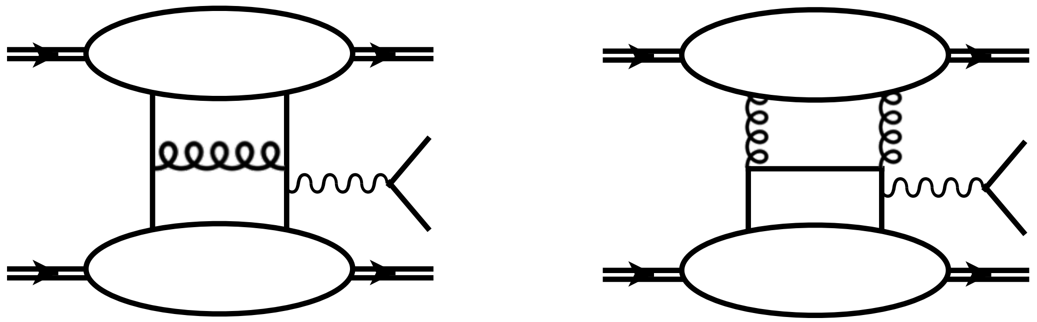

$p(p_1) + p(p_2) \rightarrow p(p_1') + p(p_2') + \gamma(q')$

Off-forward, skewed functions integrated over k_T

$\Delta = (p'-p)/2 \neq 0$

Off-diagonal matrix element of quark-quark operator

$$\langle p',\Lambda'|\bar{\psi}^q(-\frac{z}{2})\Gamma\mathscr{W}(-\frac{z}{2},\frac{z}{2})\psi^q(\frac{z}{2})|p,\Lambda\rangle$$

Gluon probes at SPD

Charmonia

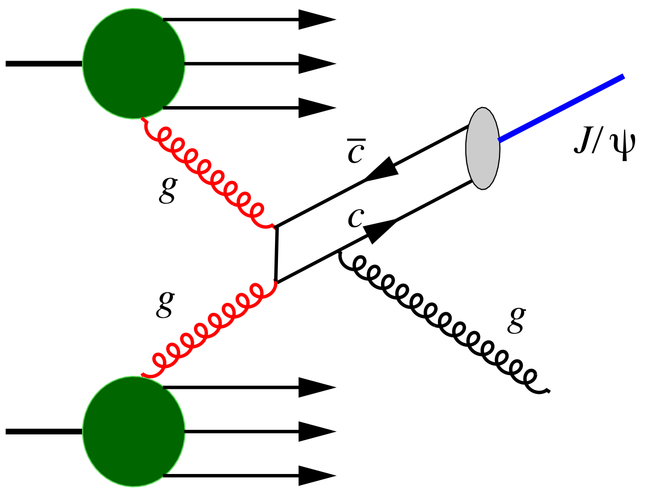

Open charm

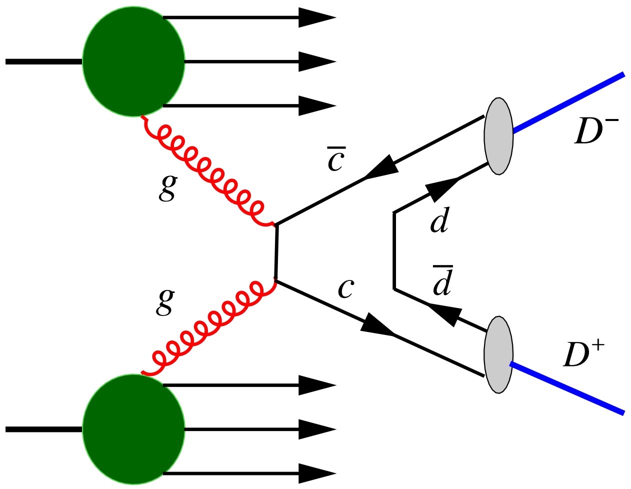

Prompt photon

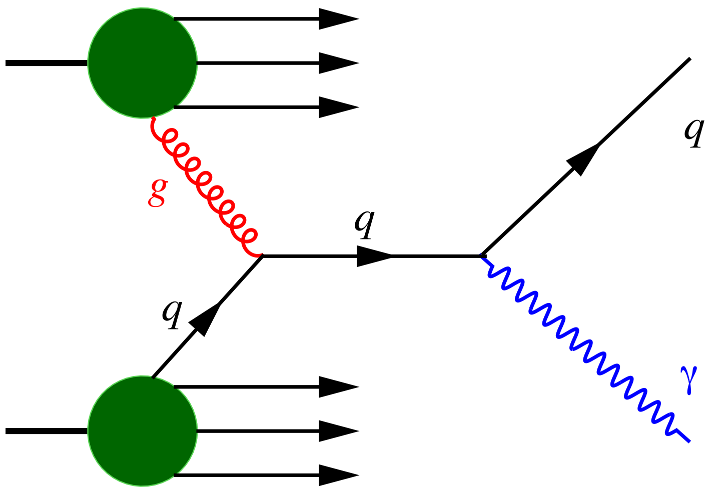

- A.Arbuzov et al., *On the physics potential to study the gluon content of proton and deuteron at NICA SPD*, arXiv:2011.15005
- Measurement of total and differential cross sections (p_T and y dependencies) in charm production to test various models
- Tests of TMD factorization
- Gluon Sivers function via SSA in gluon-induced processes
- Linearly polarized gluons in unpolarized nucleon (B-M function)
- Non-nucleonic degrees of freedom in deuteron
- Gluon polarization Δg with longitudinally polarized beams (fraction of nucleon spin carried by gluons)
- Gluon transversity in deuteron (assuming spin flip ±2, thus does not exist in nucleons)
- …